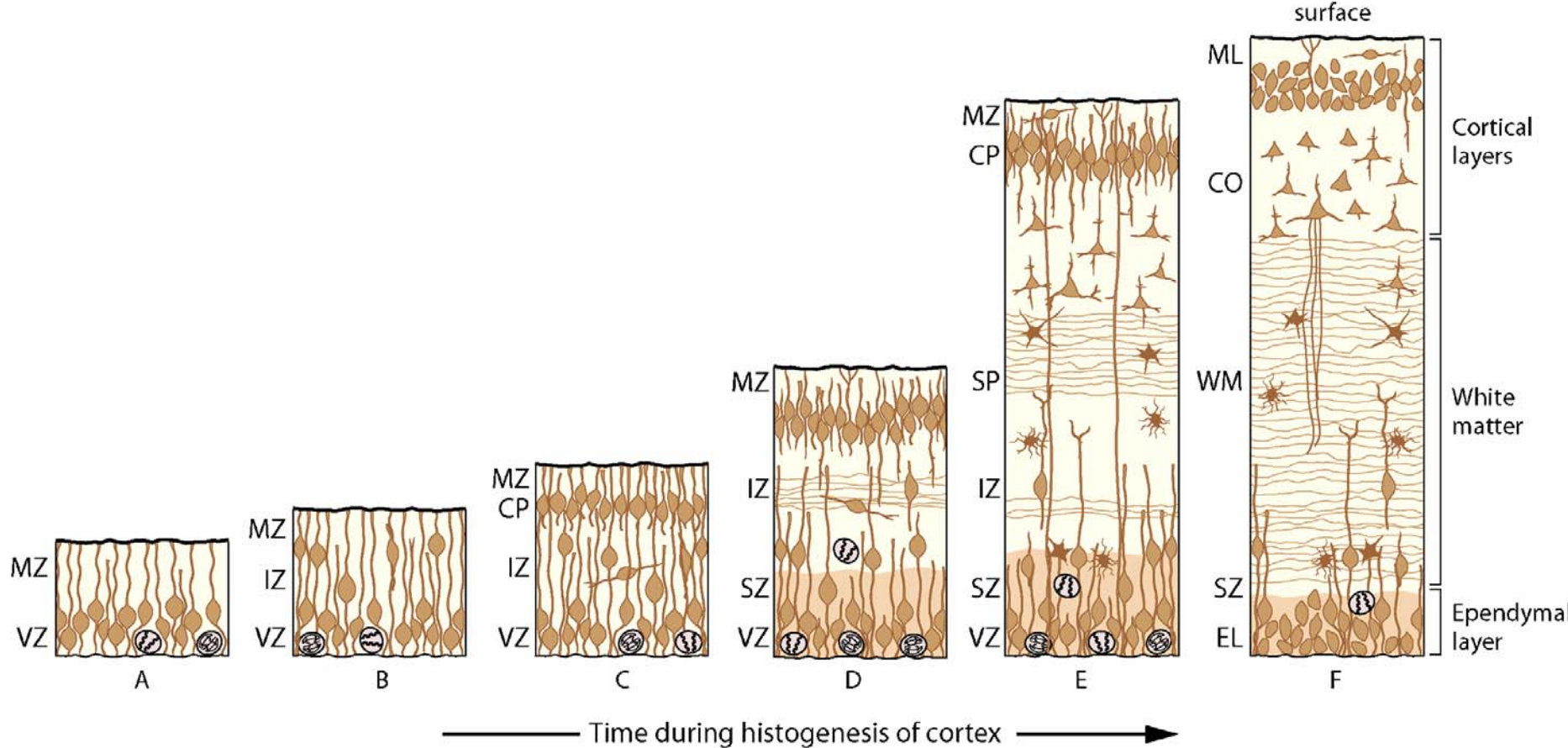
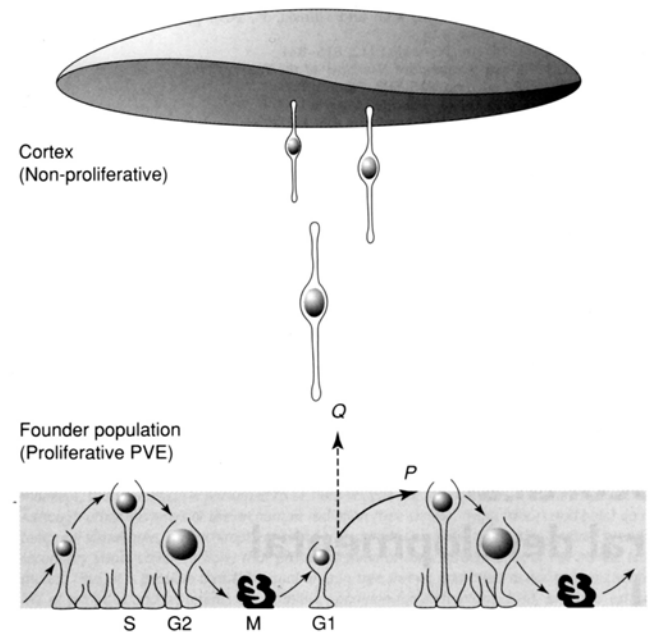
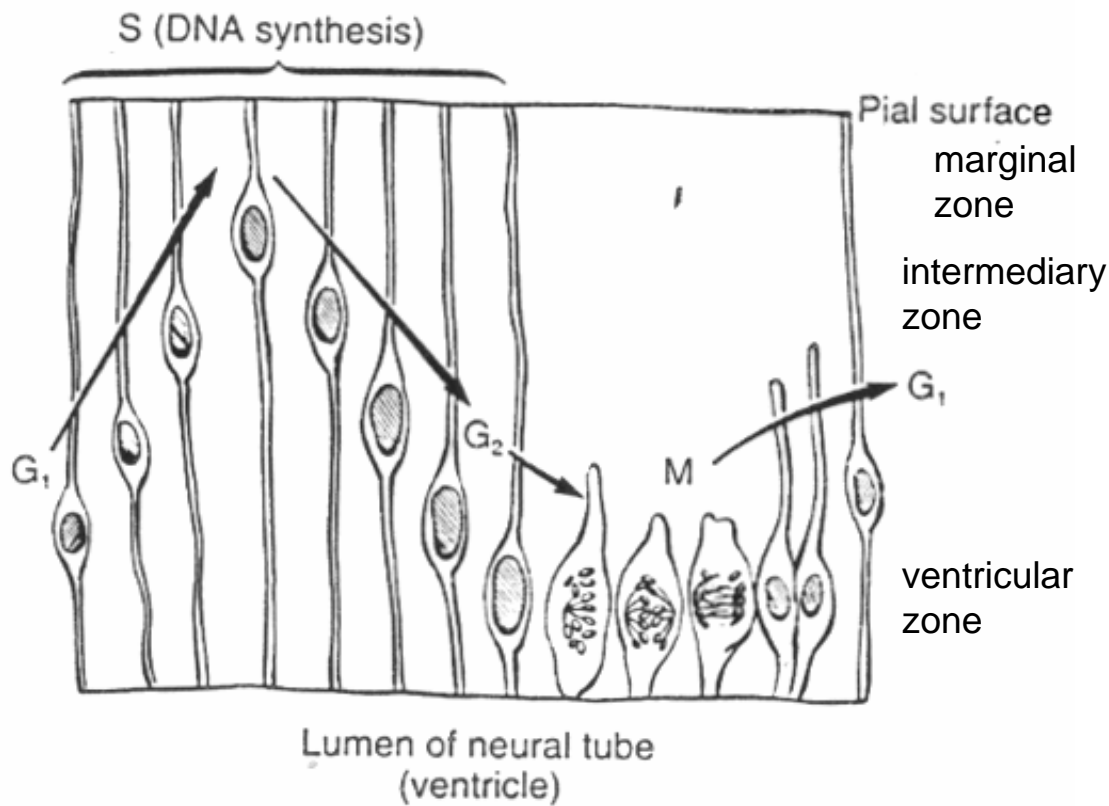


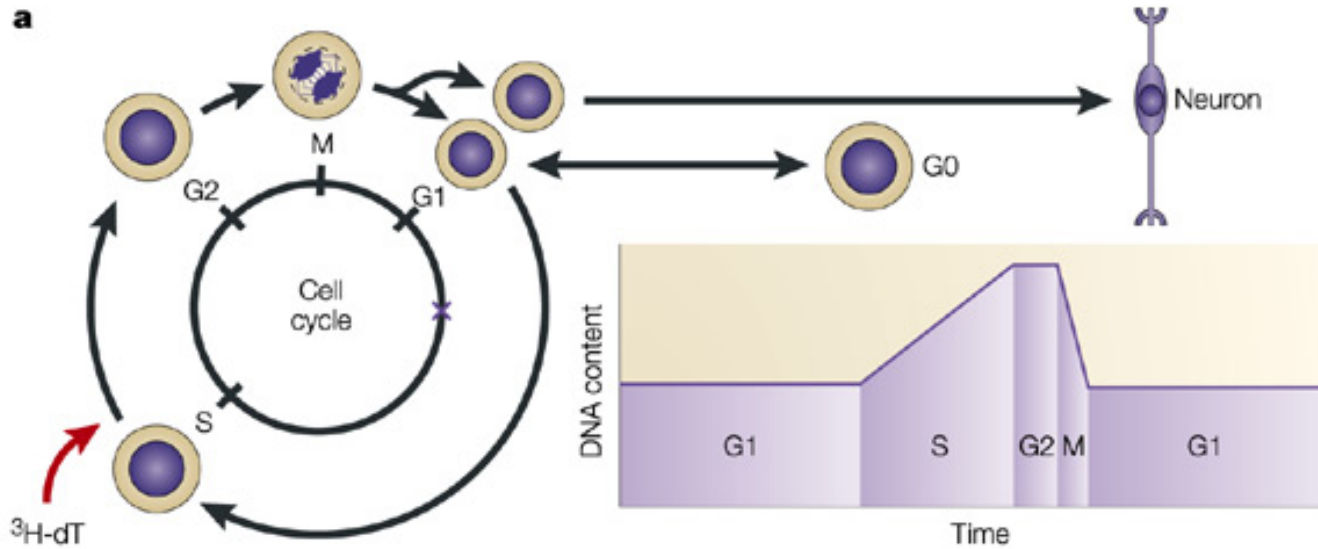
**CORTEX**



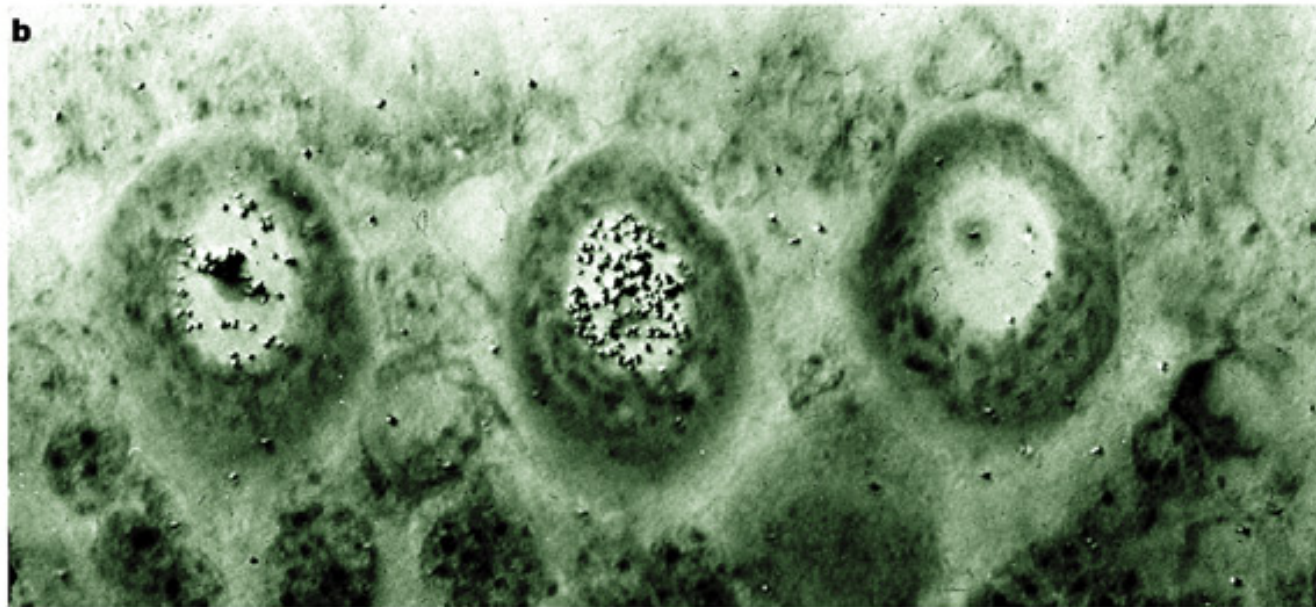
Developing wall of the telencephalic vesicle (A,B). Early stages of neural tube development, showing the ventricular zone (VZ) and marginal zone (MZ). In most brain vesicles and the spinal cord, differentiating neurons accumulate in the intermediate zone (IZ). In the telencephalic vesicle, neurons destined for cerebral cortex migrate through the intermediate zone and accumulate in the cortical plate (CP) and the subplate (SP) a transient layer of neurons that serve as temporary synaptic targets for cortical afferents (D-F). These plates form layers 2 through 6 of the cortex. The subventricular zone (SZ) is a secondary germinal zone that gives rise to interneurons and glia; WM=white matter; CO=layers 2-6; ML=stratum moleculare (after Sidman and Rakic)

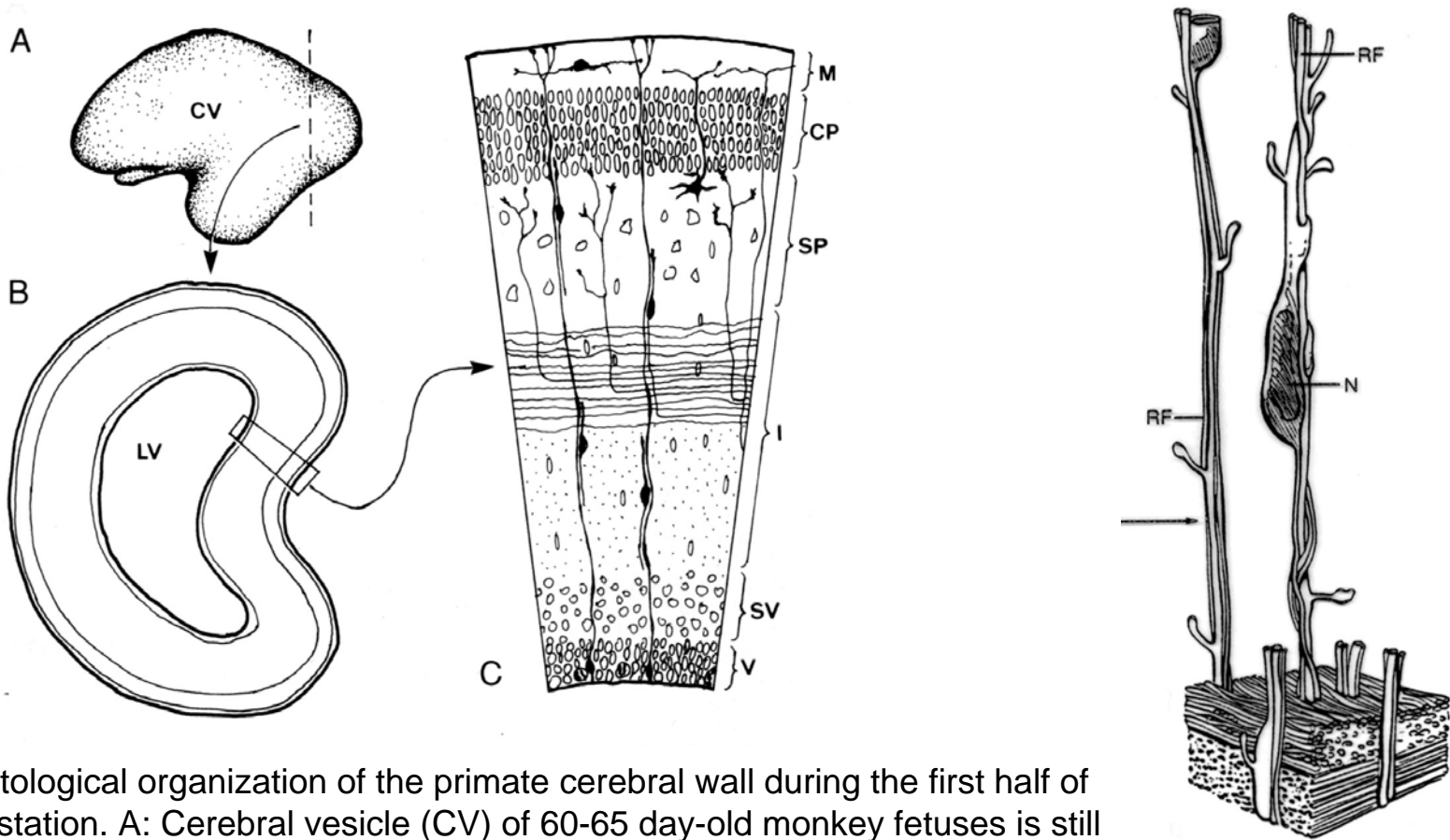


**Cell proliferation in the neuroepithelium of the recently closed neural tube.** The wall of the neural tube is composed entirely of proliferating neuroepithelial cells at this stage and appears as a pseudostratified epithelium in histologic sections. This effect is created by interkinetic nuclear migrations occurring during G1 to S (DNA synthesis), and G2 phases of the cell cycle. During mitosis (M), the cells retract their distal processes, become rounded, and divide next to the lumen of the ventricle. (From Cohen). A fraction of the cells becomes postmitotic permanently (Q) and a fraction continues to cycle (P). The cells of the Q fraction migrate to an ever-expanding cortex in which they differentiate and grow or might be eliminated by histogenetic cell death (Caviness et al., 1995)



Incorporation of  $^3\text{H}$ -thymidin as a marker of cell division. (a) DNA synthesis during different phases of cell cycle (G1, G2 gap phases, M-mitotic division; S=synthesis phase.  $^3\text{H-T}$  is readily incorporate into DNA during the S-phase. Intensive radiolabeling indicates the time of the neuron's birthday. In cases in which the cell has not divided, the cell is not labeled. (b) Purkinje cells in the middle and on the left are heavily labeled, whereas the neuron on the right can be interpreted as not divided (Rakic, 2002).





Cytological organization of the primate cerebral wall during the first half of gestation. A: Cerebral vesicle (CV) of 60-65 day-old monkey fetuses is still smooth and lacks convolutions. B coronal section across the occipital lobe at level indicated by a vertical broken line in (A). C: A block of tissue dissected from the upper bank of calcarine fissure. At this early stage six embryonic layers can be recognized: ventricular zone (V), subventricular (SV), intermediate zone (I), subplate (SP), cortical plate (CP) and marginal zone (M). Note the presence of spindle-shaped migrating neurons moving along radial glia fibers, which span the full thickness of the cortex. Afferents from the brainstem, thalamus and other cortical areas accumulate in the SP where they make transient synapses before entering the cortical plate. LV=lateral ventricle (Rakic, 1995).

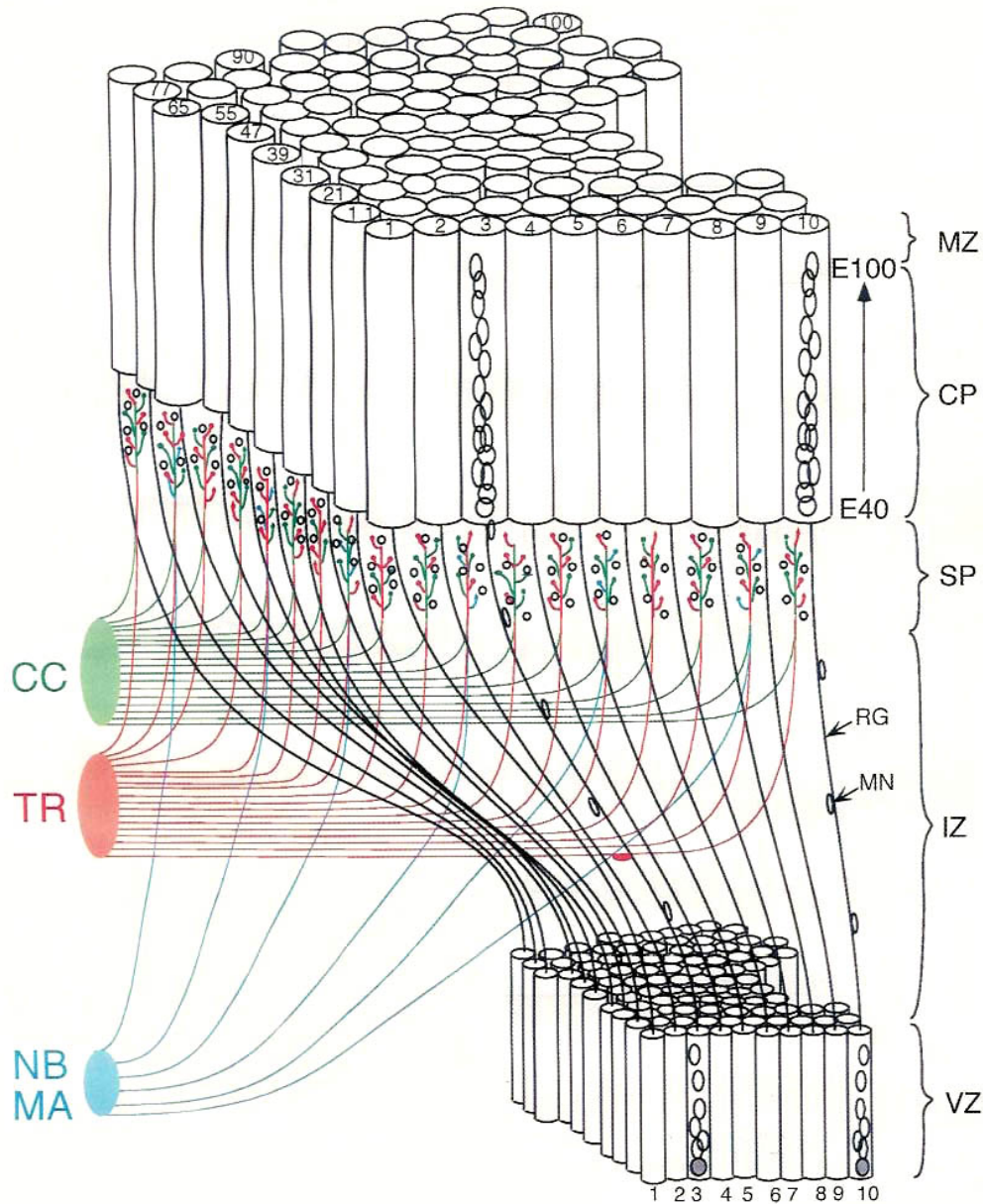
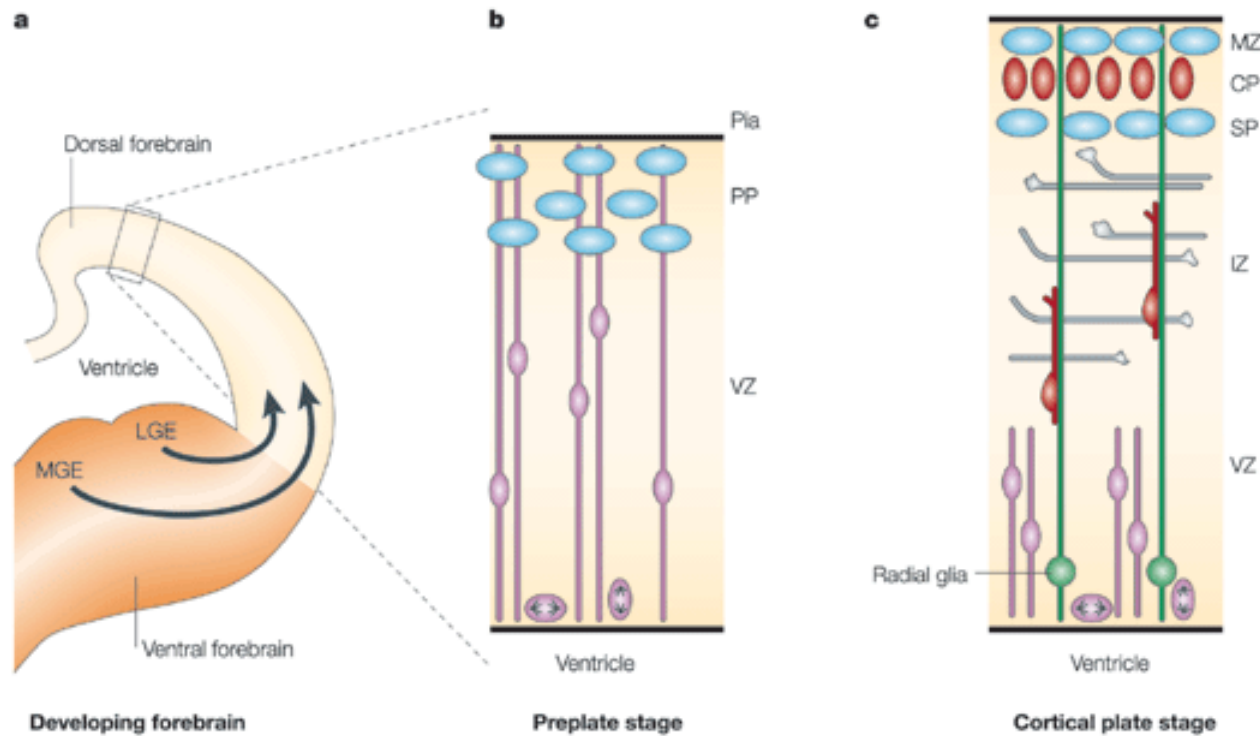
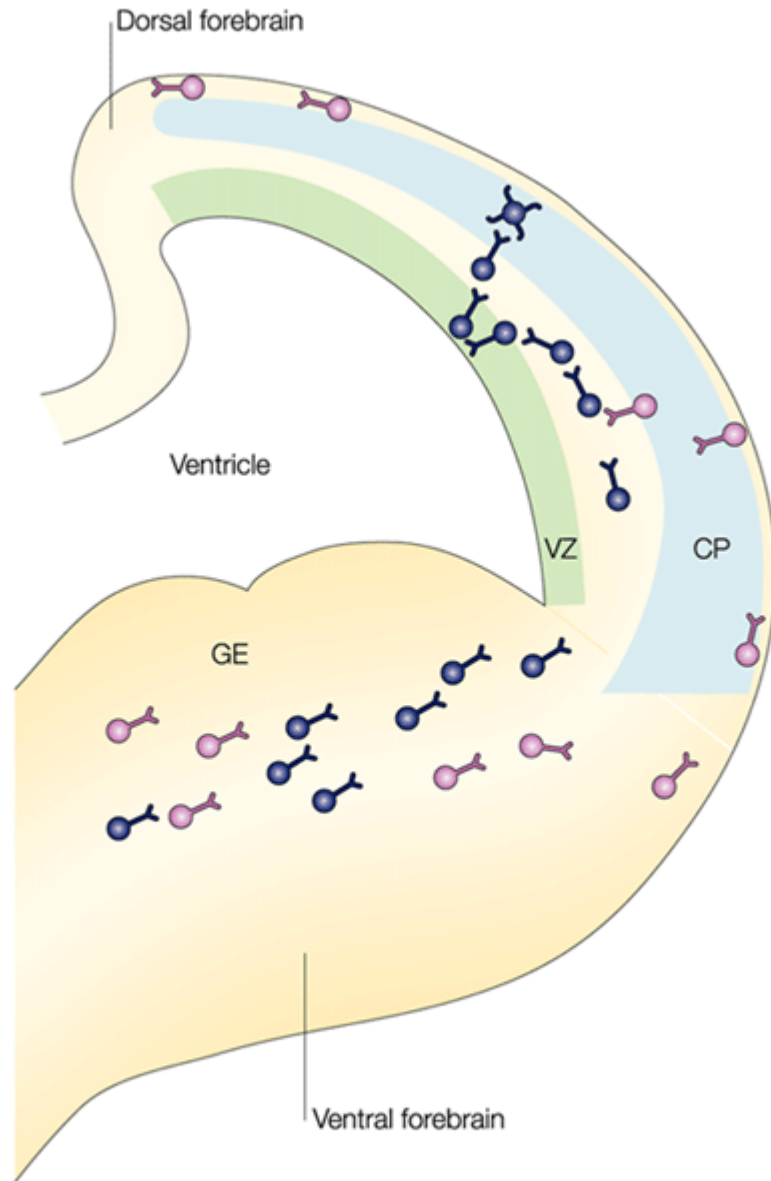


Diagram of the radial unit hypothesis. Radial glial cells (RG) in the ventricular zone (VZ) project their processes in an orderly map through the various cortical layers, thus maintaining the organizational structure specified in the ventricular layer. After their last division, cohort of migrating neurons (MN) first traverse the intermediate zone (IZ) and then the subplate zone (SP) where they have an opportunity to interact with 'waiting' afferents that arrive sequentially from the nucleus basalis (NB), monoaminergic axons (MA), from the thalamic radiation (TR) and the contralateral cortex (CC). After newly generated neurons bypass the earlier generated ones that are situated in the deep cortical layers, they settle at the interface between the developing cortical plate (CP) and the marginal zone (MZ), and eventually, form a radial stack of cells that share a common site of origin but are generated at different times. (Rakic, 1995)

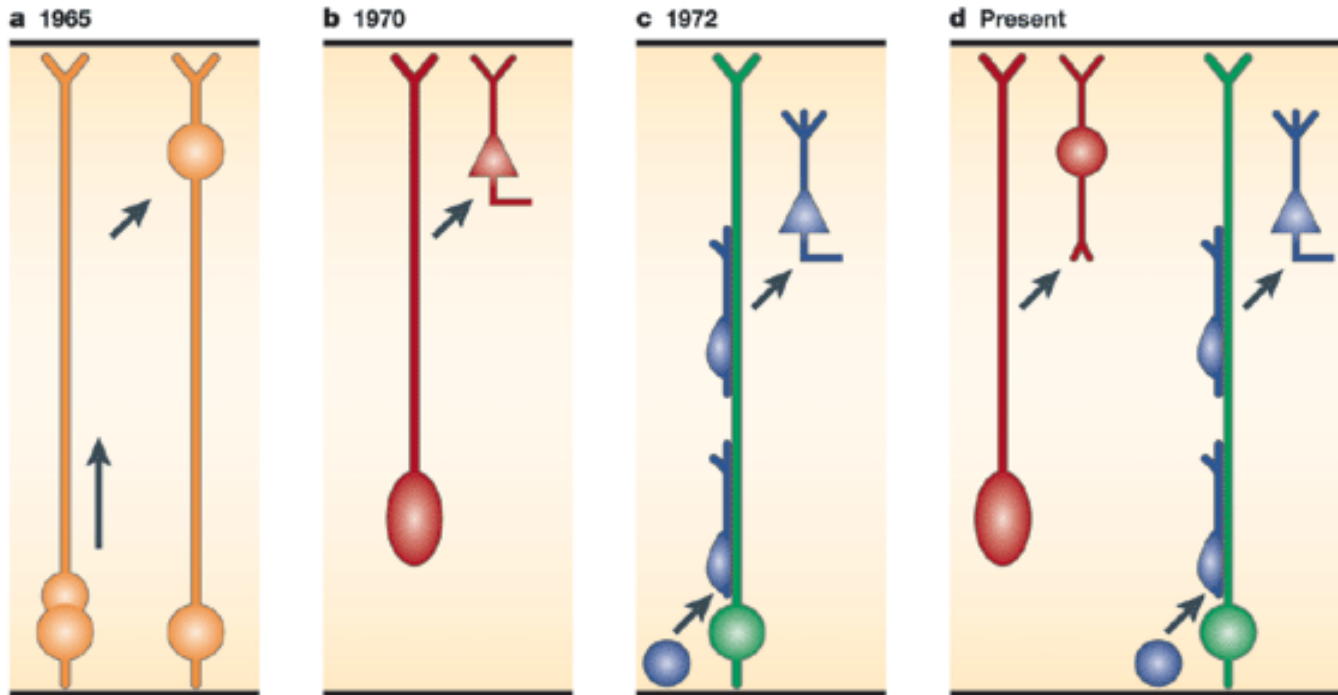


Nature Reviews | Neuroscience

Schematic diagram of a section through the developing rodent forebrain. The lateral and medial ganglionic eminence (MGE, LGE) of the ventral forebrain generate the neurons of the basal ganglia and the cortical interneurons, the latter follow tangential routes to the cortex (arrows). In the dorsal forebrain (boxed are in a) migration begins when the first cohort of postmitotic neurons moves out of the ventricular zone (VZ) to form the preplate (PP). Subsequent cohorts of neurons (pyramidal cells) migrate aided by radial gli, through the intermediate zone (IZ) to split the PP into outer marginal zone (MZ) and inner subplate (SP). CP=cortical plate. (Nadarajah and Parnavelas, 2002).

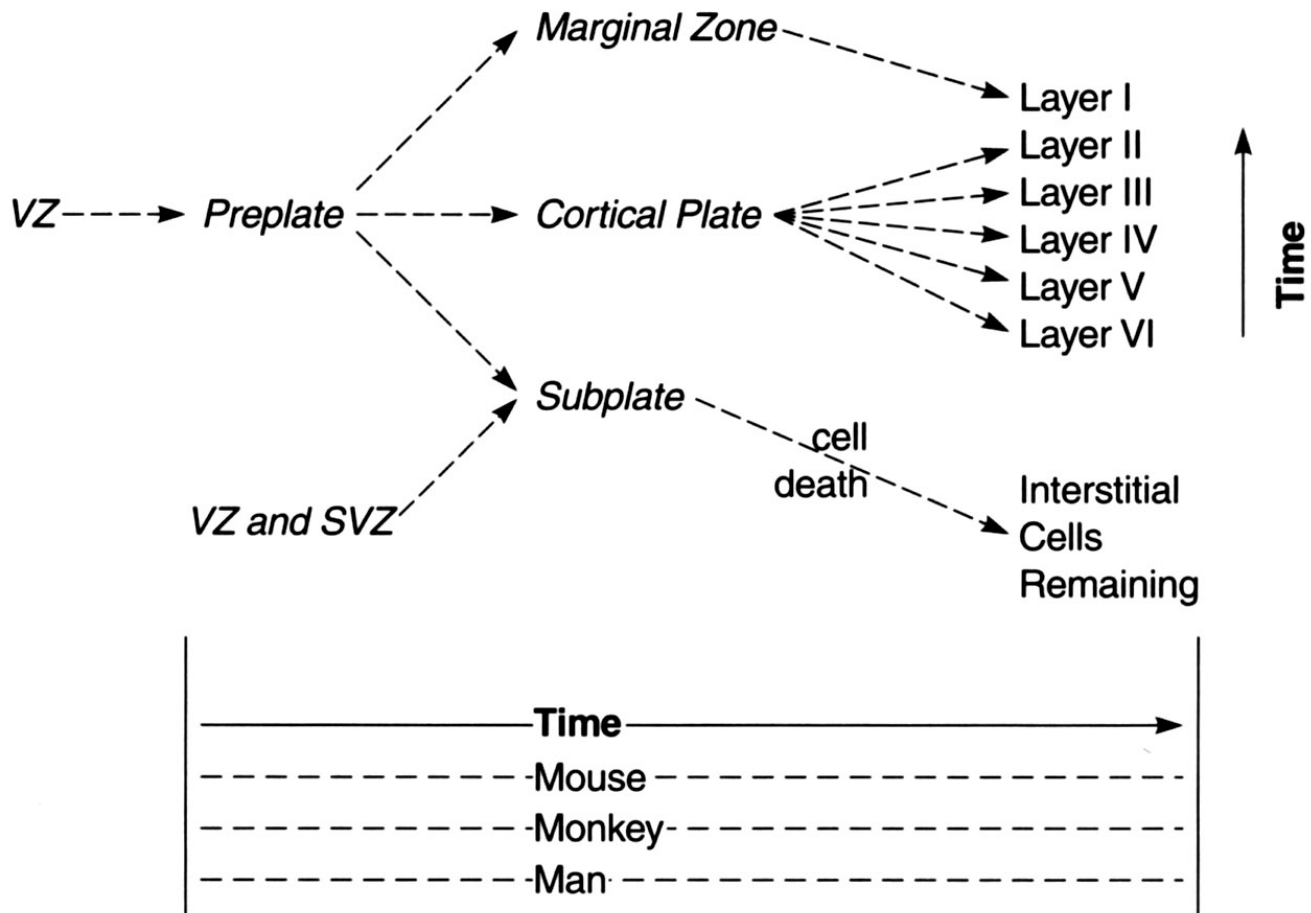


Movement of cortical interneurons in the developing cerebral cortex. Interneurons that arise in the ganglionic eminence (GE) migrate into the neocortex through the intermediate zone (blue cells) and through the marginal zone (pink cells). A subset of interneurons (blue cells) that migrate through the intermediate zone are attracted to the ventricular zone by chemoattractants that are secreted in the ventricular zone (VZ). These interneurons might receive positional information in the VZ that is required for their subsequent migration to the correct layers of the developing cortex (Nadarajah and Parnavelas, 2002).

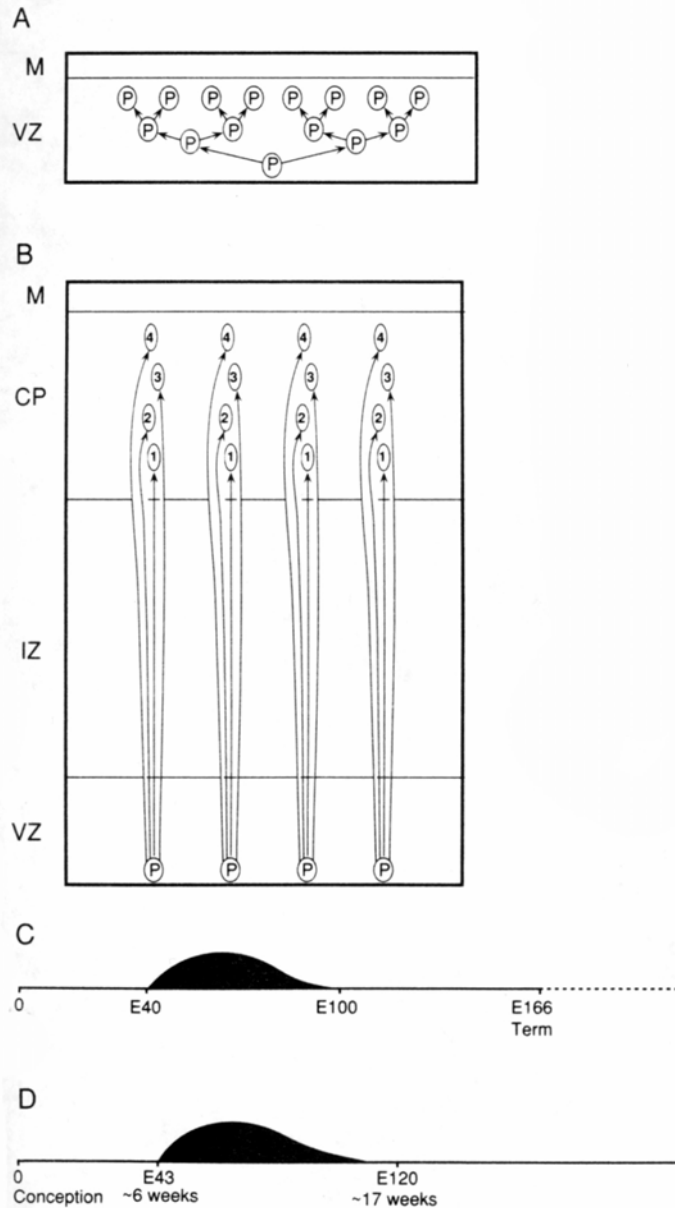


Nature Reviews | Neuroscience

Models of cortical neuronal migration. Berry and Rogers suggested that after cell division, the nucleus of one daughter cell moves towards the cortical plate through the long radial processes, while the other cell remains in the ventricular zone (a). In a similar model, Morest suggested that young neuroblasts lose their ventricular attachments and translocate their somata through radially oriented processes that terminate at the pial surface (b). Subsequently, Rakic proposed that young postmitotic neurons use radially oriented glial fibers as a scaffold to reach their positions in the cortical plate (c). Evidence now indicates that somal translocation is the predominant mode of movement during early corticogenesis, whereas glia-guided migration is more prevalent at later stages, when the cerebral wall is considerably thicker (Parnavelas, 2002).

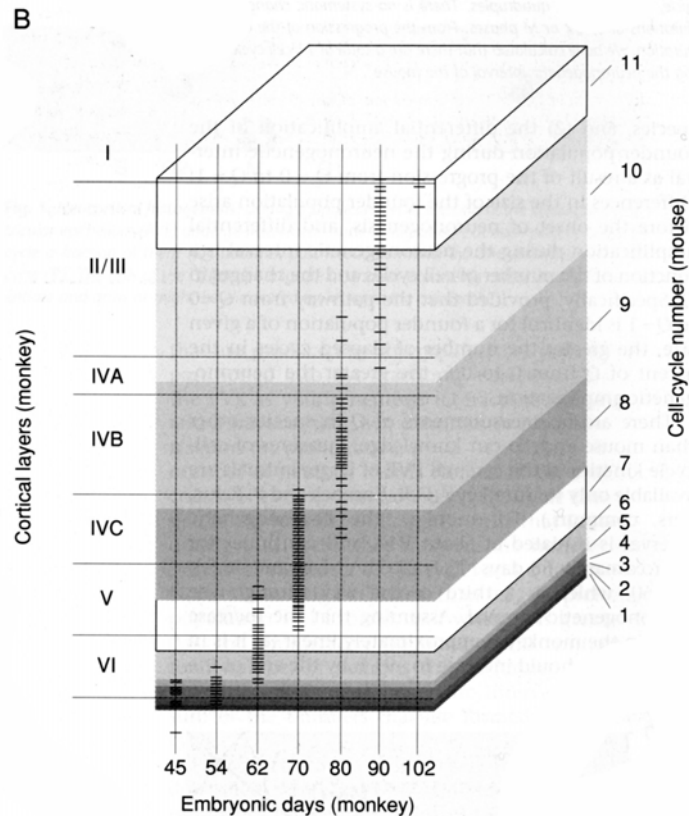
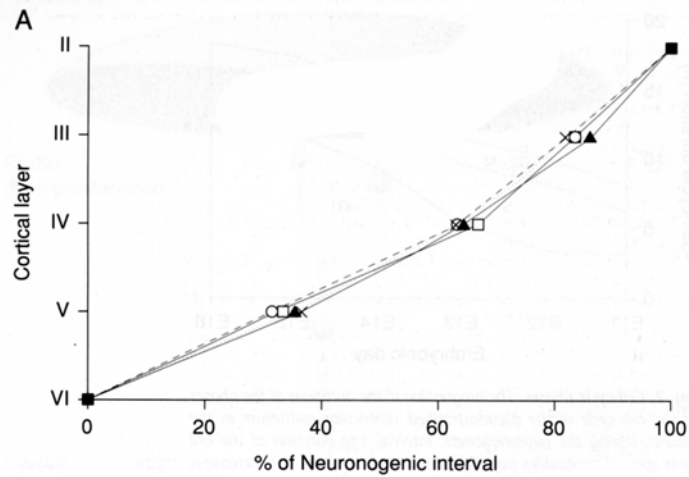


Schema of processes in generation of the neocortex (Mountcastle, 1998)

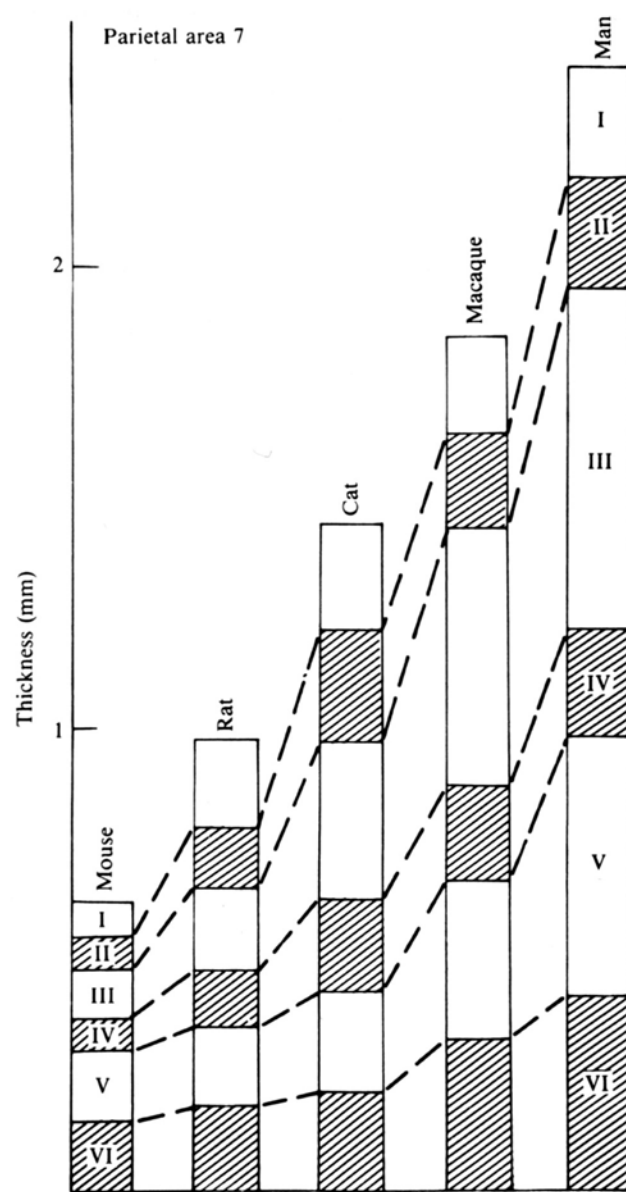
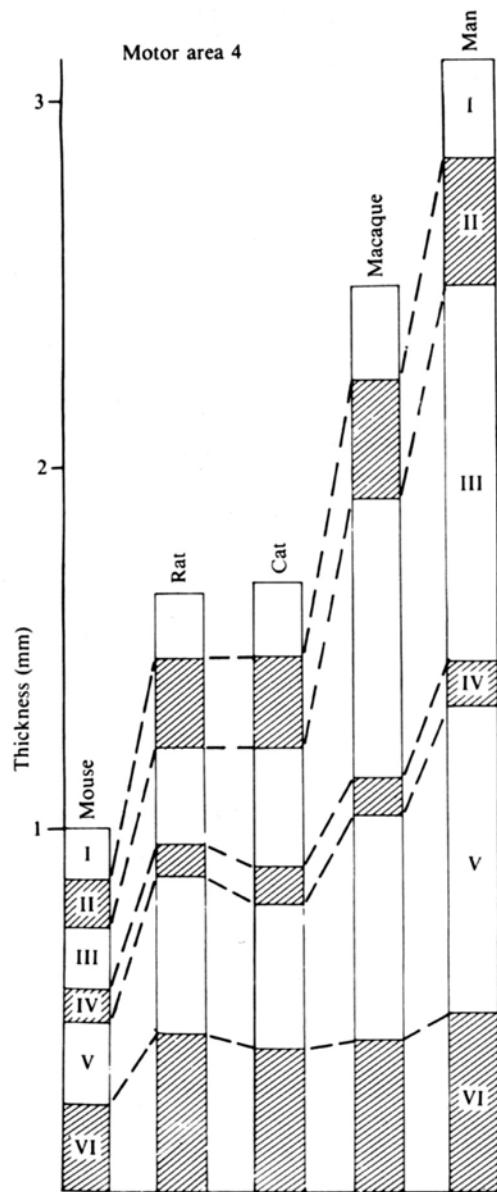


The relationships of modes of cell division to duration of corticogenesis. A: Schematic model of symmetrical cell division that predominate before the 40<sup>th</sup> embryonic day (E40). At this early embryonic age, the cerebral wall consists of only the ventricular zone (VZ), where cell proliferate, and the marginal zone (M) where some of them extend their radial processes. Symmetric division produces two progenitors (P) during each cycle, and causes rapid horizontal lateral spread. B: model of asymmetrical division that becomes predominant in the monkey after E40. During each asymmetrical division, a progenitor (P) produces one postmitotic neuron that leaves the ventricular zone, and another progenitor that remains within the proliferative zone and continues to divide. Postmitotic cells migrate rapidly across the intermediate zone (IZ) and become arranged vertically in the cortical plate (CP) in reverse order of their arrival (1-4). C: Diagrammatic representation of the time of neuron origin in macaque monkey. D: Estimate of the time of neuron origin in the human neocortex (Rakic, 1995).





Scaling of neurogenetic processes across species. A: The time of production of neurons for each layer of the cortex is compared in four different species, mouse (squares), rat (triangles), cat (circles) and monkey (crosses), as a function of the percentage of the neurogenetic interval in each species that has elapsed at the time the cortical layer is produced. B: The proportion of neurons generated at each of the 11 cell cycles in the neurogenetic interval of the mouse is shown as a volume that reflects the proportional contribution to a final cortical volume. An overlay of the schedule of neurogenesis of the successive layers of the monkey visual cortex, scaled to the mouse time base, illustrates the commonality of scaling of the time of origin, number and laminar positions of neurons generated in the two species. (Caviness, Takahashi, Nowakowski, 1995).



Comparison of total cortical thickness and thickness of each cortical layers in area 4 (left) and 7 (right) of mouse, rat, cat, macaque monkey and man. The total number of cells is virtually the same in the vertical dimension of the cortex, except for primate area 17 (Mountcastle, 1998)

*Table 4-2.* Number of neurons beneath pial patches ( $25 \times 30 \mu\text{m}$ ) in several areas of the cerebral cortex in five mammals.

Mammal	Translaminar cell count ( $\pm$ SD)						Means
	Motor	Sensory	Frontal	Temporal	Parietal	Visual	
Mouse	73.4 $\pm$ 4.5	75.2 $\pm$ 4.6	74.5 $\pm$ 6.8	74.3 $\pm$ 4.4	70.4 $\pm$ 6.8	75.4 $\pm$ 4.30	73.8 $\pm$ 4.6
Rat	72.7 $\pm$ 3.9	71.9 $\pm$ 6.8	70.1 $\pm$ 6.8	72.4 $\pm$ 6.2	70.7 $\pm$ 4.6	72.4 $\pm$ 5.3	71.6 $\pm$ 4.9
Cat	69.8 $\pm$ 5.1	71.6 $\pm$ 6.8	72.6 $\pm$ 4.2	76.5 $\pm$ 4.9	74.3 $\pm$ 6.7	73.8 $\pm$ 6.7	73.6 $\pm$ 4.9
Monkey	74.1 $\pm$ 6.3	73.5 $\pm$ 6.3	75.3 $\pm$ 7.5	73.8 $\pm$ 6.9	77.0 $\pm$ 6.7	180.0 $\pm$ 9.2	—
Man	68.7 $\pm$ 6.5	69.7 $\pm$ 3.9	69.4 $\pm$ 5.8	72.4 $\pm$ 5.0	70.0 $\pm$ 8.4	174.0 $\pm$ 10.6	—

*Note:* Numbers transformed from original counts of Rockel et al. (1974) to account for section shrinkage. Patches of area  $25 \times 30 \mu\text{m} = 750 \mu\text{m}^2$  were noted to display linear shrinkage of 18 percent. Original size of the patches was therefore  $25/.82 \times 30/.82 = 1,116 \mu\text{m}^2$ . A conversion factor of  $750/1,116 = 0.672$  was therefore multiplied by the original counts.

Golgi stain

Nissl stain

Weigert stain

I. Molecular layer

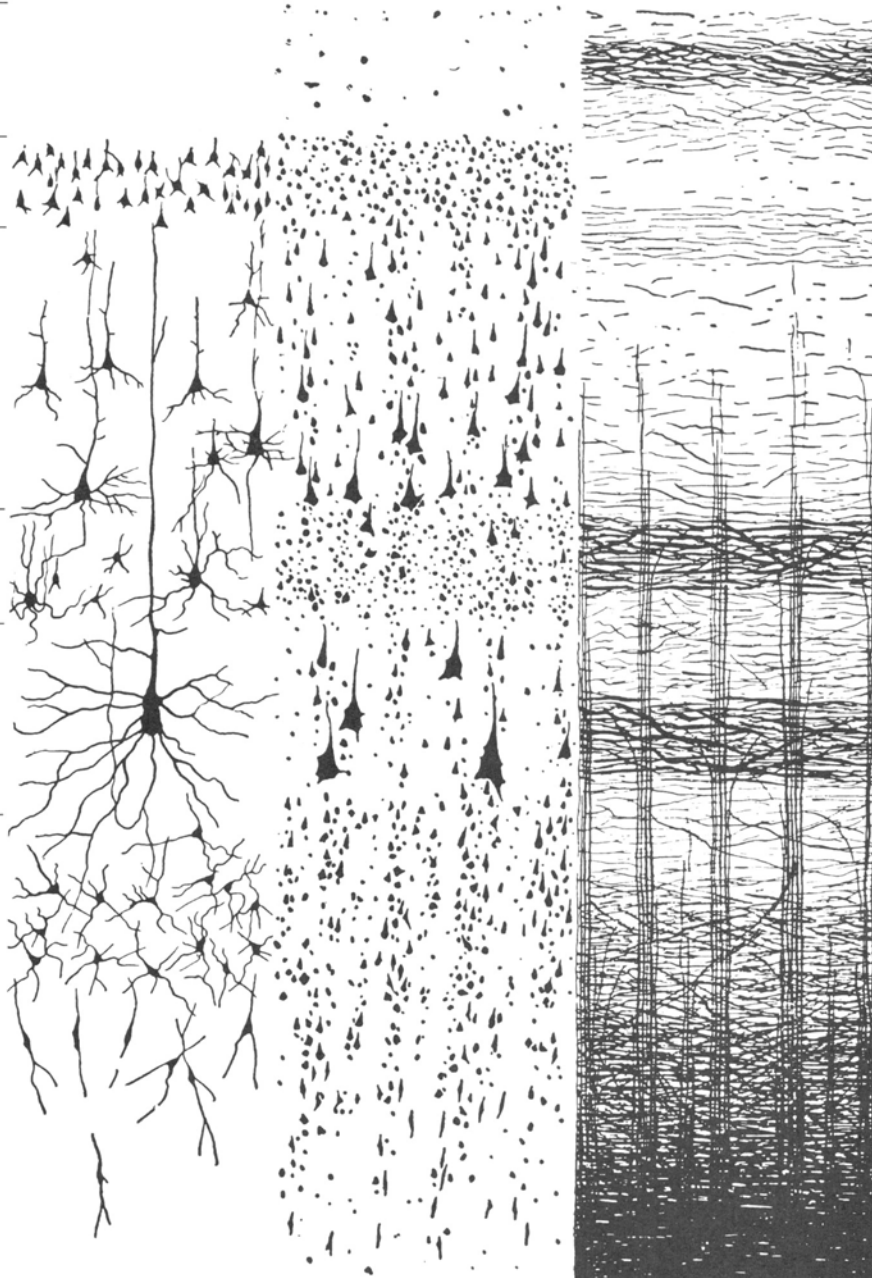
II. External granular layer

III. External pyramidal layer

IV. Internal granular layer

V. Internal pyramidal layer

VI. Multiform layer



Cross section of neocortex stained by three different methods. The Golgi stain reveals the complete axonal and dendritic arborizations of a small percentage of neurons. The Nissl method stains the cell bodies of all neurons showing their shape and packing densities. The Weigert method stains myelin, revealing horizontally and vertically oriented bands (Brodman, 1909; Nolte)

Outer band of Baillarger

Inner band of Baillarger

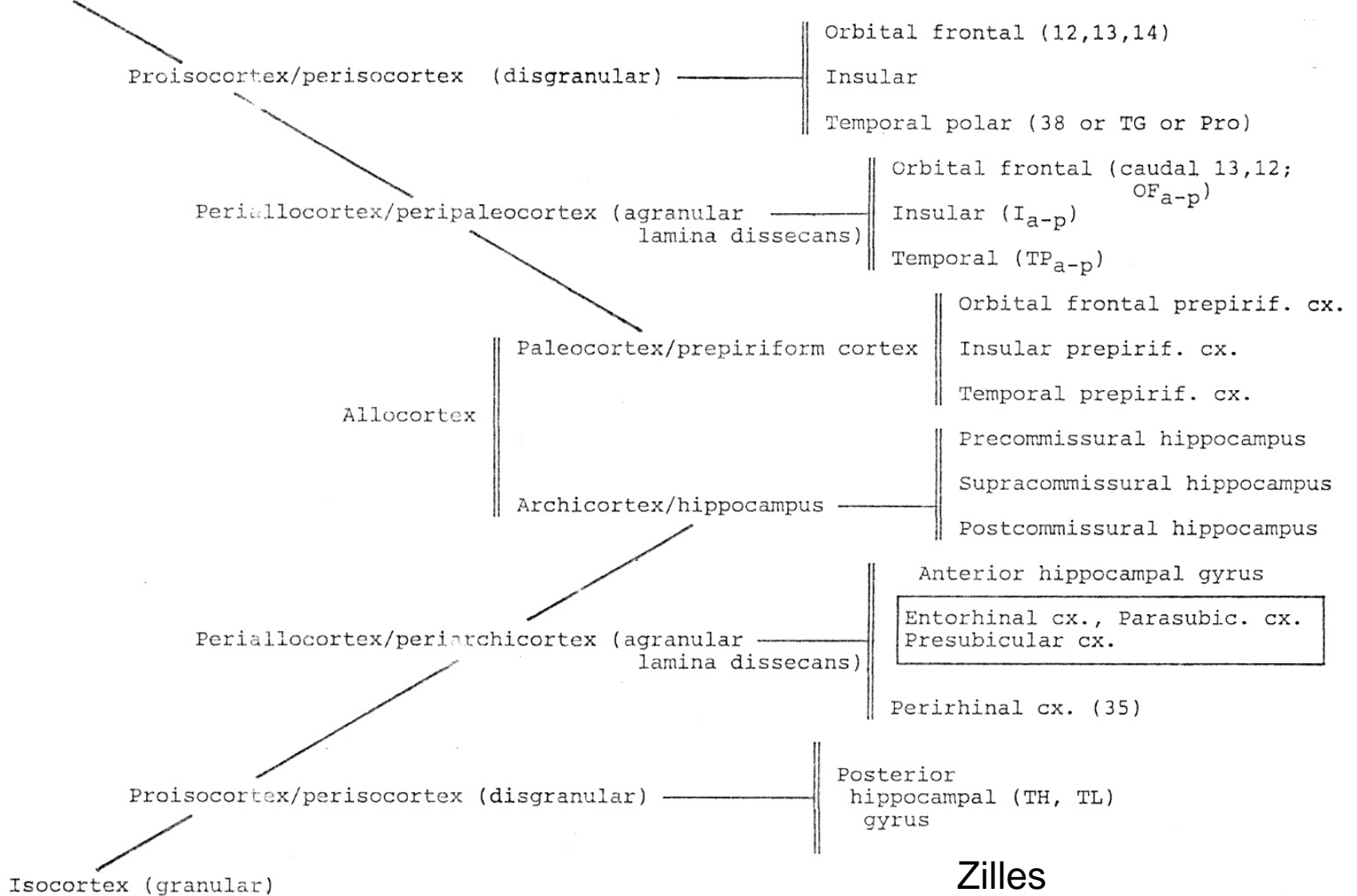
Cortical layers.

	AGRANULAR	DISGRANULAR	GRANULAR	
External stratum.	I. (molecular layer)			Supragranular
	II & III.			
Internal stratum	(lamina dissecans)			Granular
	V & VI.			Infragranular

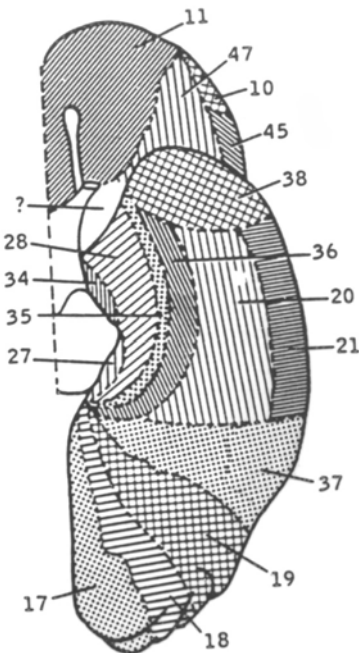
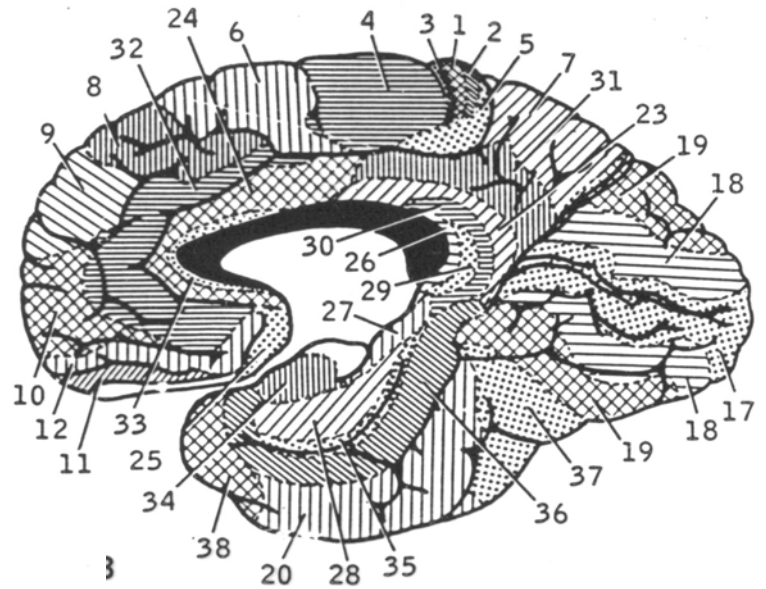
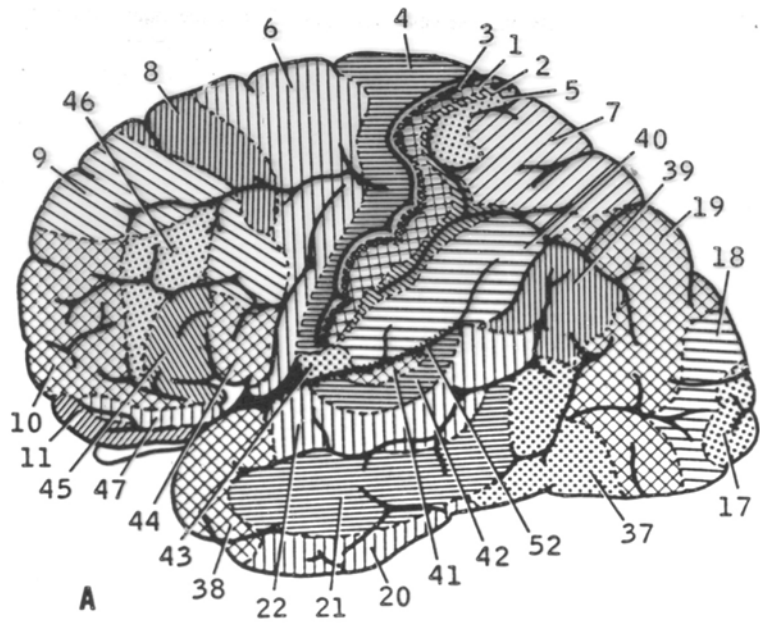
# SCHEME FOR DEVELOPMENT OF CORTICAL AREAS

Cortical radiation.

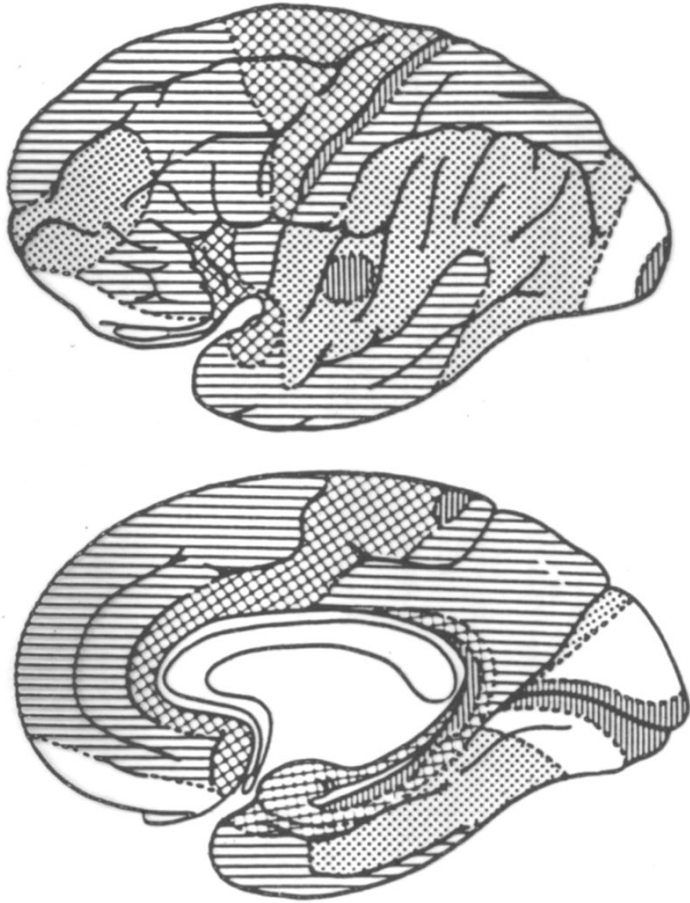
Isocortex (granular).



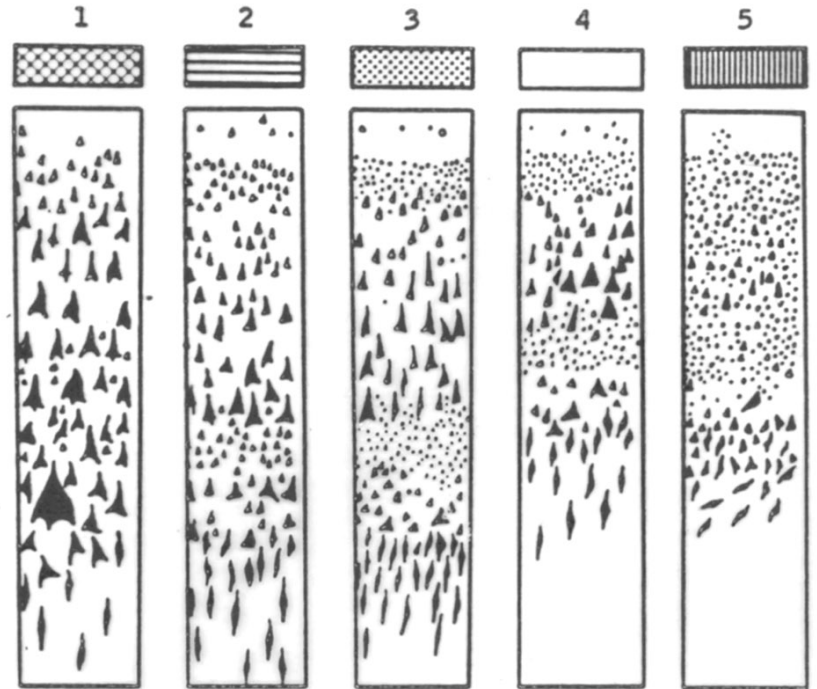
Zilles

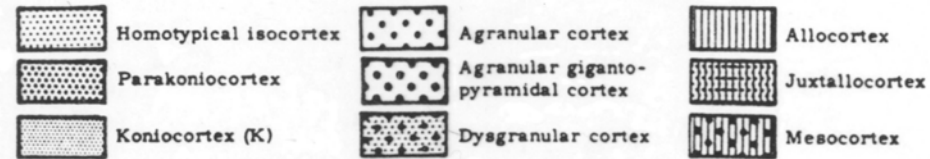
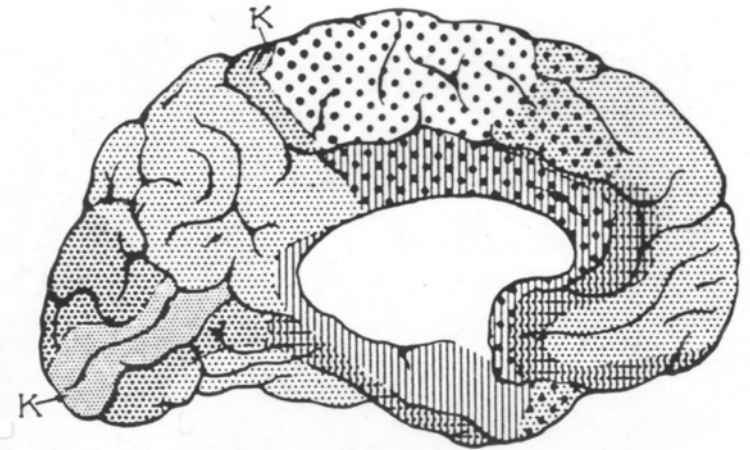
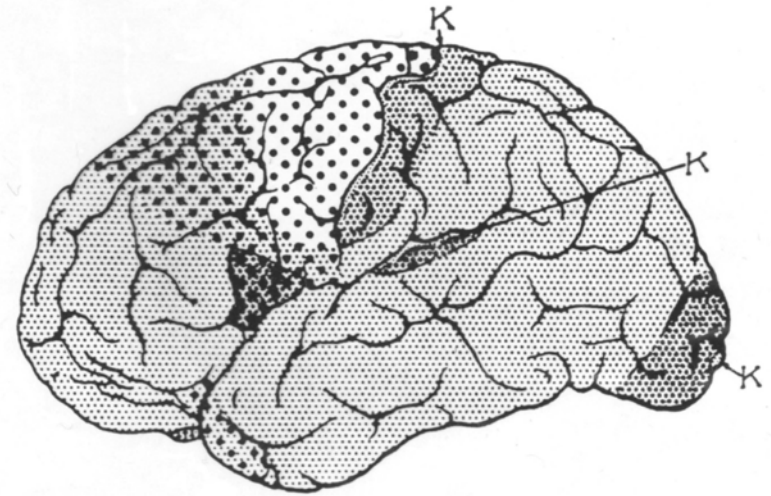
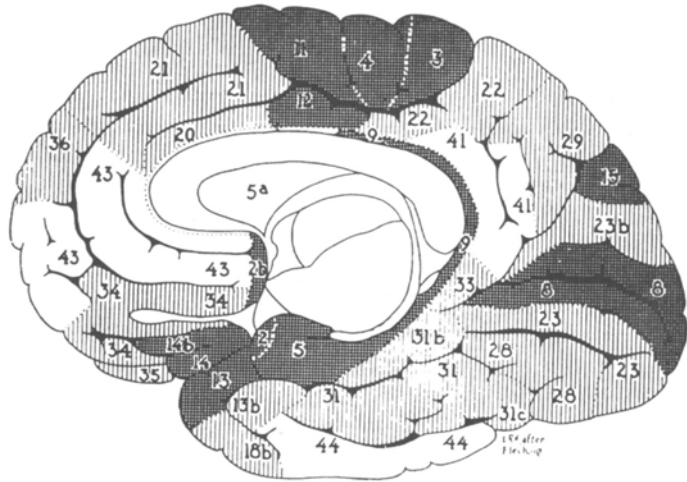
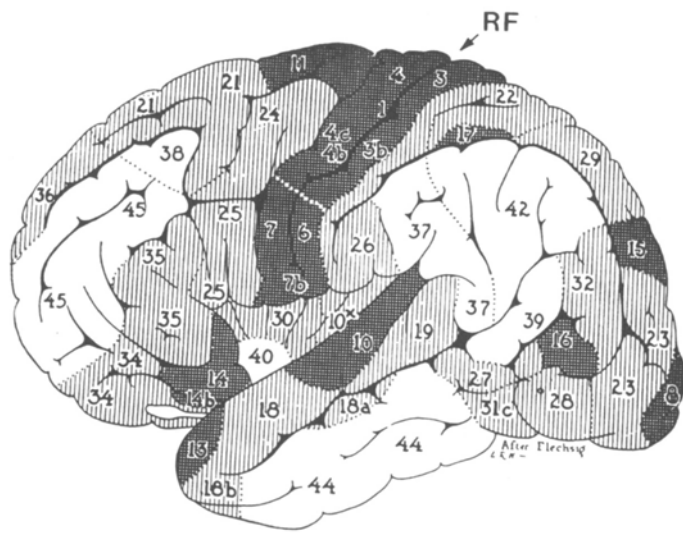


Cytoarchitectural zones of the human cerebral cortex, according to Brodmann.



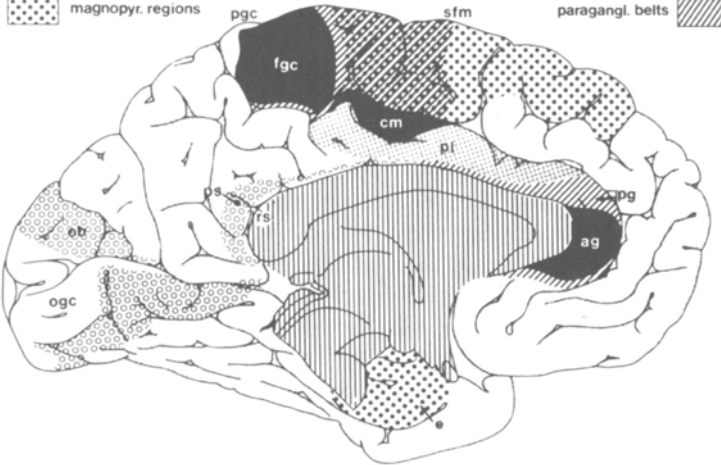
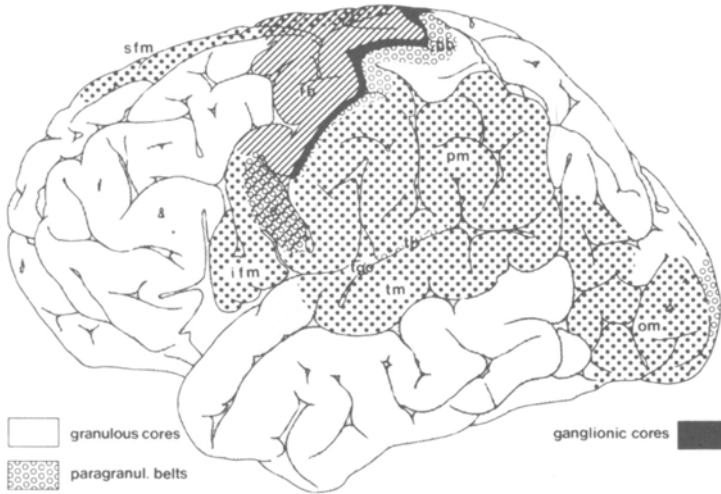
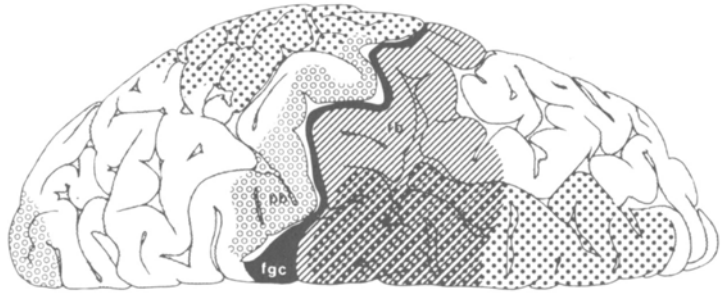
The five fundamental types of cerebral cortex, according to von Economo: 1, agranular; 2, frontal; 3, parietal; 4, polar; and 5, granular.





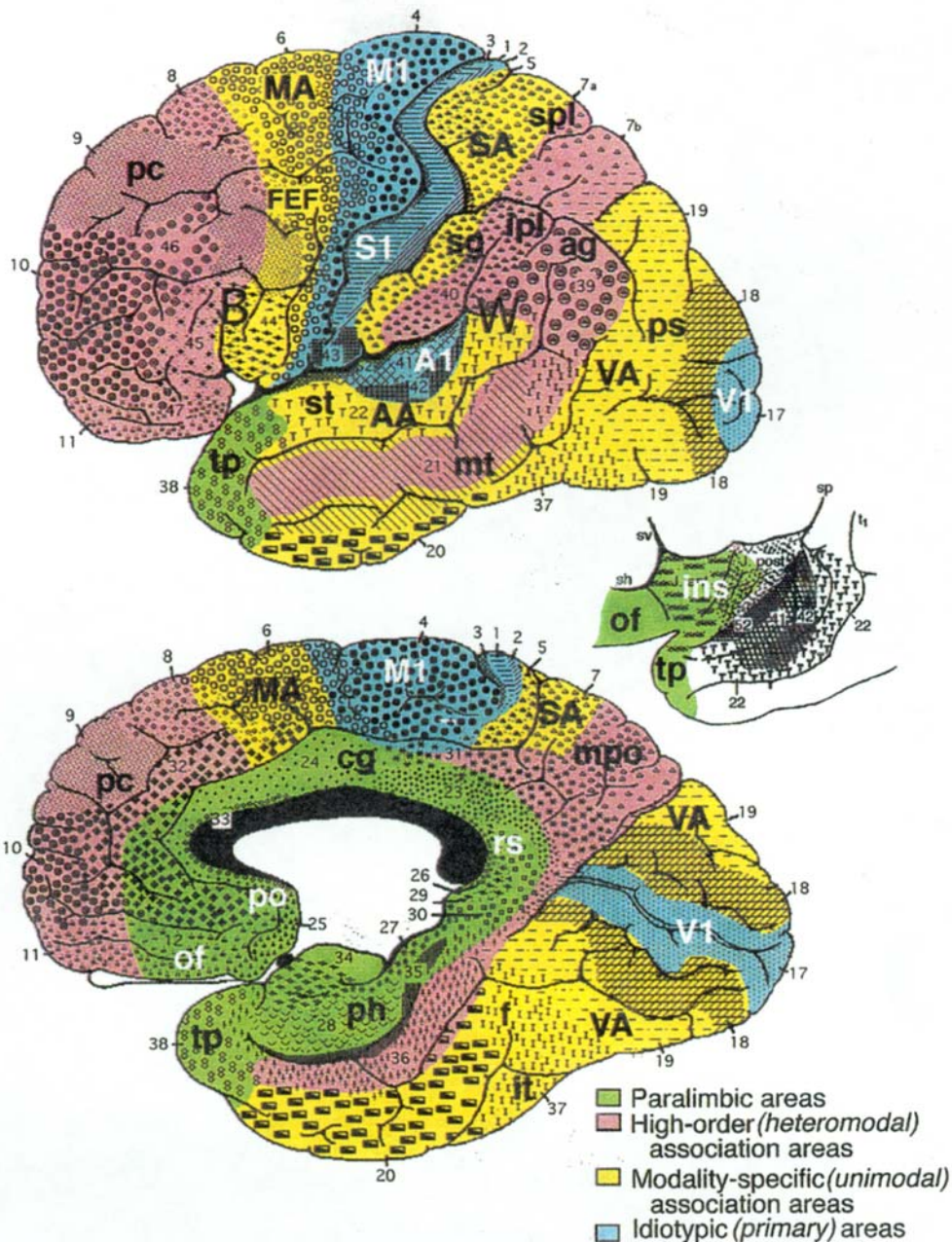
Flechsig's myeloarchitectural map (1920). Cortical fields are numbered in their order of myelination. Shaded zones with low numbers are those whose afferent and efferent fibers are myelinated earliest, unshaded areas with high numbers are myelinated later in ontogenesis and in the neonatal period.

Baily and von Bonin's cytoarchitectural map.

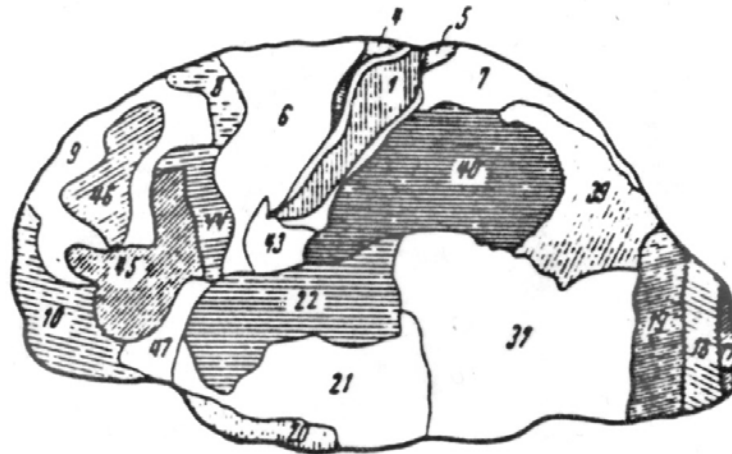
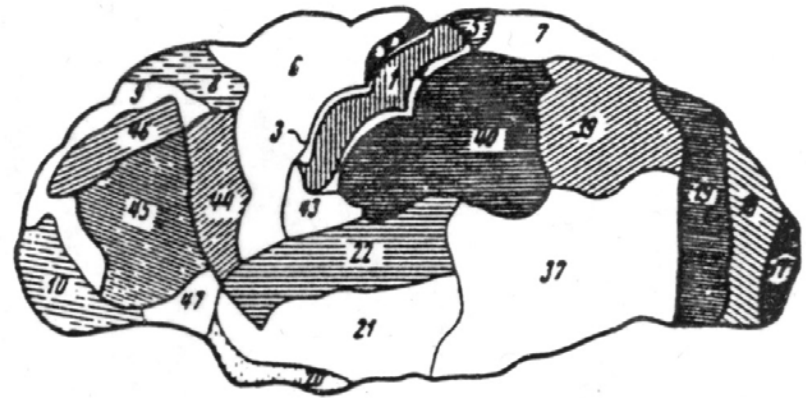
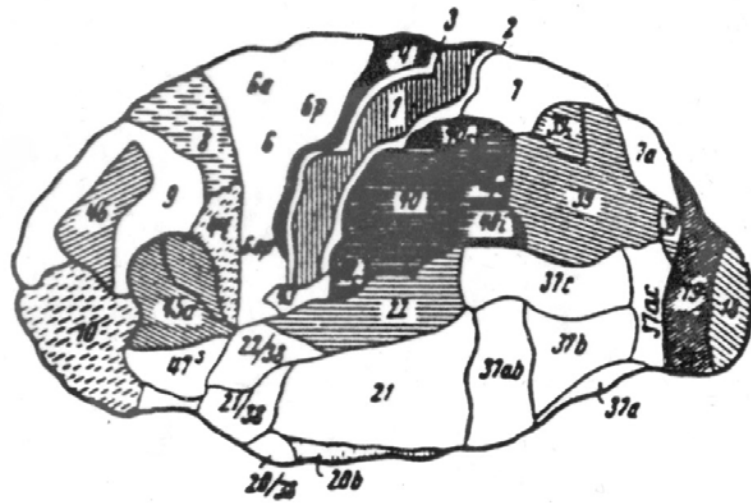


A map of the major regions of the human neocortex, prepared with the method of pigment staining (Braak, 1980).

# Distribution of functional zones in relationship to Brodmann's map of the human brain



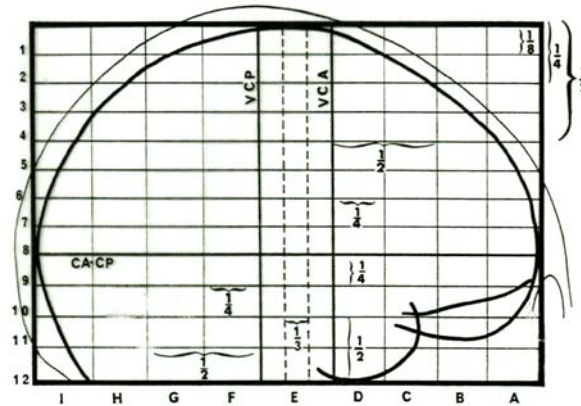
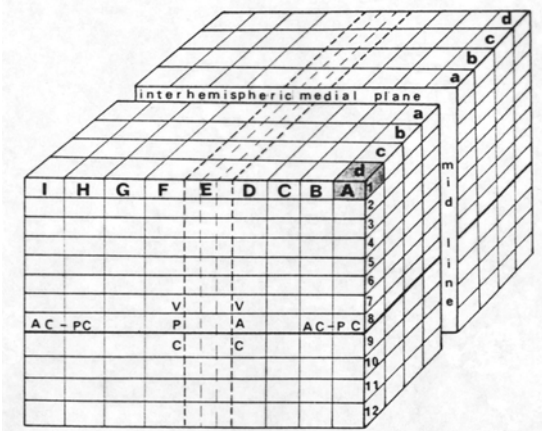
. Much of the information is based on experimental evidence obtained from animals and needs to be confirmed in humans. AA=auditory assoc. cortex; ag: angular gyrus; A1= primary auditory cortex; B: Broca's area; cg=cingulate cortex; f=fusiform gyrus; FEF=frontal eye fields; ins=insula; ipl=inferior parietal lobule; it=inferior temporal gyrus; MA=motor association cortex; mt-middle temporal gyrus; M1=primary motor cortex; of=orbitofrontal cortex; pc=prefrontal cortex; ph=parahippocampal region; po=parolfactory area; ps=peristriate cortex; rs=retrosplenial area; SA somatosensory association cortex; sg=supramarginal gyrus; spl=superior parietal lobule; st=superior temporal gyrus; S1=primary sensory cortex; tp=temporopolar; VA =visual association cortex; V1 primary visual cortex; W=wernicke's area



Cytoarchitectural maps of the human cortex and the variability of the individual regions (Sarkisov, 1960)

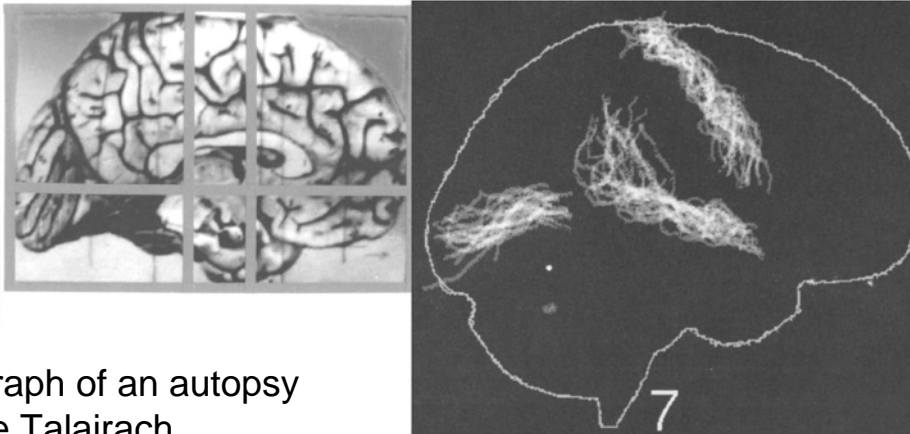
# Intersubject registration. Atlasing.

**A**



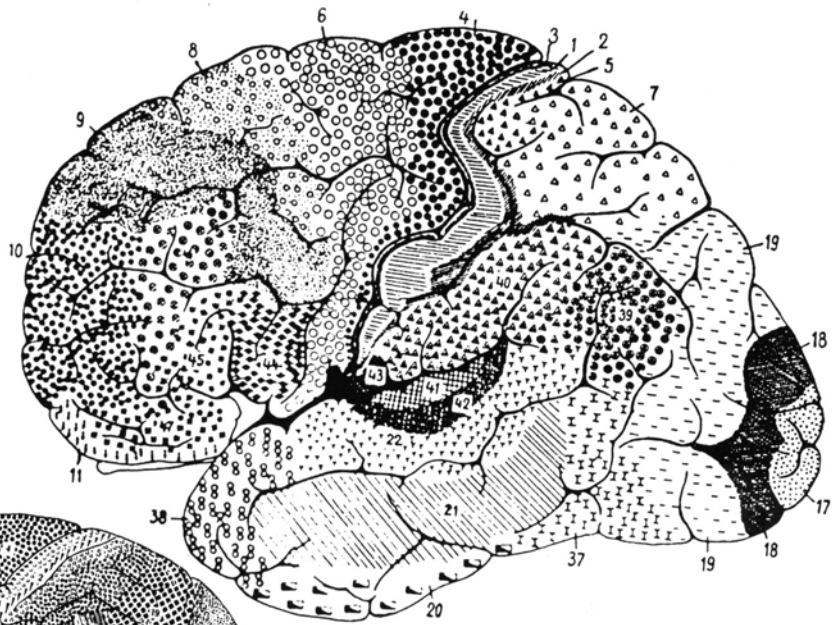
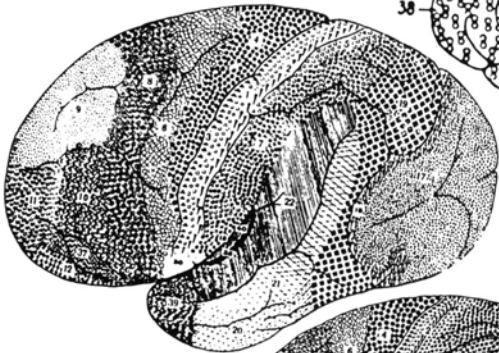
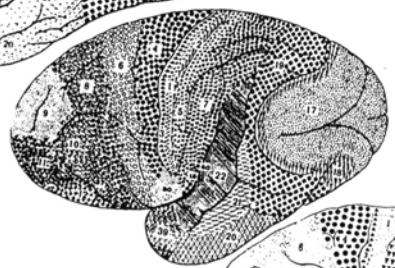
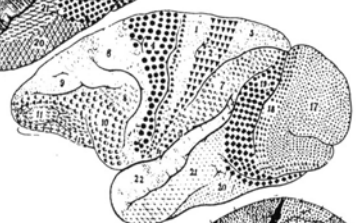
**A:** In the Talairach-Tournoux (1988) atlas the brain is divided into orthogonal parallelograms, the dimension of which vary with the principal axes of the brain. Each of these volumes is defined by a capital letter, a lower case letter and a number.

**B**

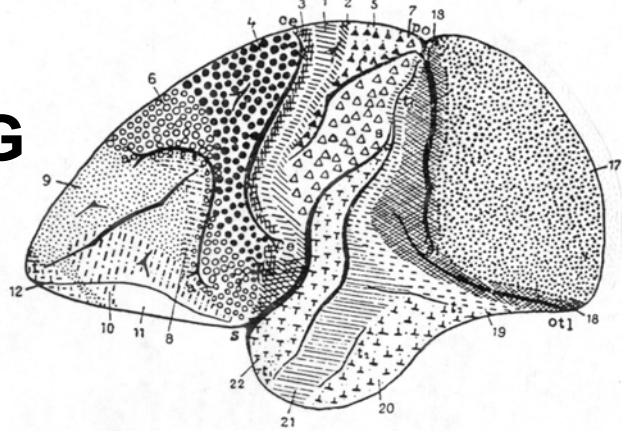
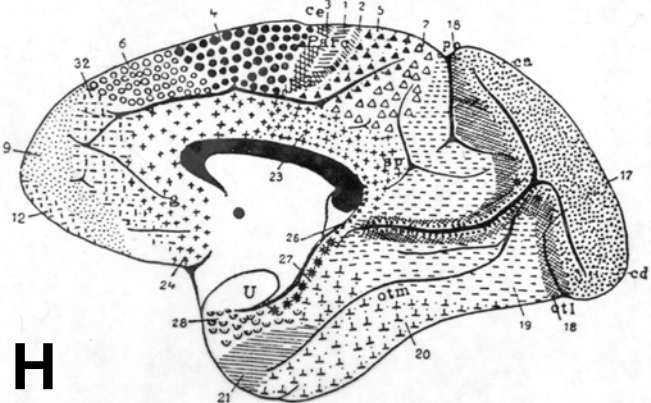


**B:** Photograph of an autopsy brain in the Talairach proportional grid system (Mai et al., 1997)

**C:** Three cortical landmarks (right calcarine sulcus, right precentral gyrus, and right superior temporal gyrus [STG] and its posterior extension) from 22 subjects have been mapped into a common frame of reference using a linear image registration algorithm incorporating 7 parameters. Note the marked variability of the posterior aspect of the STG (Woods, 1996).

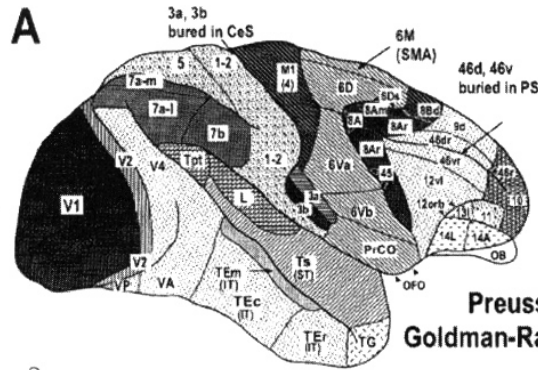
**A****B****C****D****E****F**

1CM

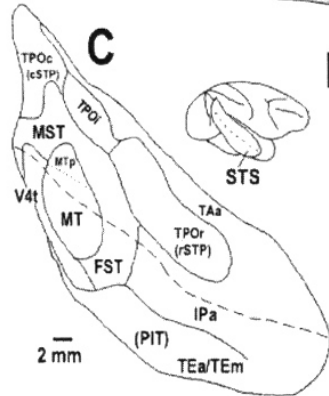
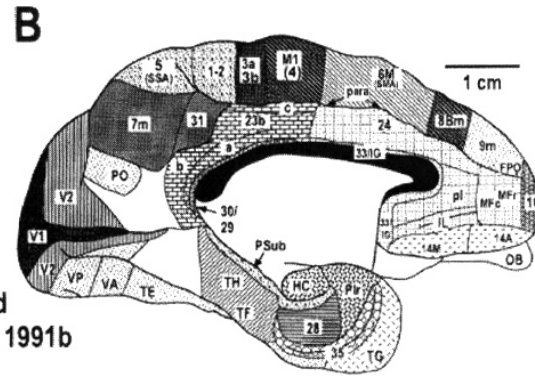
**G****H**

Cytoarchitecture of a series of primates and an insectivore. A: man, B: orangutan, C: gibbon, D: macaque; E: lemur; F: an insectivore; G, H: Brodmann's map of a monkey (A: Brodmann, 1912; B-E: Mauss, 1910; G, H: Vogt and Vogt, 1919)

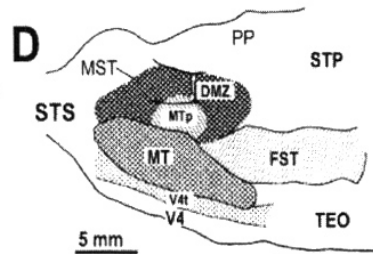
# CYTOARCHITECTONICS OF MONKEY CORTEX



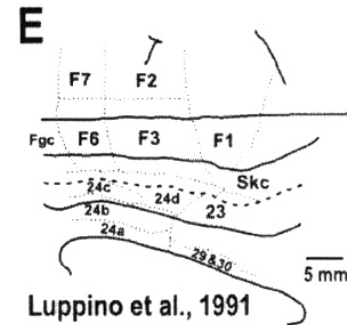
Preuss and Goldman-Rakic, 1991b



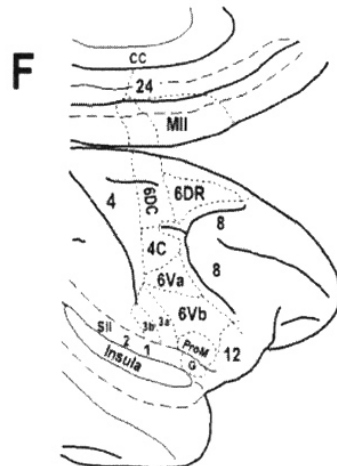
Cusick et al., 1995



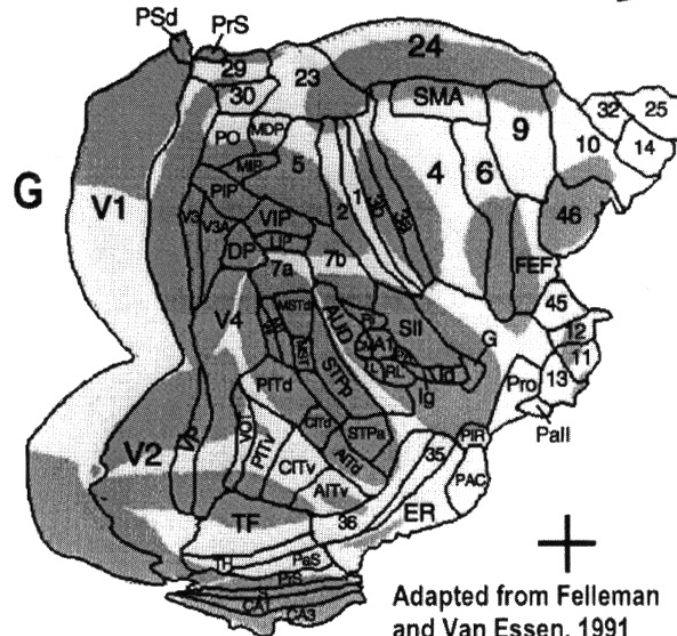
Desimone and Ungerleider, 1986



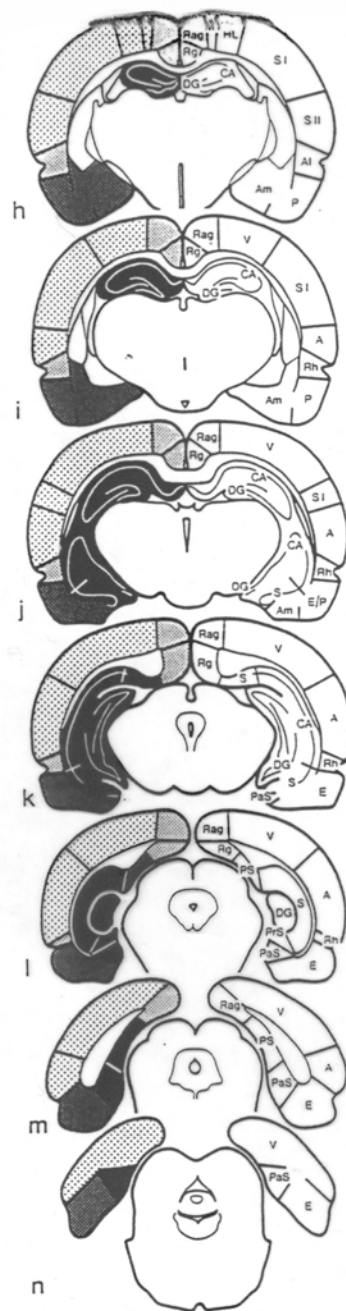
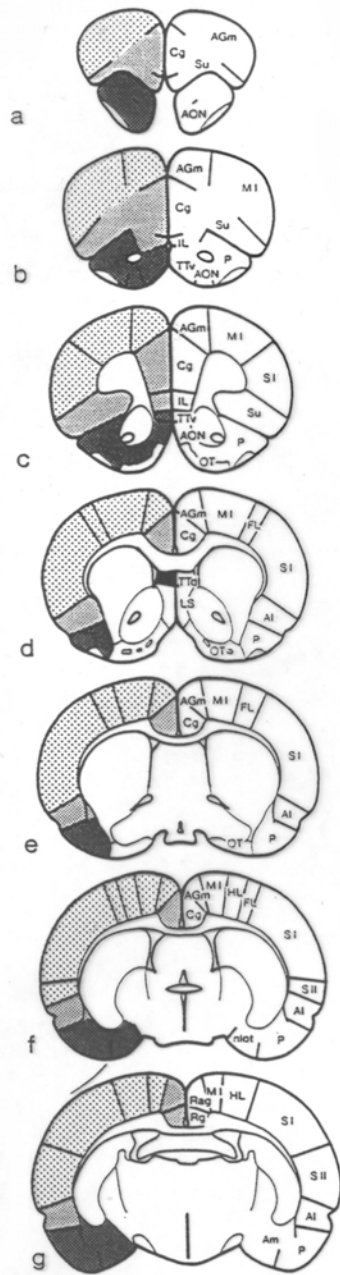
Luppino et al., 1991



Barbas and Pandya, 1987



Adapted from Felleman and Van Essen, 1991



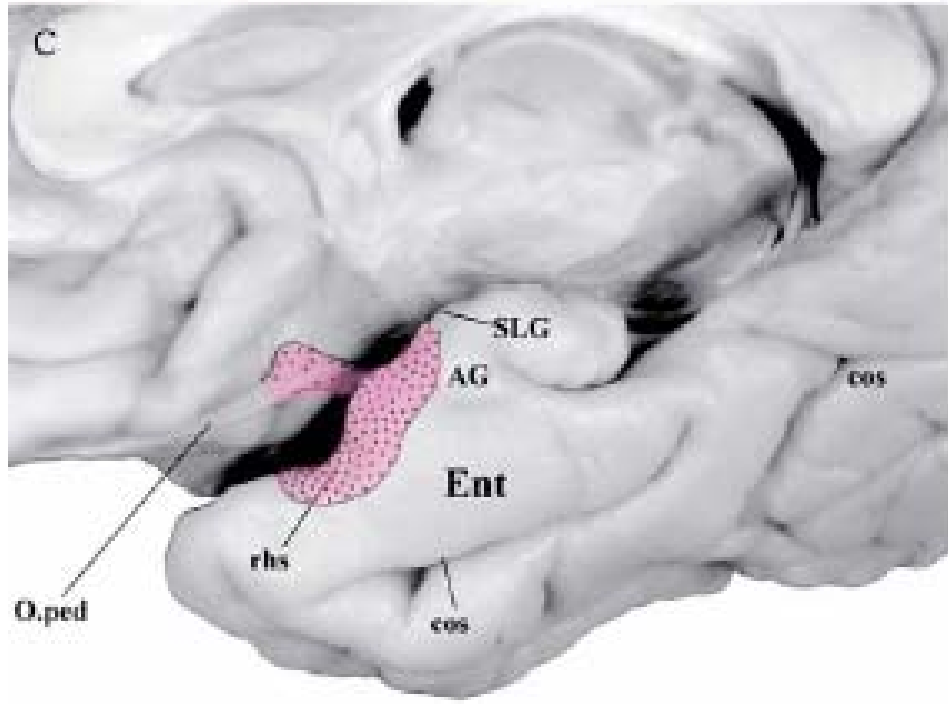
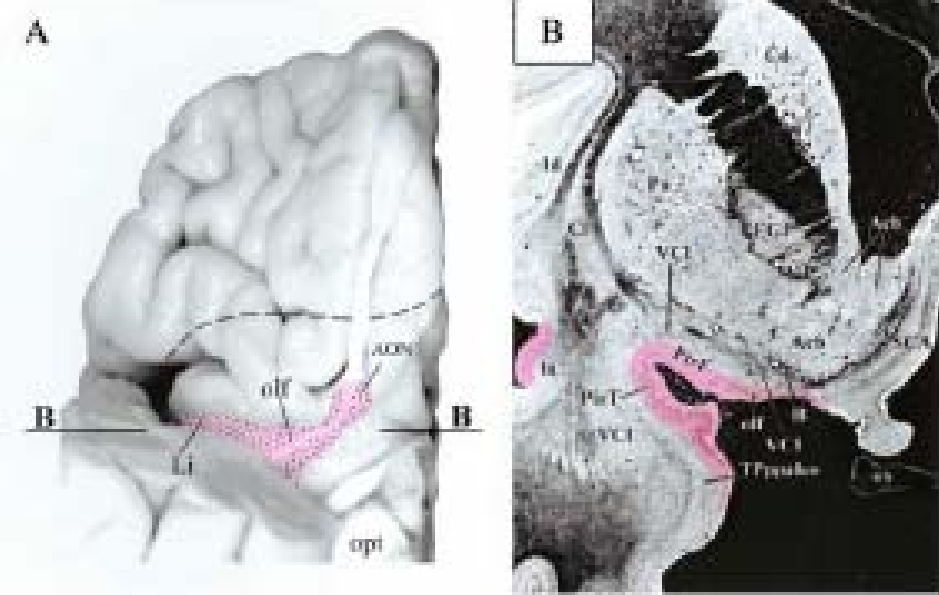
The subdivision of the cerebral cortex in rat. The neo (iso) cortex is stippled; the mesocortex is shown in light tone and is divisible into medial and lateral subdivisions; and the two subdivisions of the allocortex, the paleocortex and the archicortex, are shown respectively in dark tone and solid black (McGeorge and Faull, 1989)



D

# OLFACTORY (piriform cortex) AREAS IN HUMANS

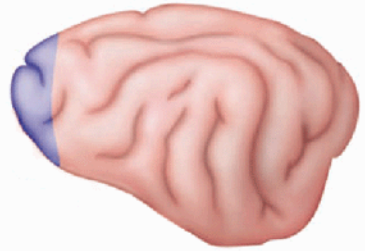
A: Orbital surface with a typical sulcal H-pattern. The approximate olfactory bulb projection area in the caudal orbital area is colored in magenta. The hyphenated line across the posterior half of the orbital cortex indicates the approximate rostral border of the limbic lobe. Limen insulae (Li) provides continuity between the orbital olfactory cortex and the temporal and insular parts of the olfactory cortex. The line labeled B-B indicates the level for the coronal section shown in B. SLG semilunar gyrus; cos collateral sulcus; AG: ambient gyrus. From Heimer and Van Hoesen, 2005. D: Brodman map (From Zilles, 1990)



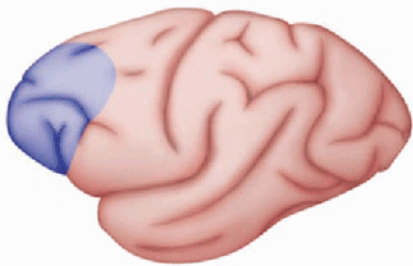
# PREFRONTAL CORTEX



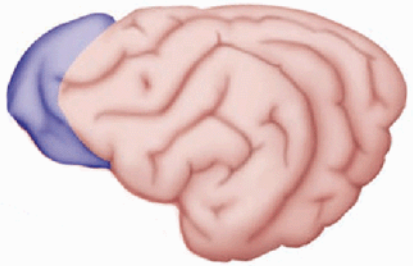
Squirrel monkey



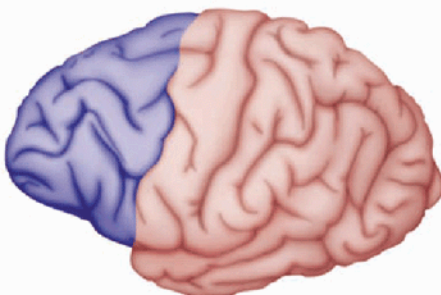
Cat



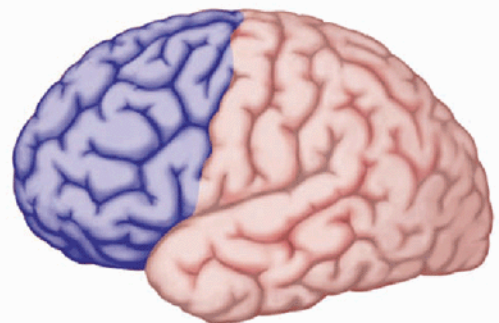
Rhesus monkey



Dog

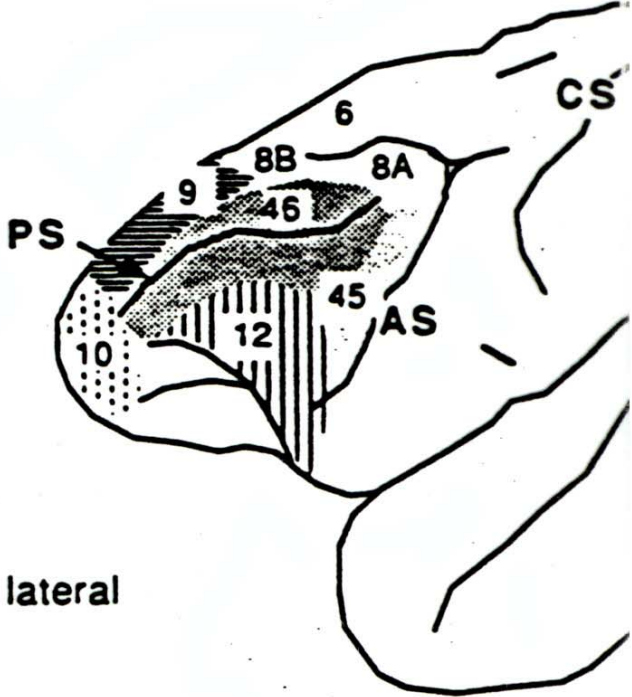
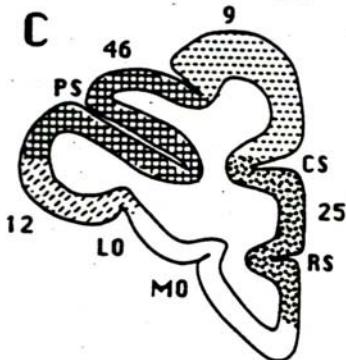
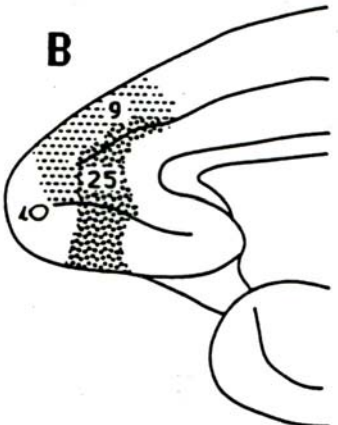
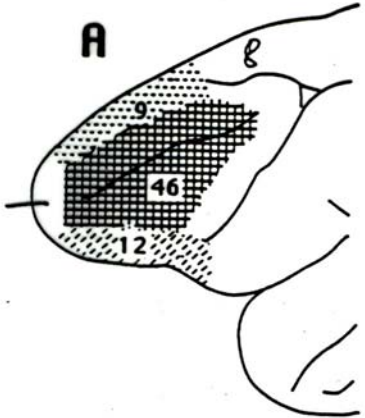


Chimpanzee

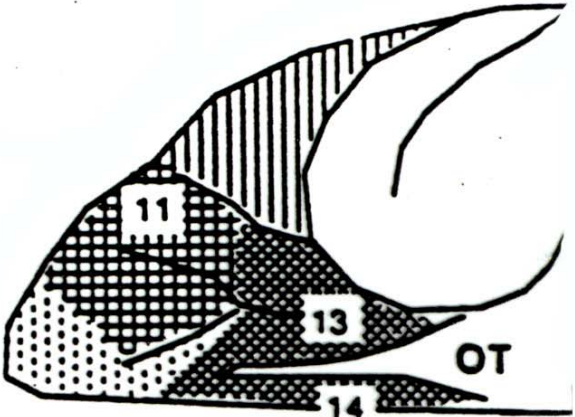


Human

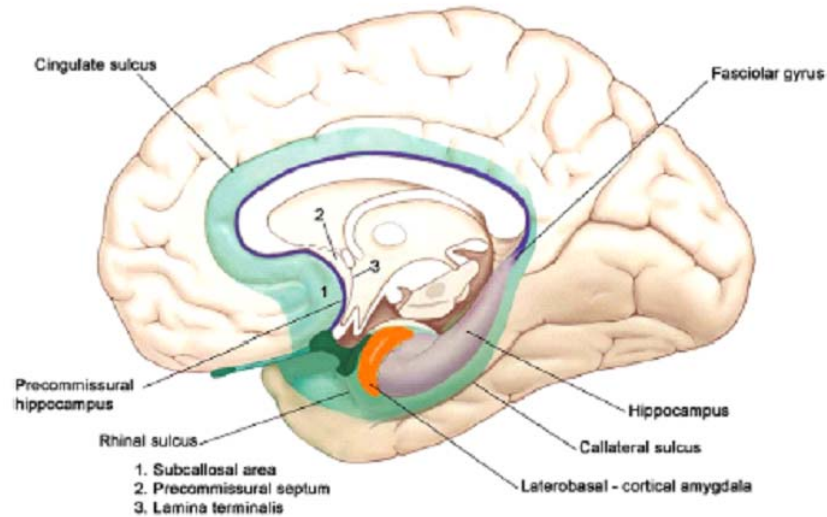
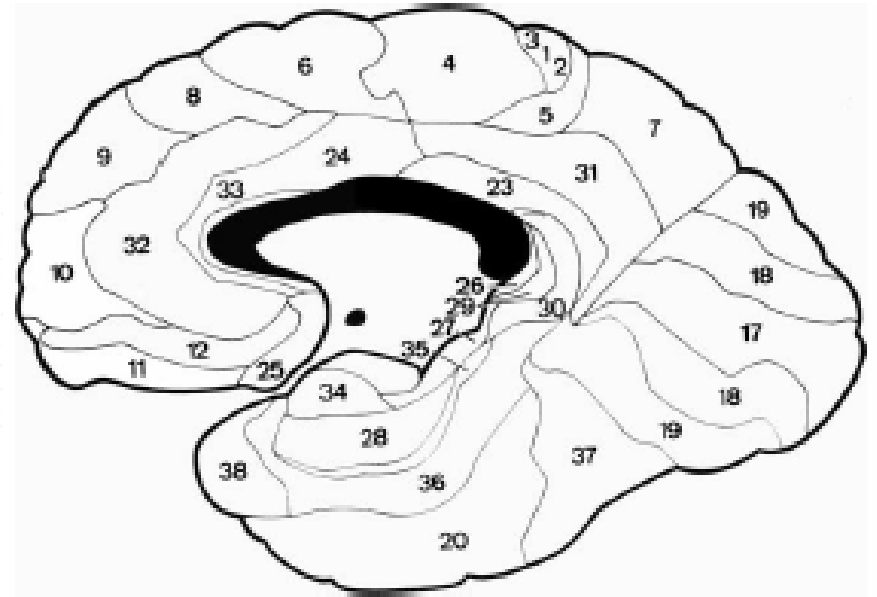
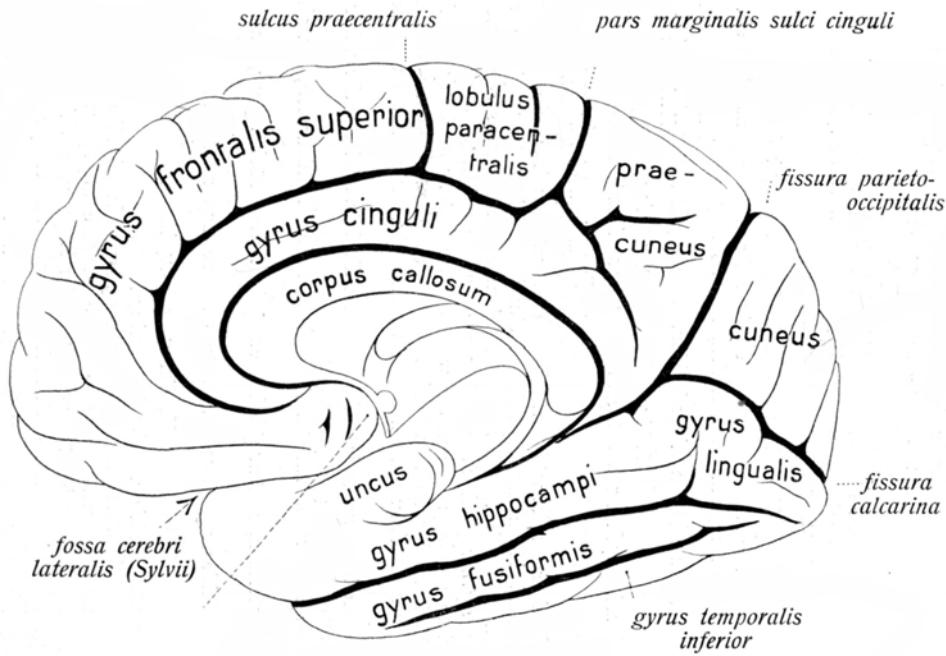
# PREFRONTAL CORTEX IN PRIMATES



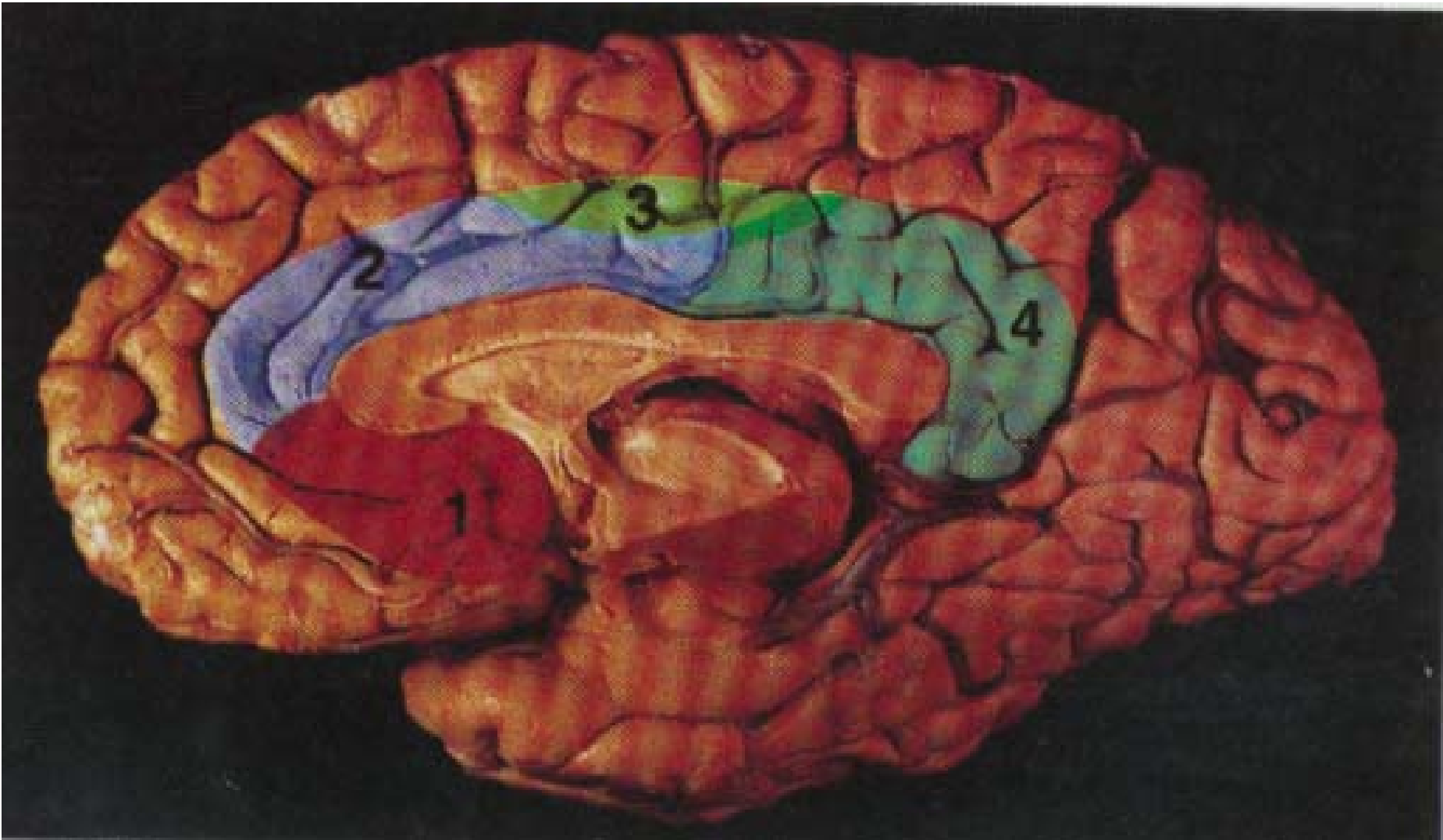
lateral



# Cingulate gyrus



## FUNCTIONAL DIVISIONS IN THE CINGULATE CORTEX



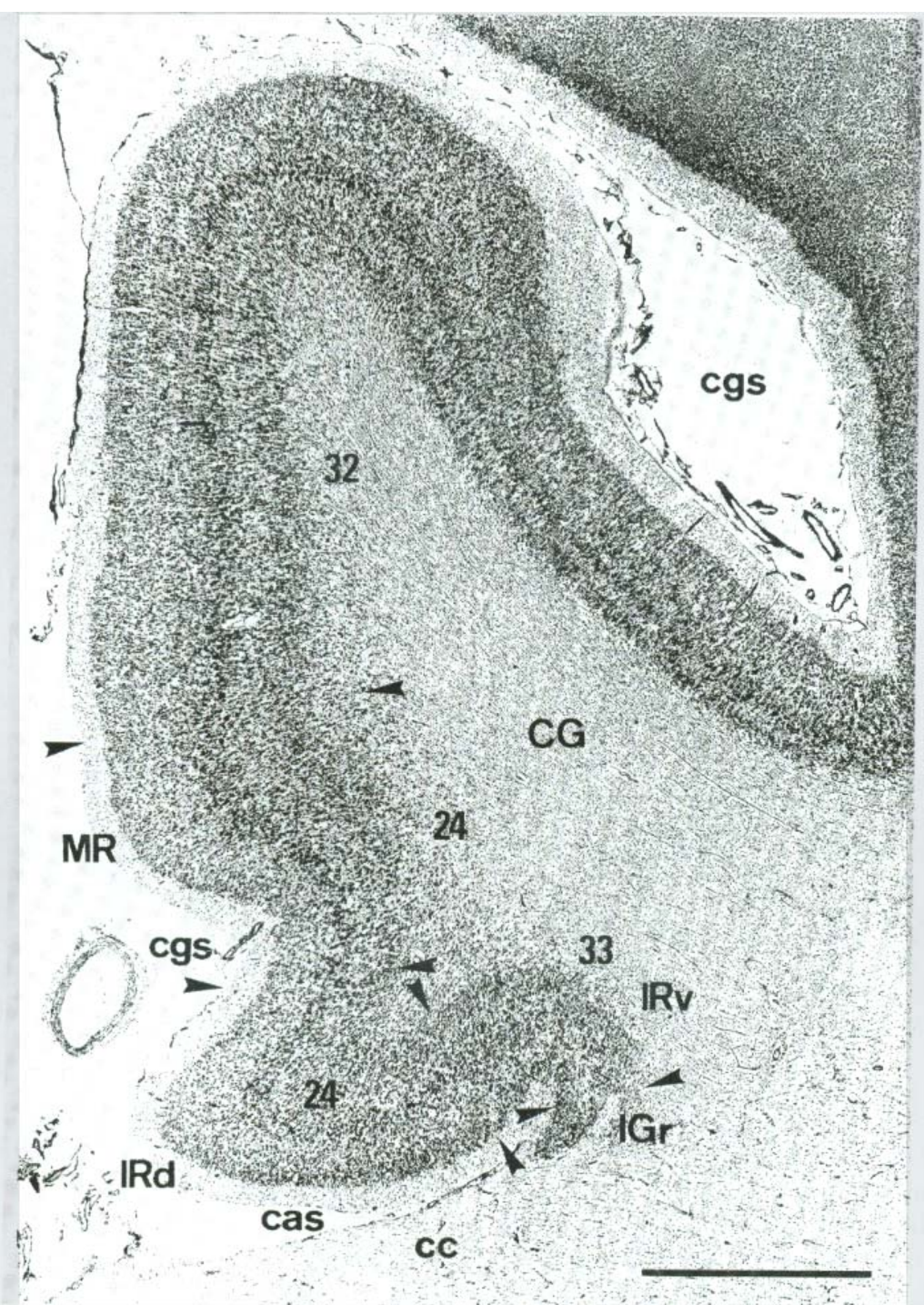
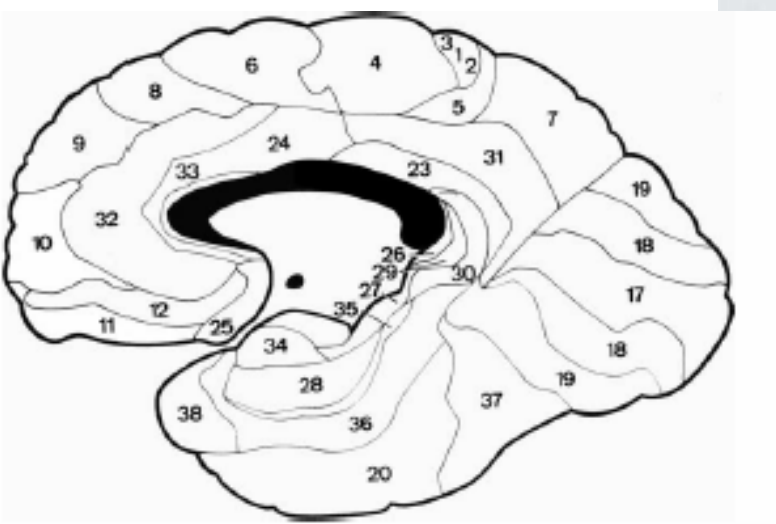
1: Visceral effector; 2: Cognitive effecor; 3: Skeletomotor effector; 4: Sensory processing region (Mega et al., 1997)

# CINGULATE CORTEX

Horizontal section through the anterior cingulate and rostrally adjoining regions showing the transition from allo- to neocortex.

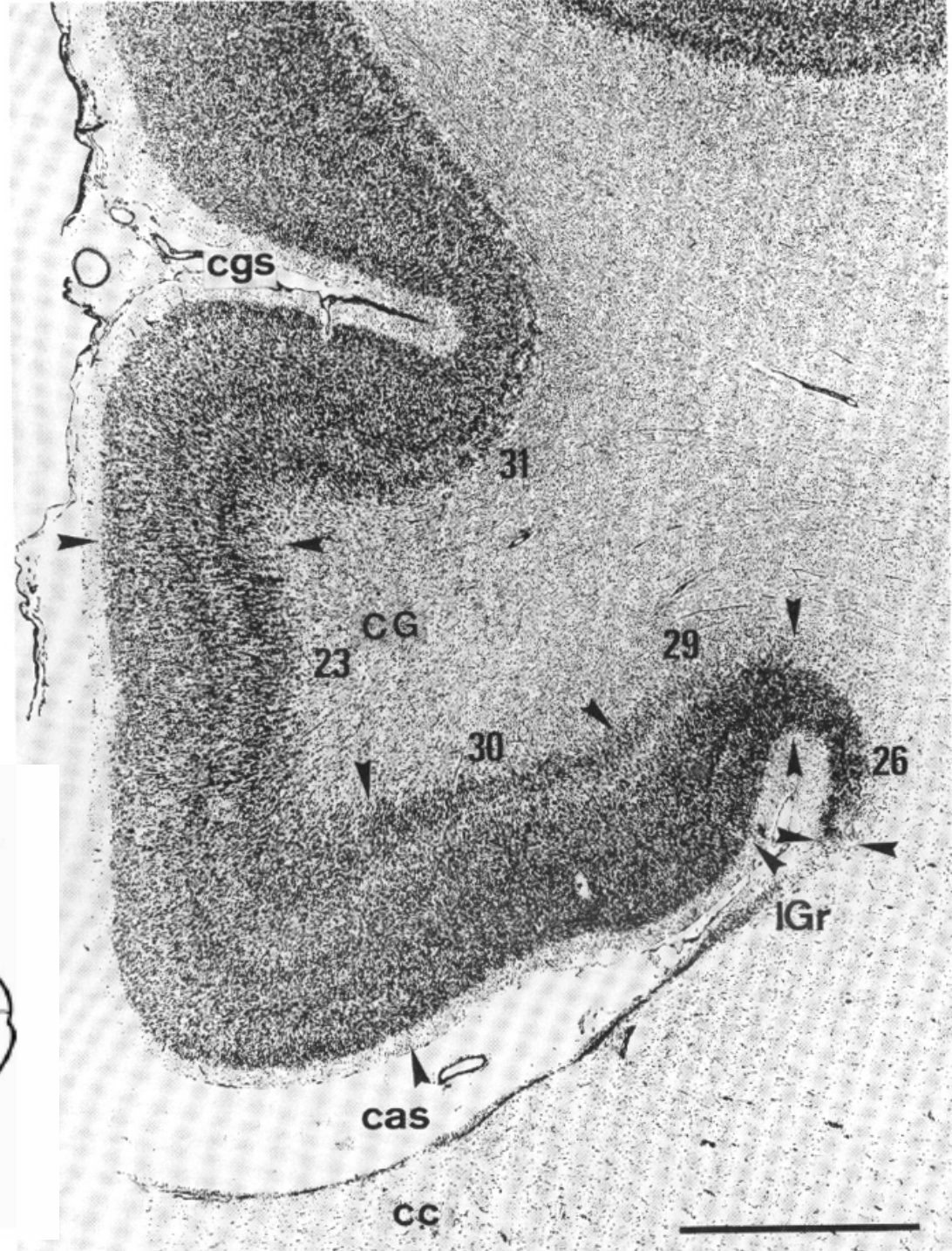
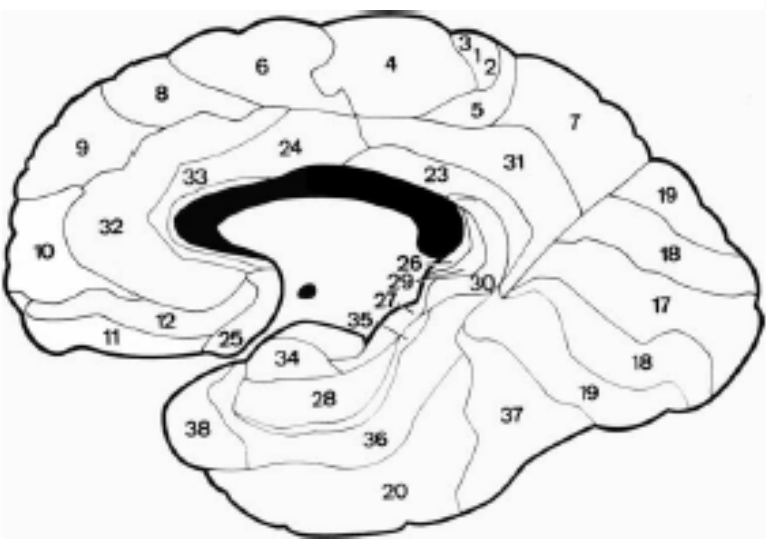
Area 33 and 24 are proisocortical, are 32 neocortical.

IGr=supracommissural hippocampus

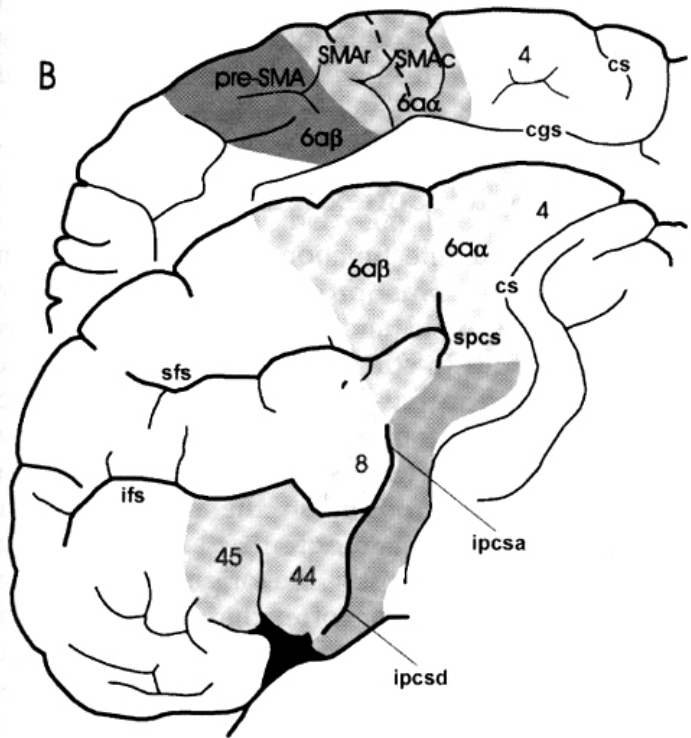
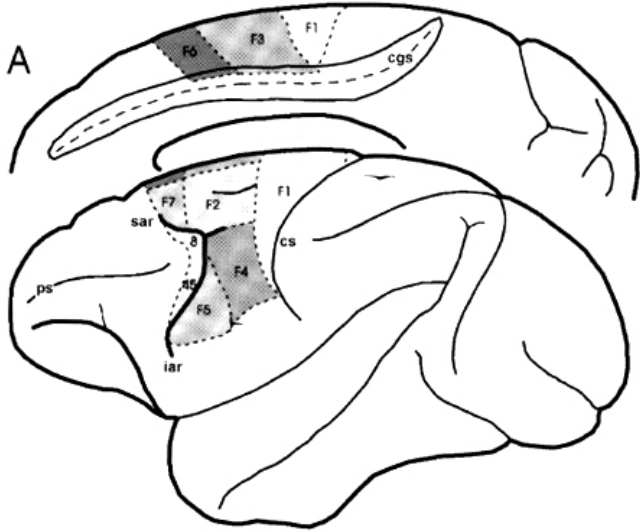


# CINGULATE CORTEX

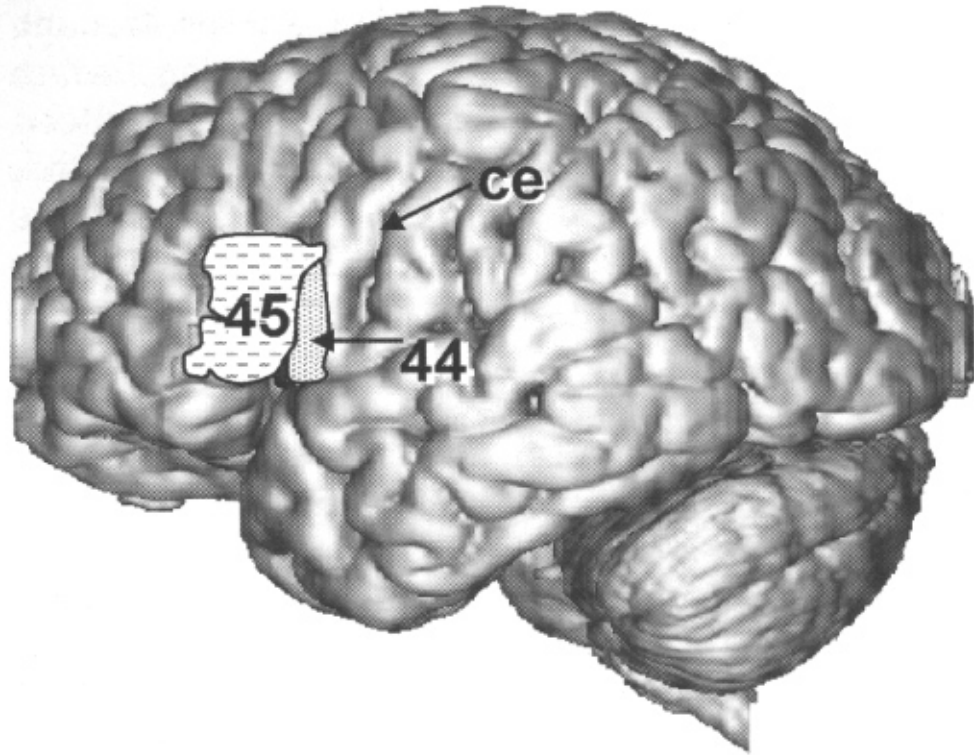
Coronal section through the post. Cingulate gyrus showing the transition from allo- to neo(iso)cortex. Areas 26, 29 belong to allocortex, area 30 is part of the proisocortex and areas 23 and 31 are classified as neocortical regions. cas=sulcus of the corpus callosum, cc=corpus callosum; CG cingulate gyrus; IGr indusium griseum (From Zilles, 2004)



# BROCA AREAS

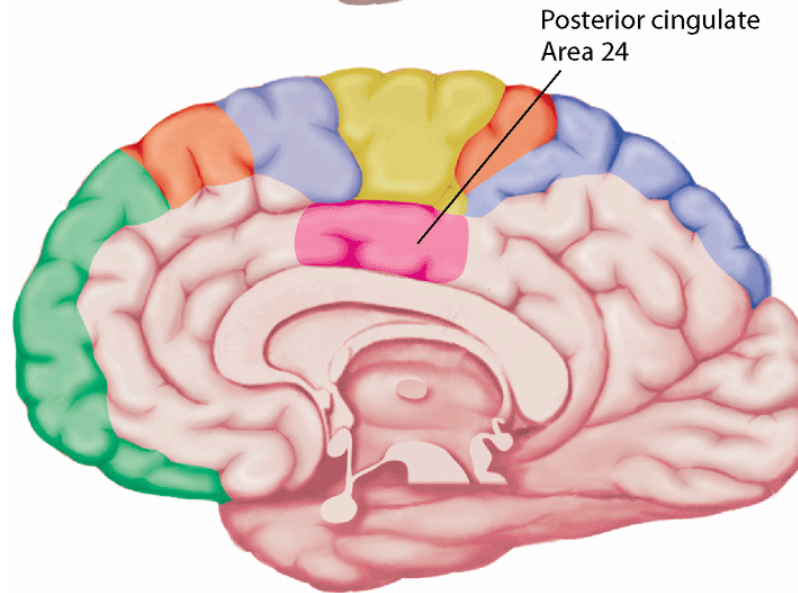
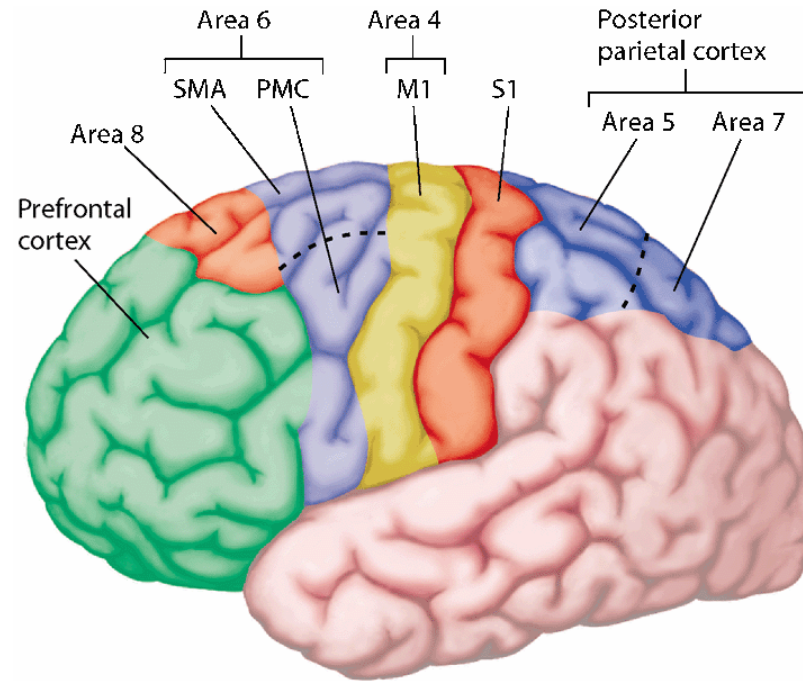


# BROCA AREAS

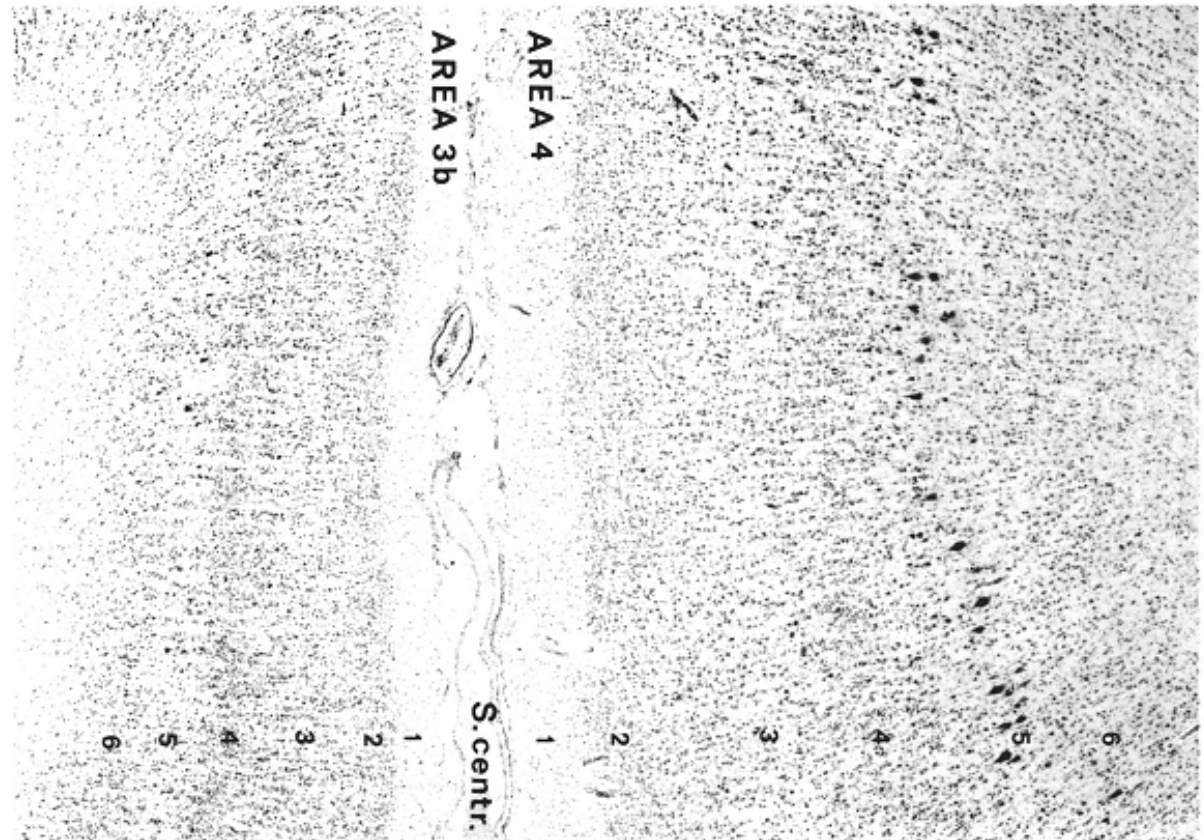
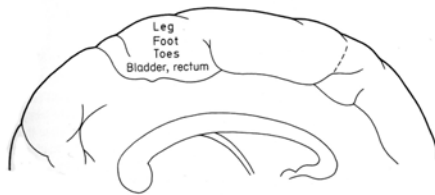
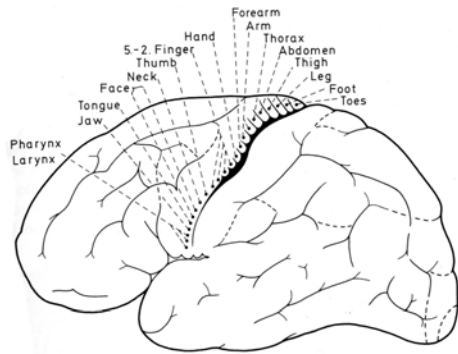


Areas 44 and 45. Cytoarchitecturally, these areas are dysgranular. The incipient layer IV is marked by asterisk. From Zilles, 2004

# CORTICAL AREAS RELATED TO MOTOR CONTROL

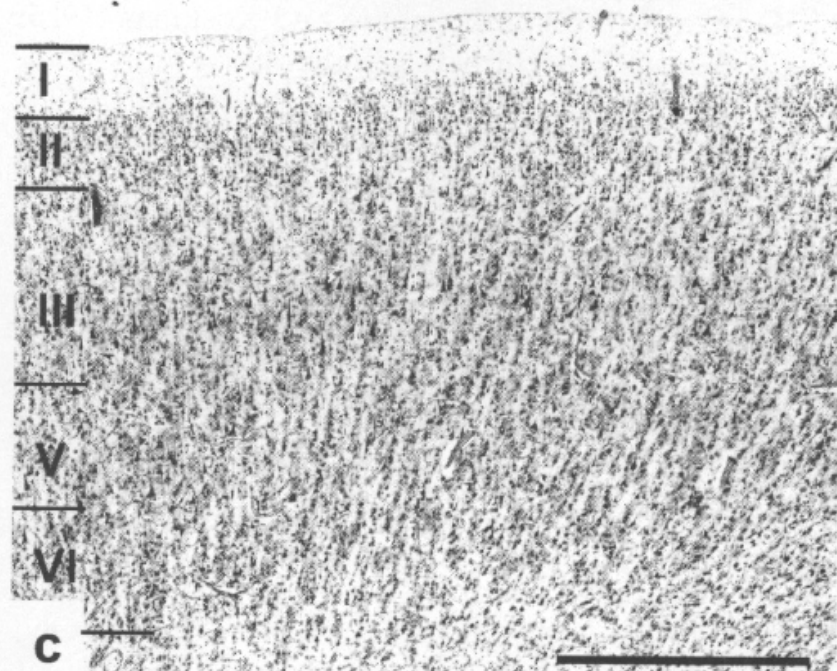
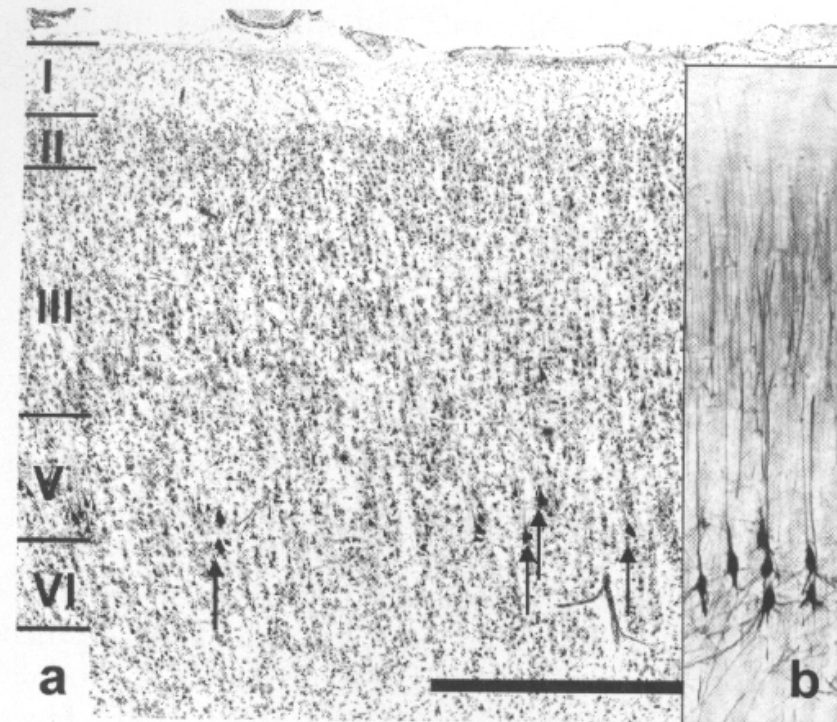


# PRIMARY MOTOR CORTEX

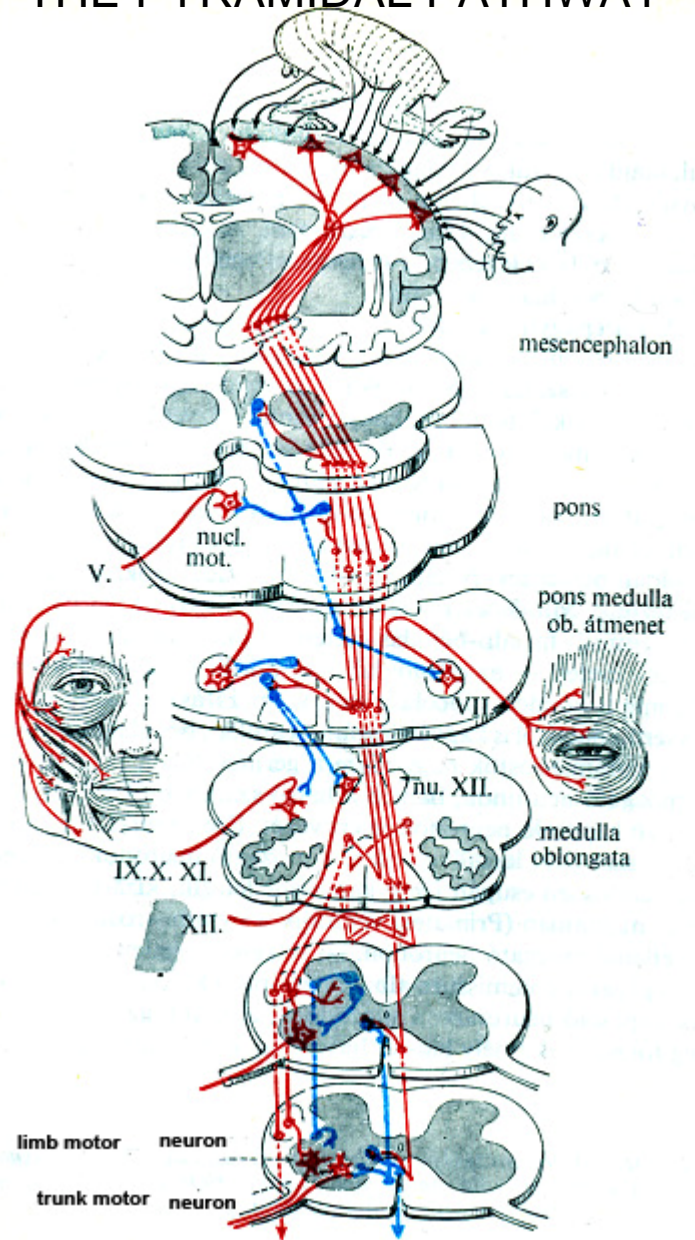
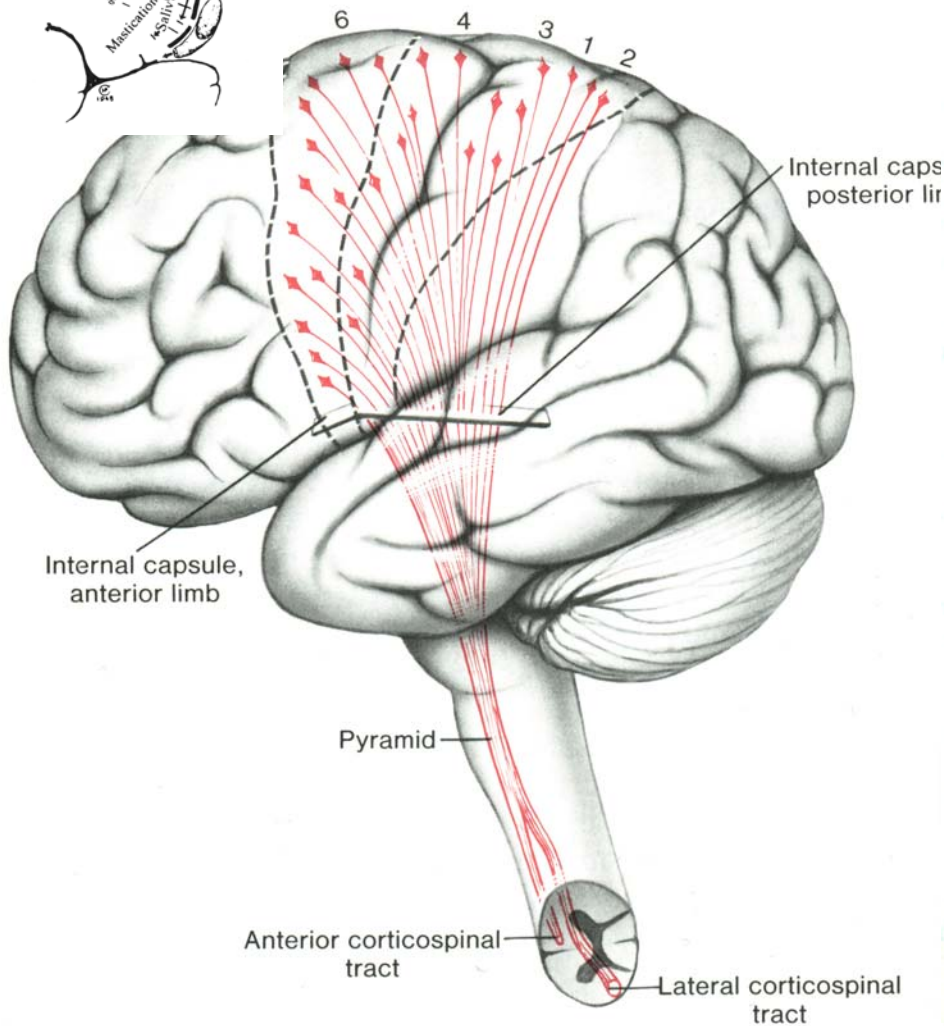
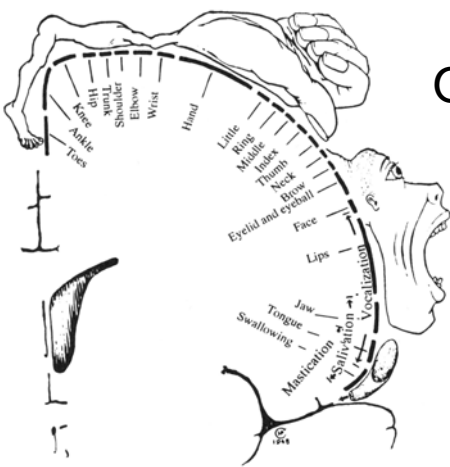


Photomicrograph of a thionin-stained section through the central region of the human brain. The six-layered structure is evident in area 4 (M1) and in area 3b (S1). Note, however, the difference in appearance of the various layers in the two areas, especially with regard to layers 4 and 5. The large pyramidal (Betz) cells in layer 5 are especially apparent (Brodal, 1992)

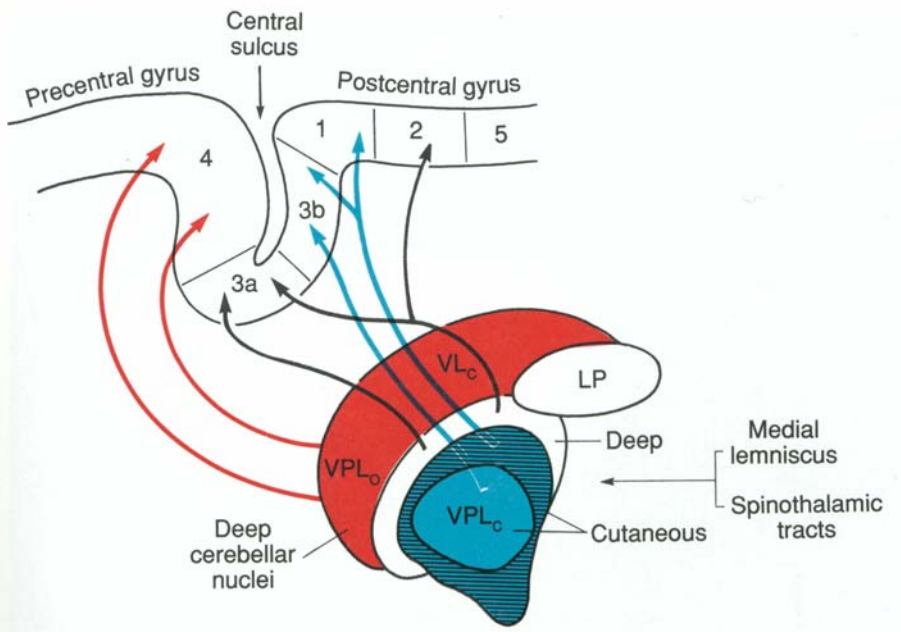
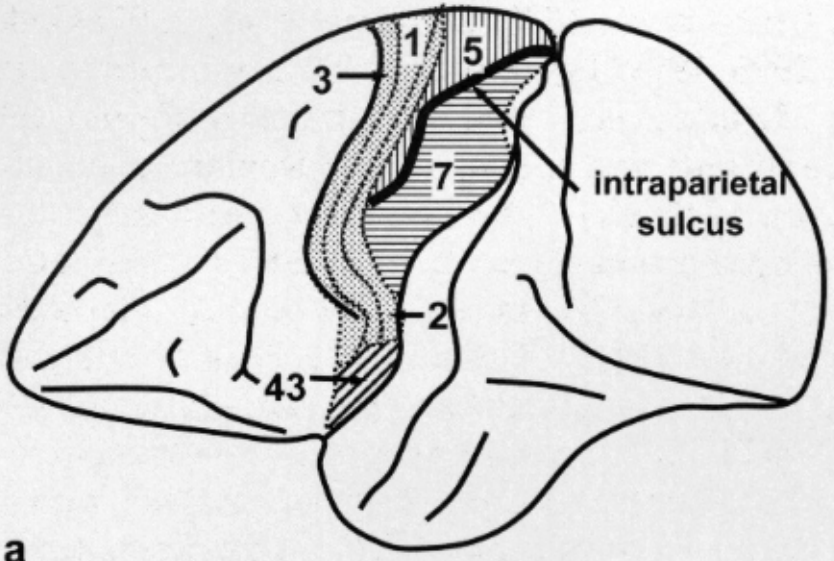
AREAS 4 (a) and 6 (c). Both are agranular. (a) Nissl staining, arrows indicate Betz cells; (b) SMI-32; (c) area 6 Nissl



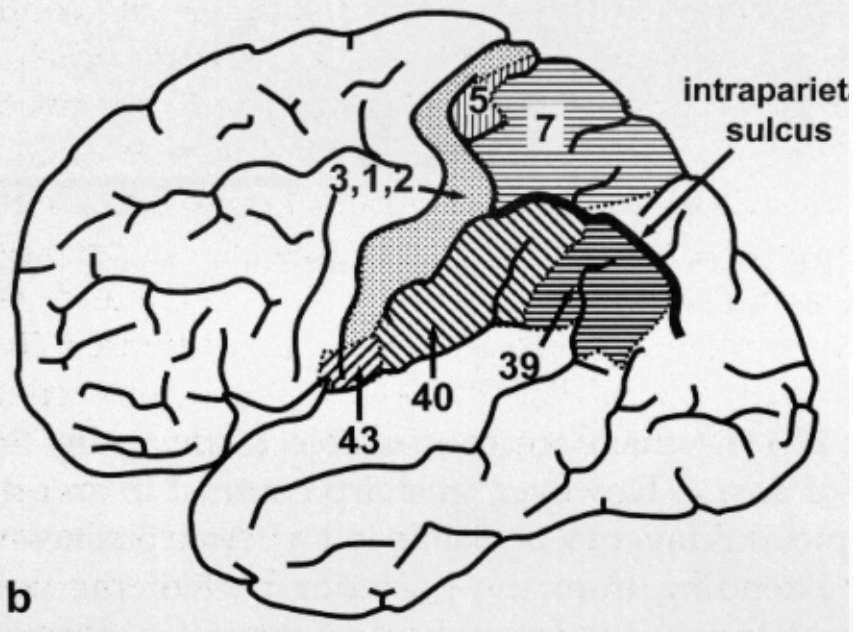
# ORIGIN AND DISTRIBUTION OF THE PYRAMIDAL PATHWAY



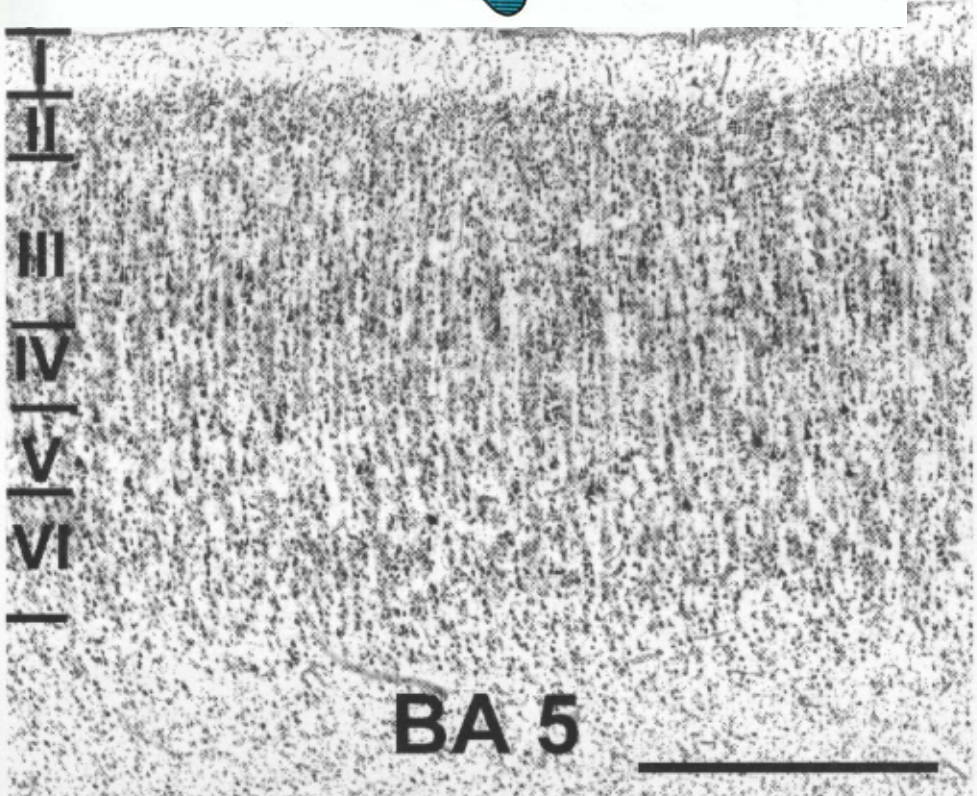
# PARIETAL LOBE



a



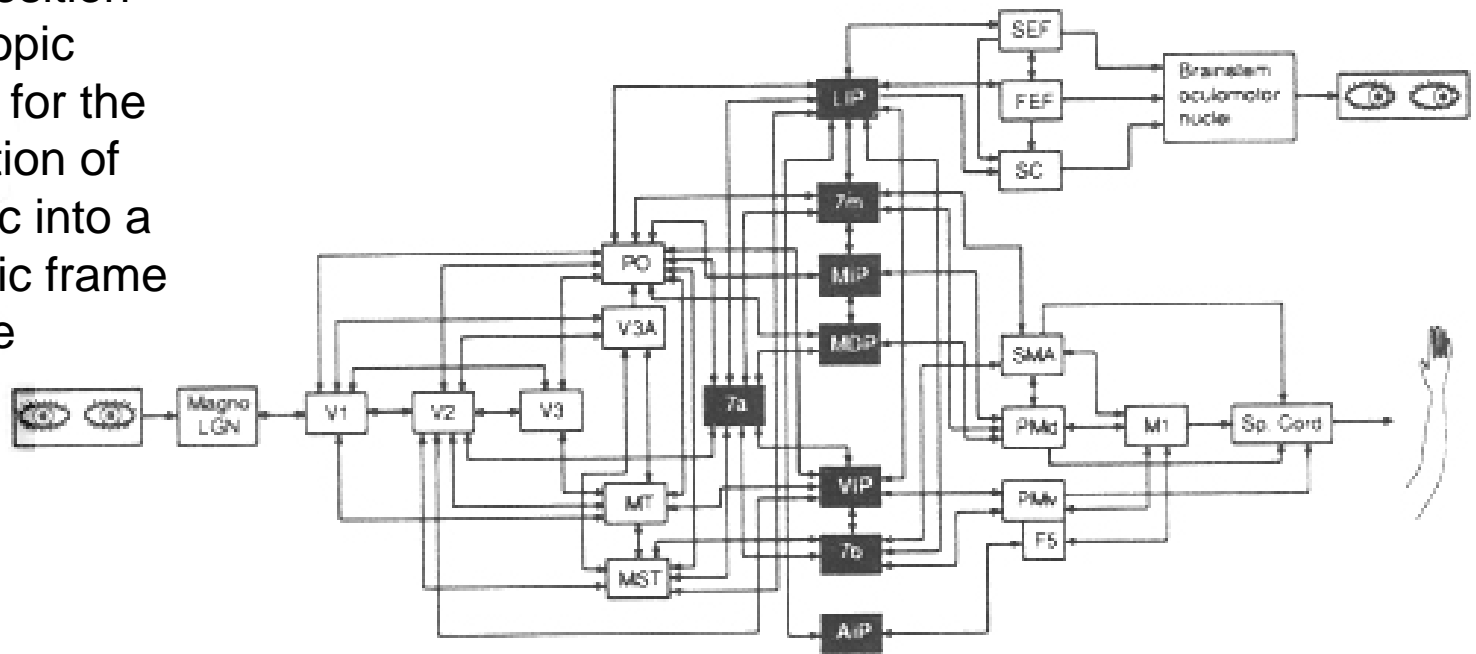
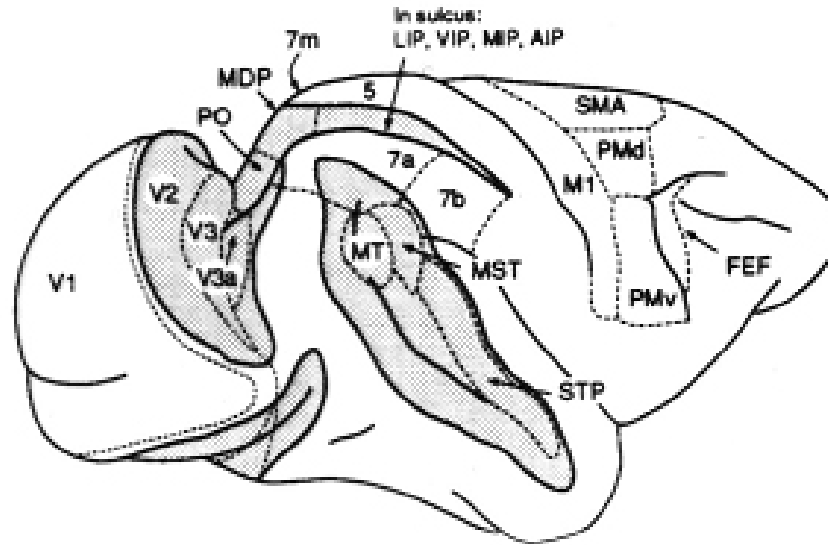
b



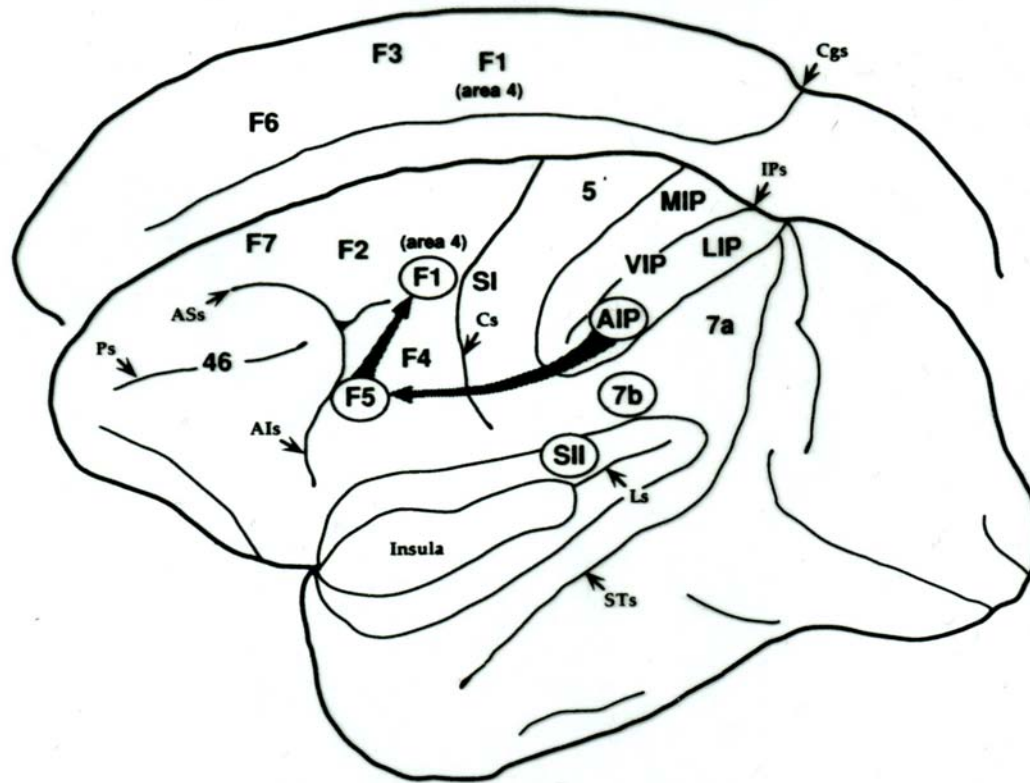
(a) macaque; (b) human. From Zilles, 2004

# PARCELLATION OF THE MONKEY PARIETAL CORTEX

Transformation of sensory and visual information for the control of hand and eye movements. The **LIP-FEF** circuit uses eye position and retinotopic information for the transformation of retinocentric into a craniocentric frame of reference

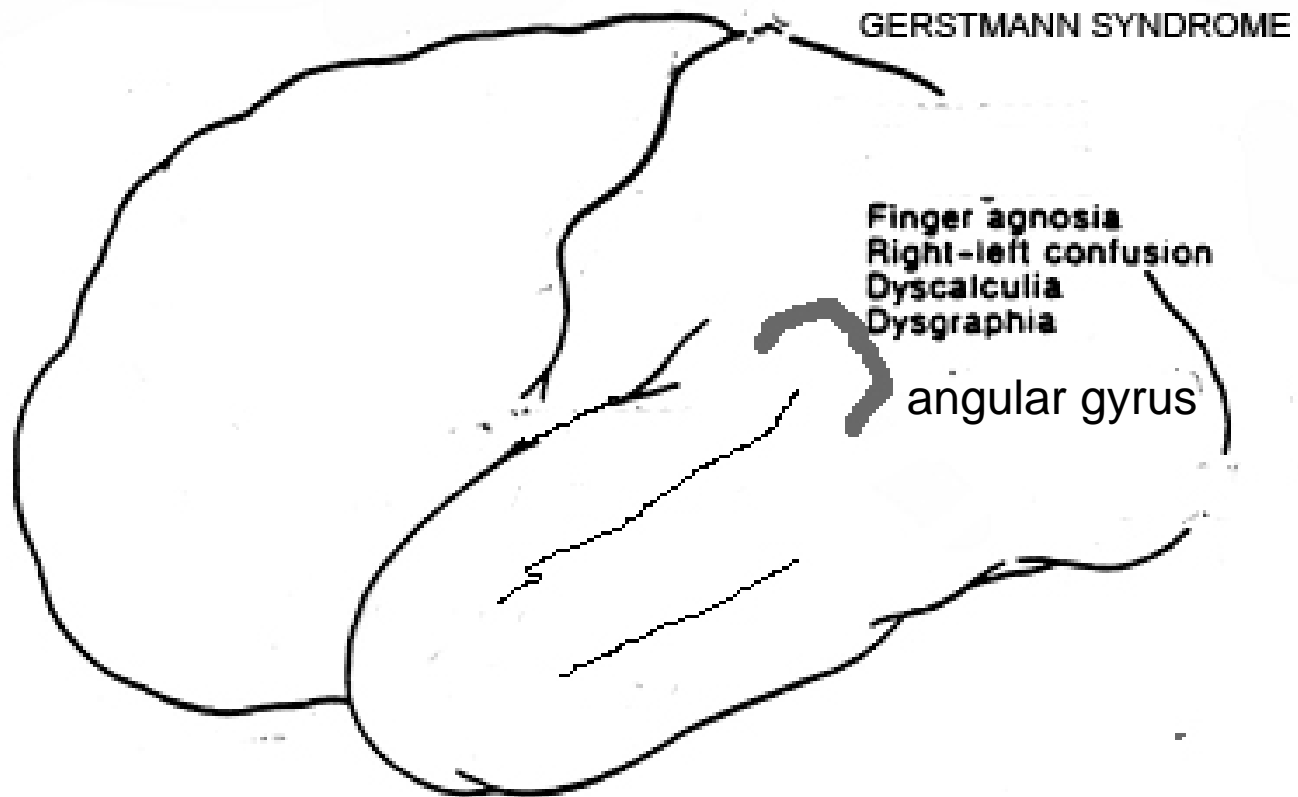


## The AIP-premotor circuit for grasping

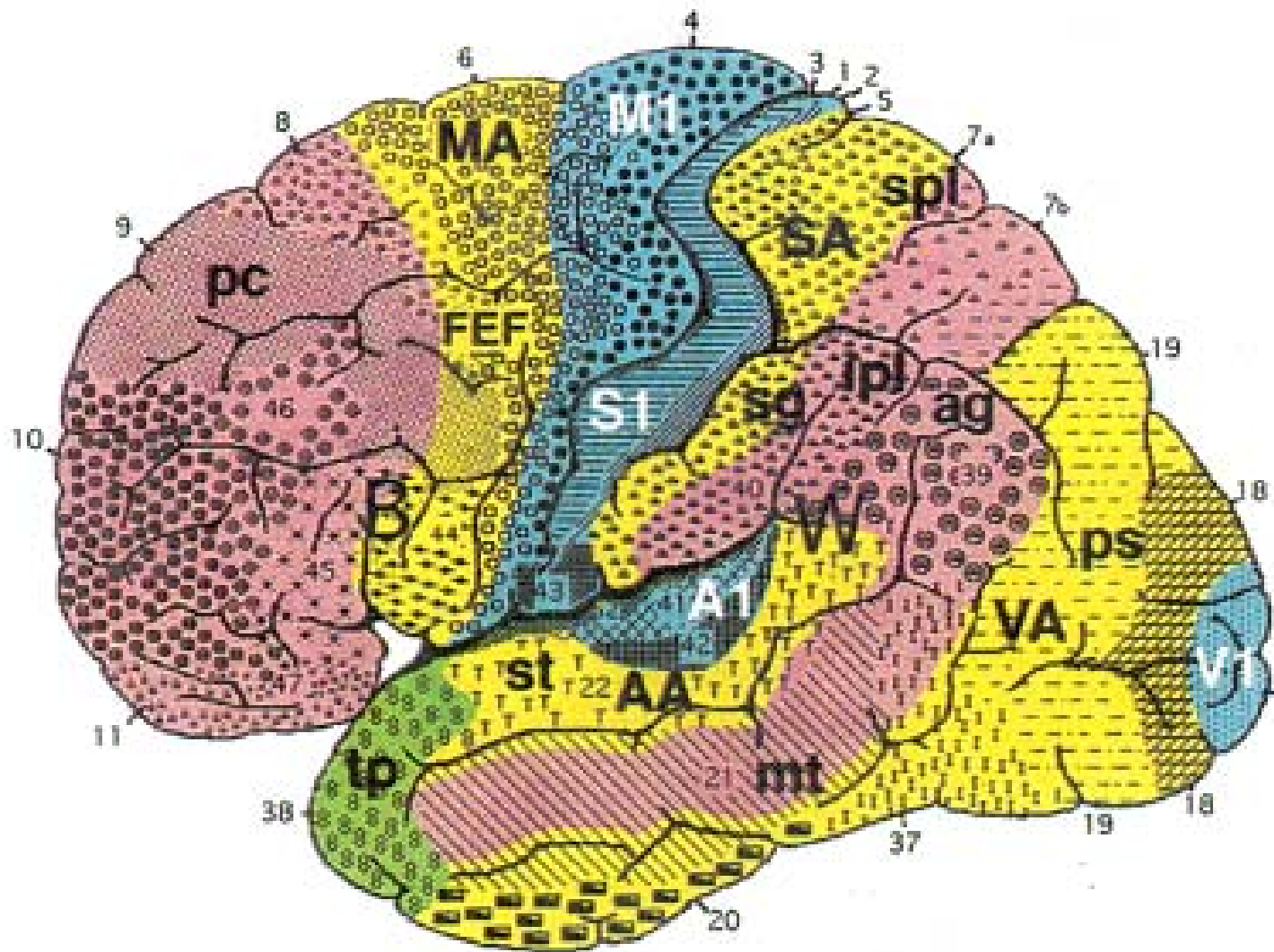


The visuomotor stream for grasping is indicated by large arrows. The AIP-premotor circuit provides a representations of intrinsic object properties (size, shape and orientation) for selection of the most appropriate way of grasping. AIP= anterior intraparietal area; VIP= ventral intraparietal area; MIP= medial intraparietal area; LIP= lateral intraparietal area; STs= superior temporal sulcus; Cs=central sulcus; AIs; ASs= inferior, superior arcuate sulcus (Jedannerod et al., 1995)

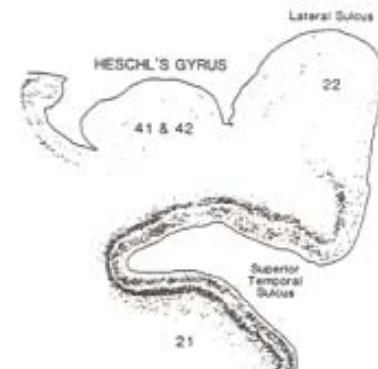
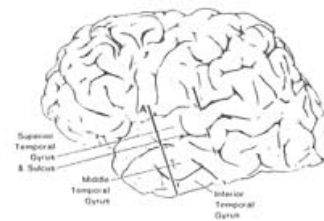
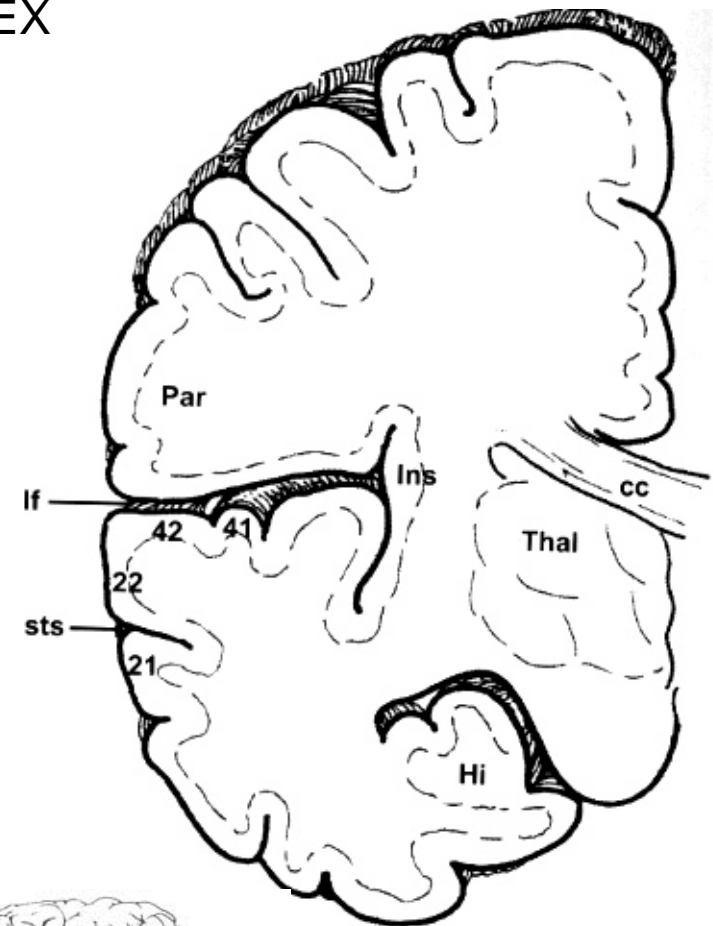
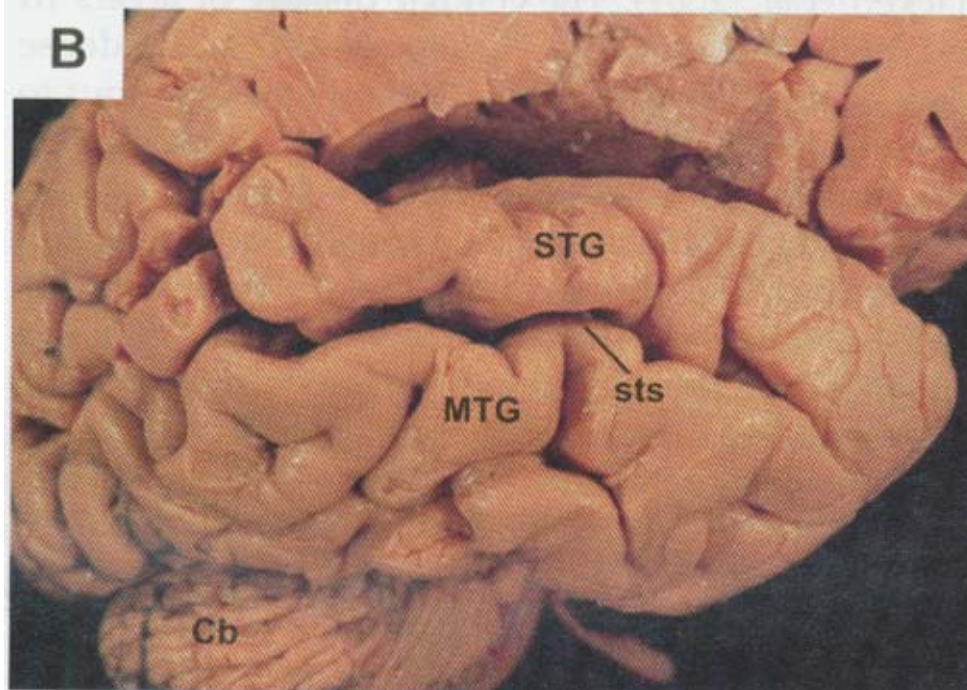
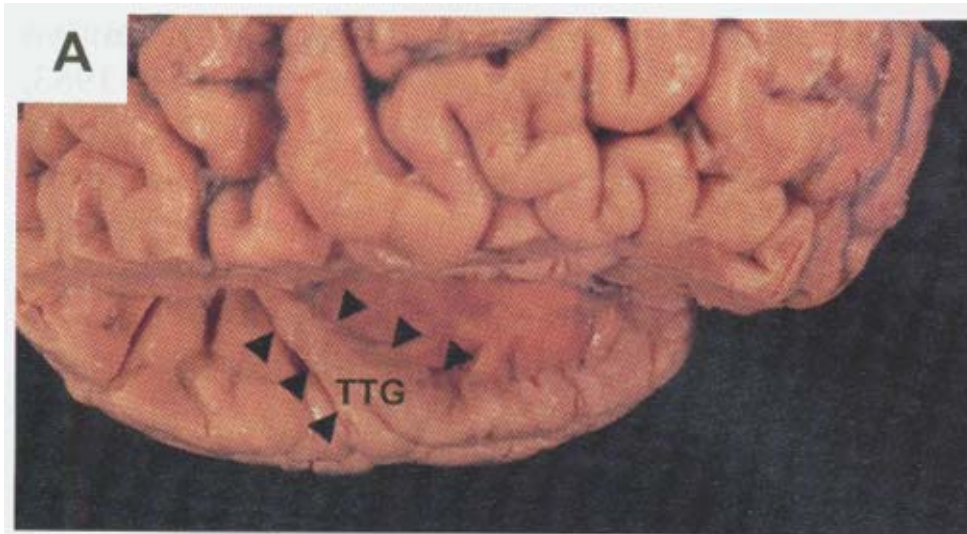
## Parietal lobe: focal lesions



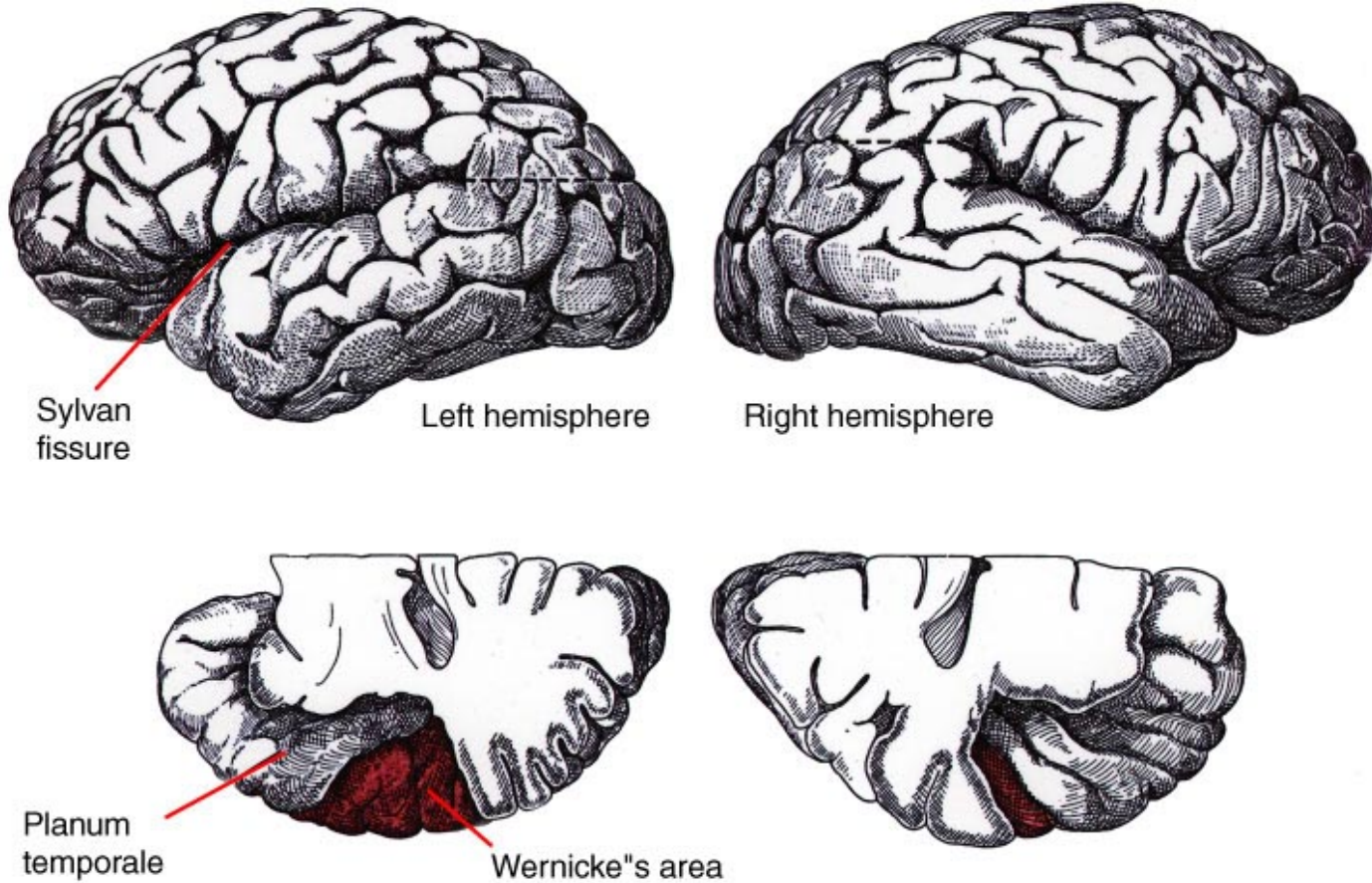
# TEMPORAL LOBE: lateral aspect



# TEMPORAL LOBE: AUDITORY CORTEX



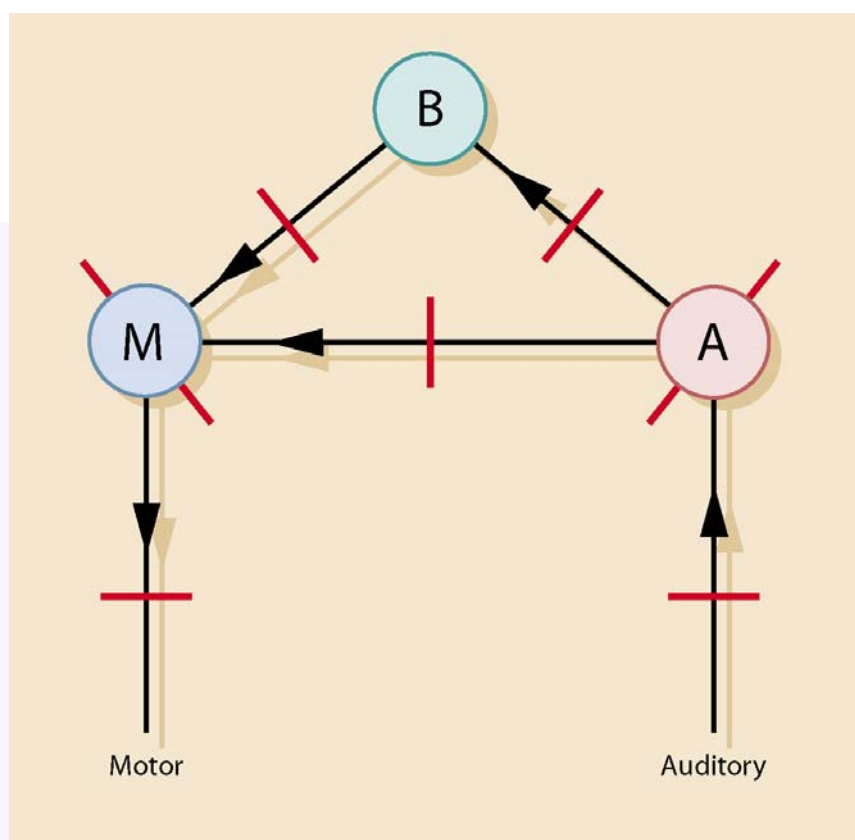
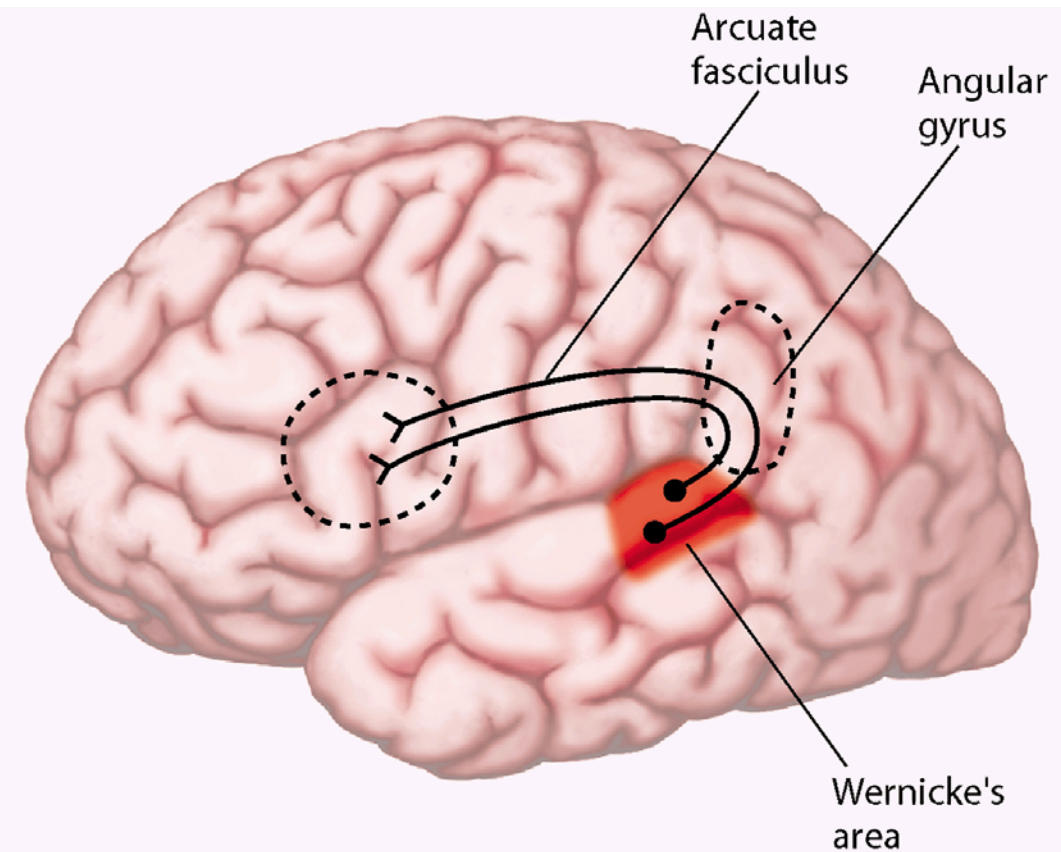
# TEMPORAL LOBE: PLANUM TEMPORALE, Wernicke area



Copyright © 2002, Elsevier Science (USA). All rights reserved.

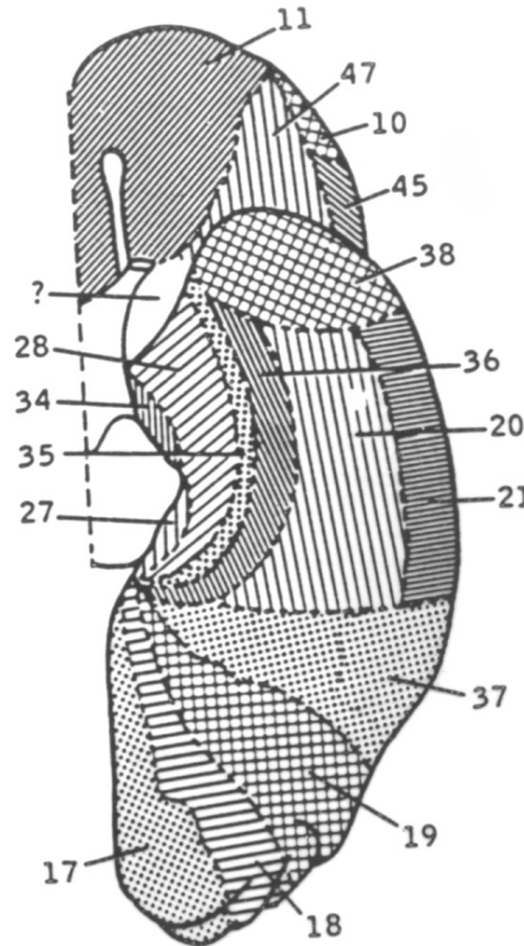
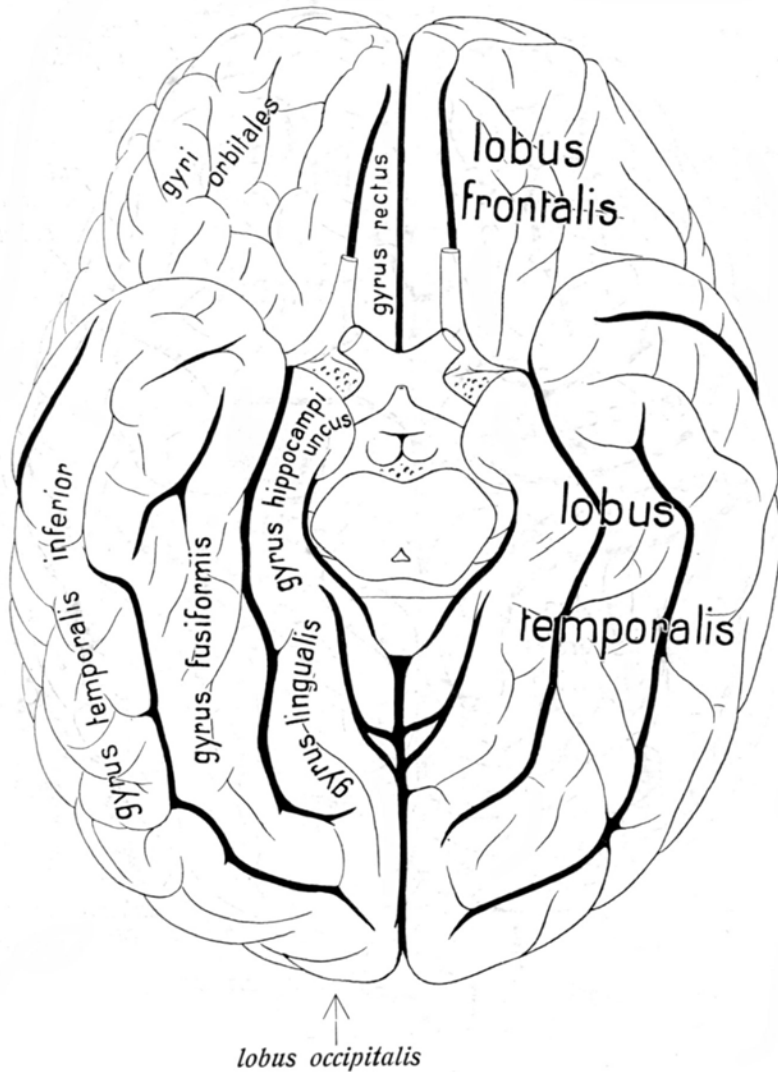
Depiction of a horizontal slice through the brain showing asymmetry in the size of the planum temporale related to lateralization of language

# TEMPORAL LOBE: WERNICKE AREA



Wernicke-Lichtheim-Geschwind model of language processing. The area that stores permanent information about word sounds is represented by *A* (*Wernicke area*). The speech planning and programming area is represented by *M* (*Broca area*). Conceptual information is stored in area *B* (*supramarginal, angular gyri*). From this model it was predicted that lesions in the three main areas, or in the connections between the areas, or the inputs to or outputs from these areas, could account for seven main aphasic syndromes (Caplan et al., 1994; Gazzaniga, 2002).

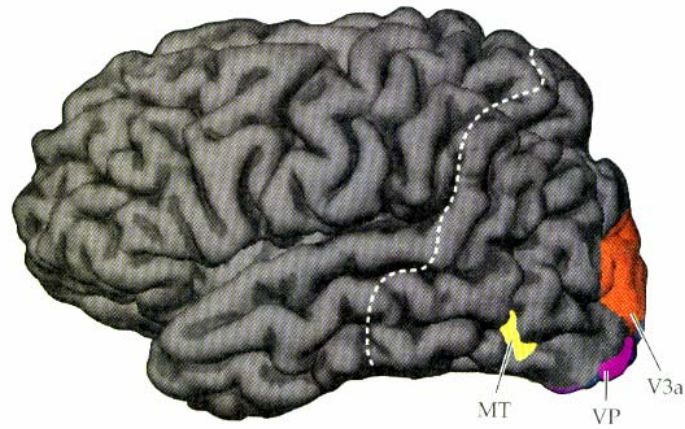
# TEMPORAL LOBE: ventral aspect



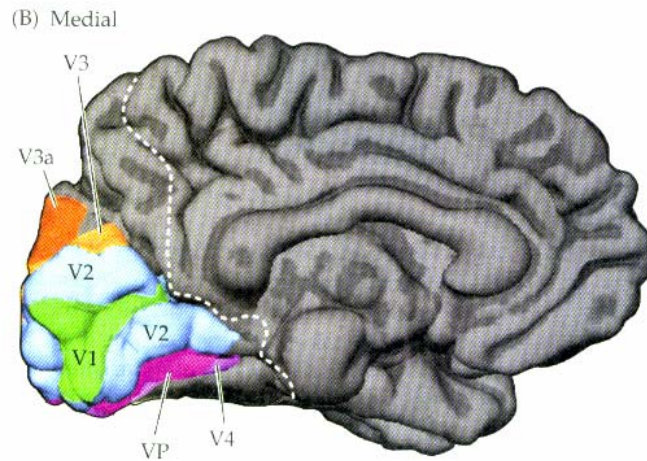
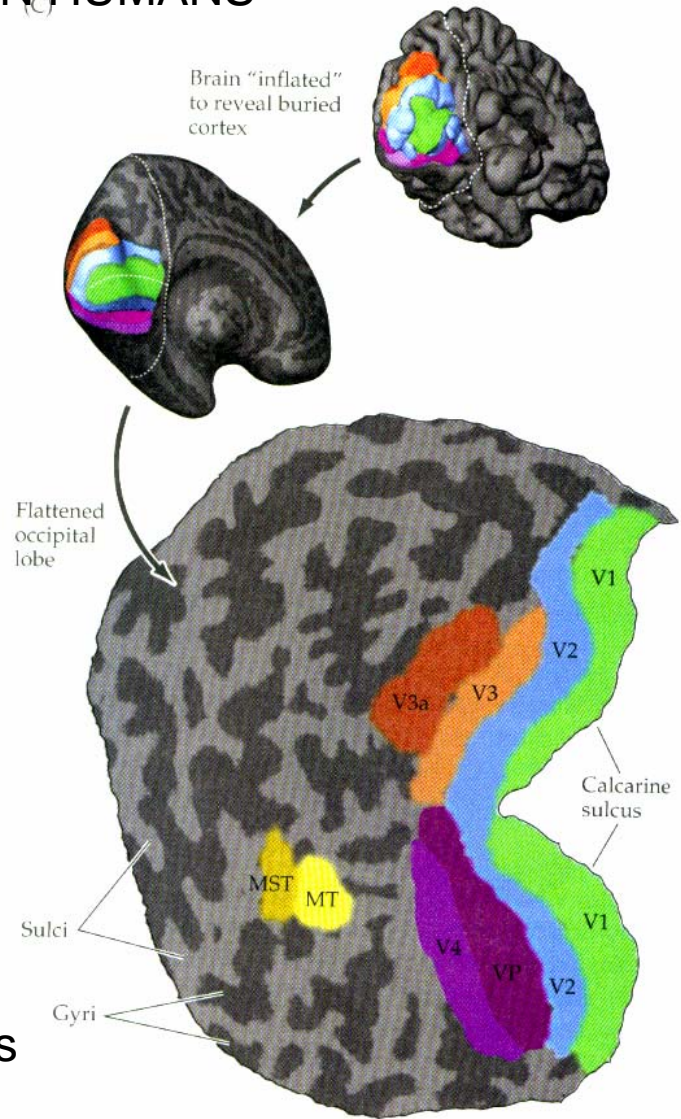
AREA 21: short term verbal memory, verbal fluency, word generation

AREA 20 (on the inf. temp gyrus) and parts of AREA 37 (on the fusiform gyr). belong to the ventral stream. The parahipp gyrus (AREA 36) and the fusiform gyr (area 20) are activated by attention to shape

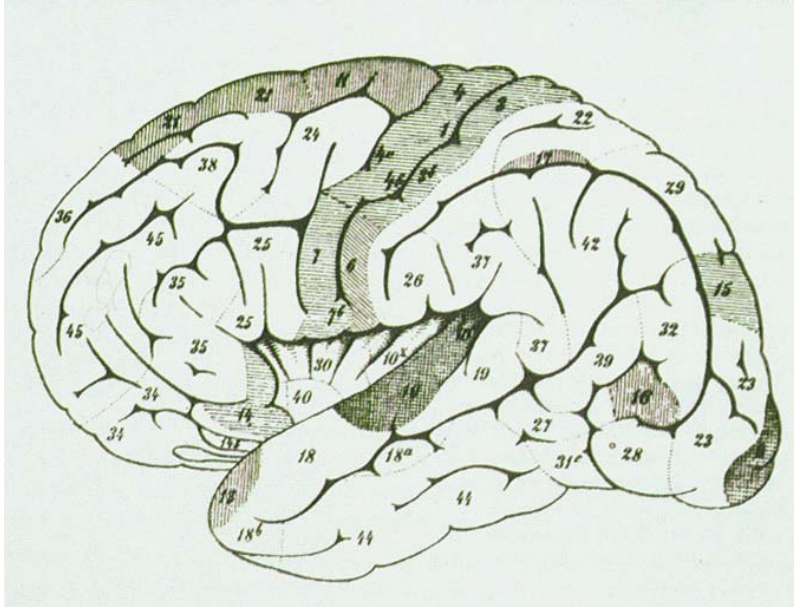
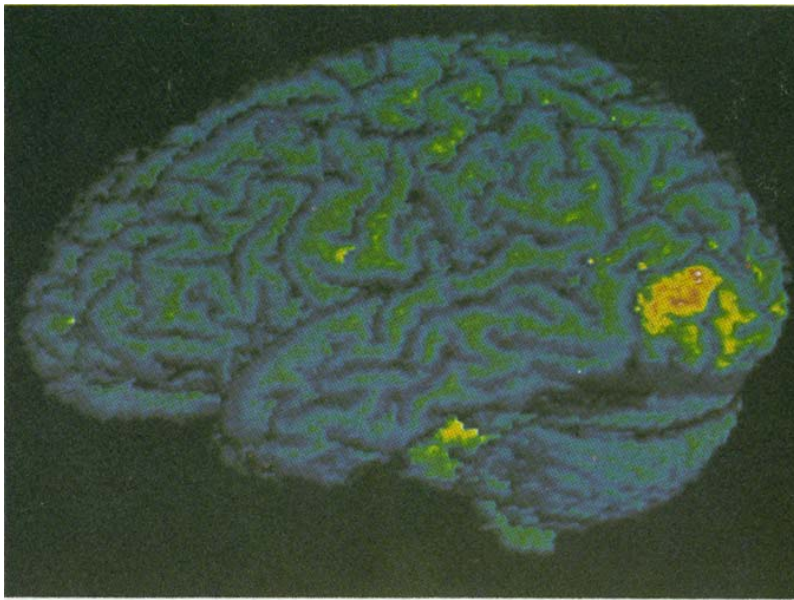
# OCCIPITAL LOBE: VISUAL AREAS IN HUMANS



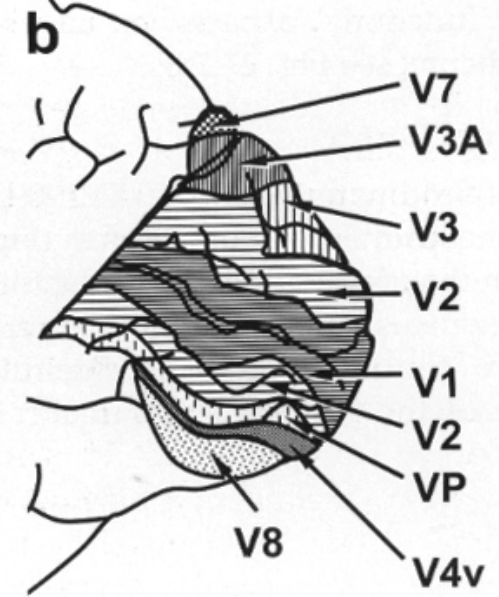
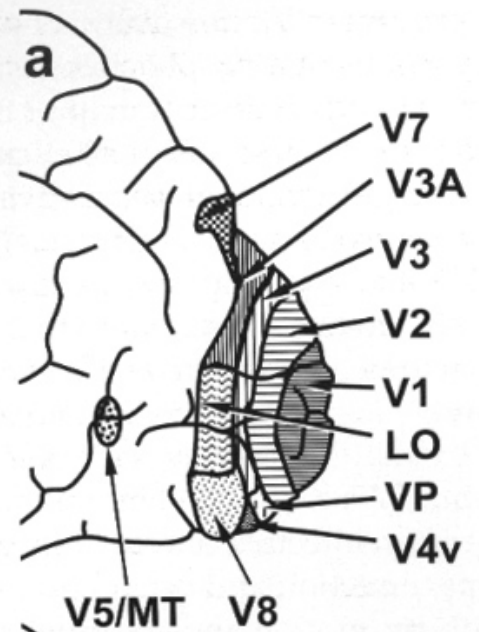
Brain "inflated" to reveal buried cortex



V4 is located on the post part of the fusiform gyrus (corr. V8 by Tootell). V5/MT is a heavily myel. Area in the i of the ascending limb of the inf. temp sulcus near the occipito temp junction on the lateral convexity. Area MST located anterior to V5

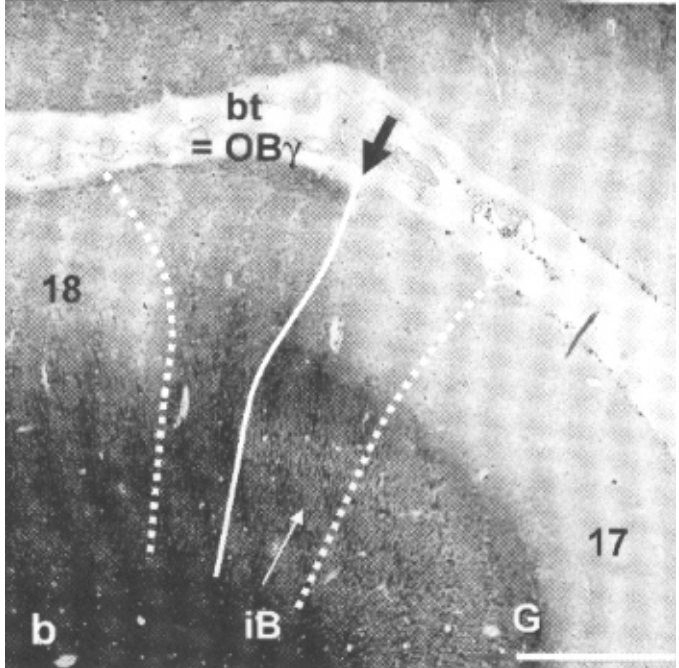
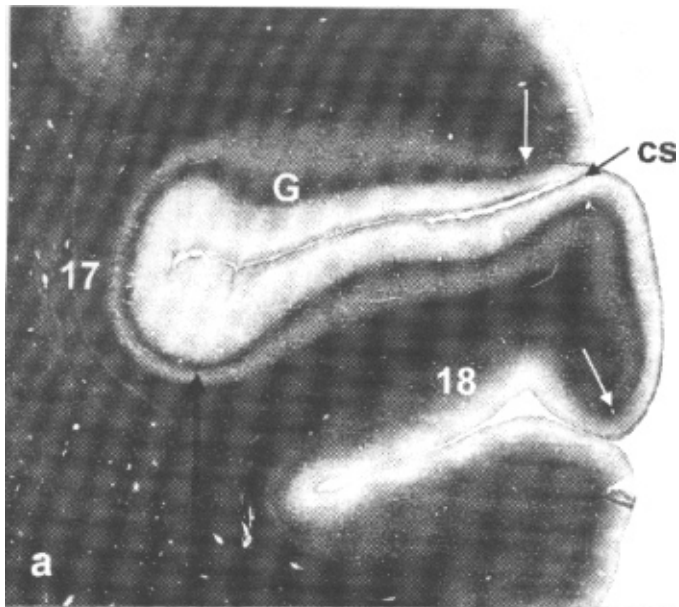


Location of the cerebral area which is active when human subjects perceive visual motion, using PET. The area is similar in location as defined Feld 16, by Flechsig found to be myelinated at birth (Zeki, 1993).

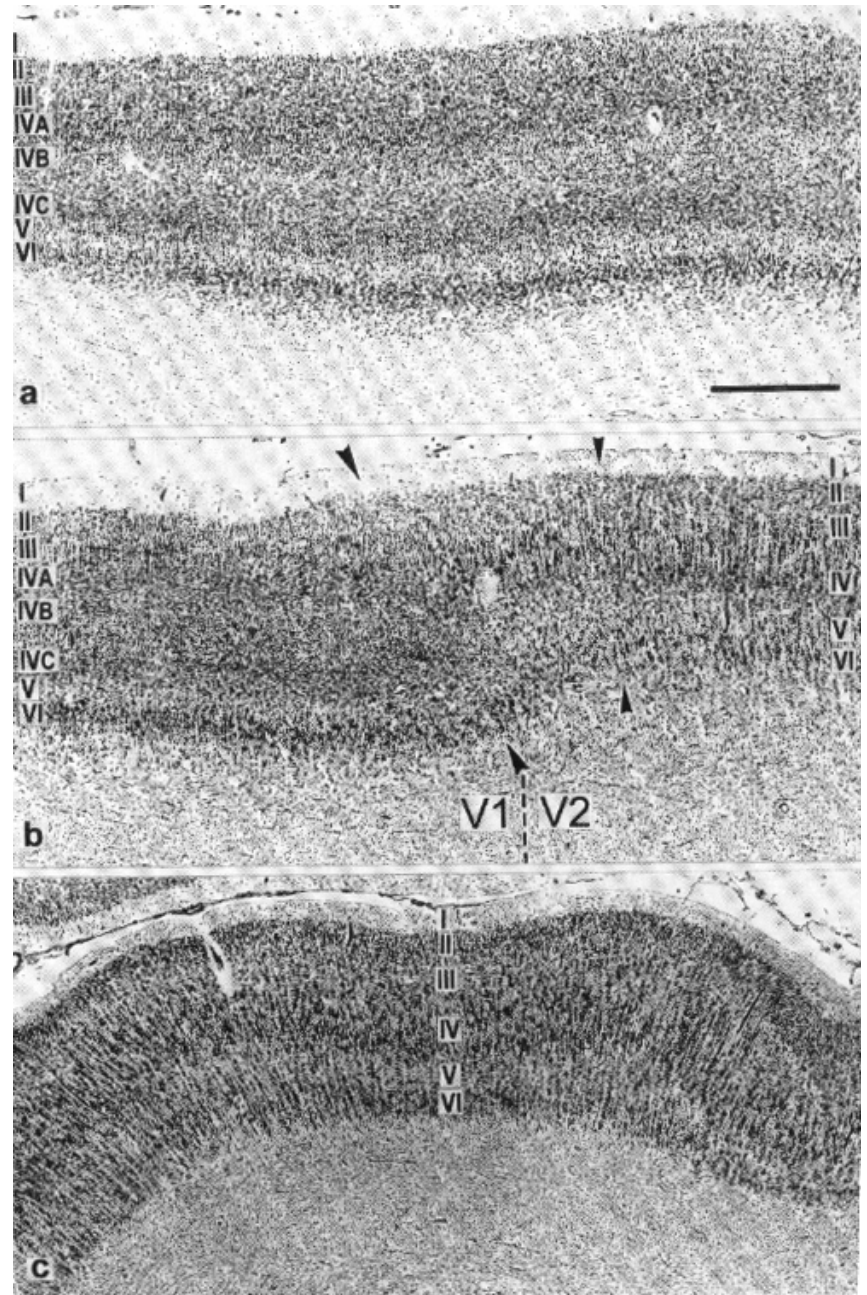


Areal map of the human visual cortex (Tootell et al., 1998)

# Myeloarchitecture of areas 17/18

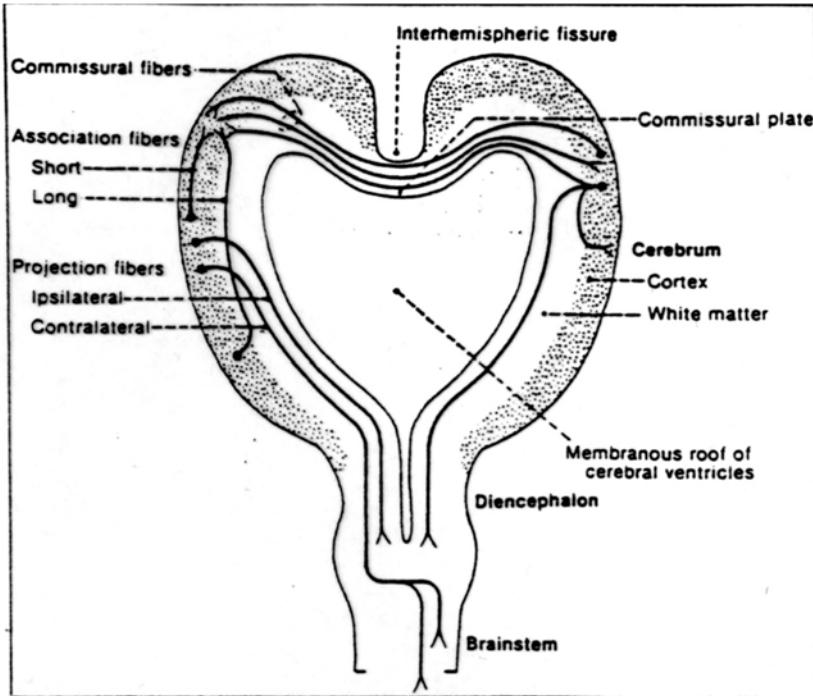


# Visual areas 17 (a,b); 18 (b) and 19 (c)

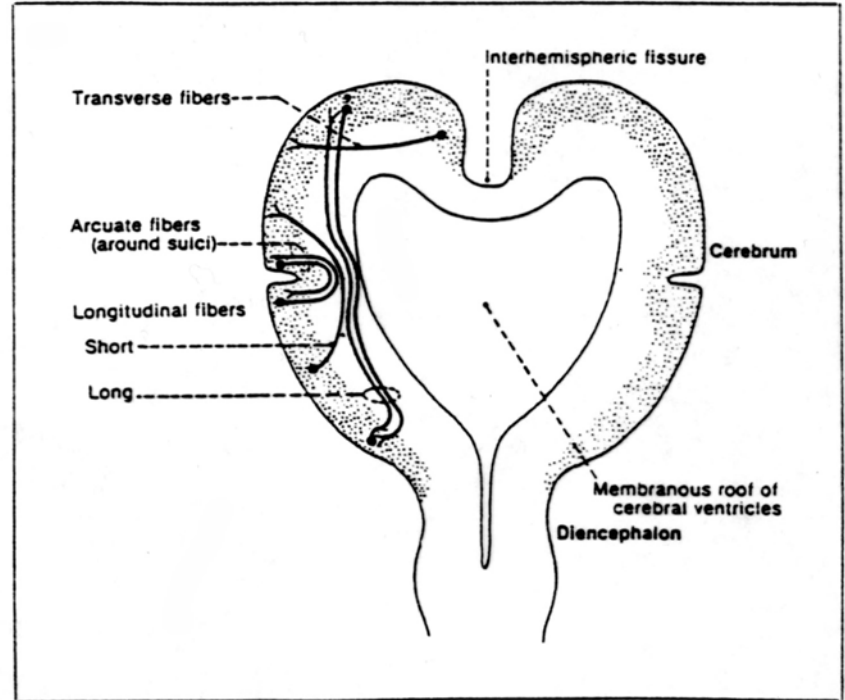


G=Gennari stripe, cs=calcarine sulcus. From Zilles, 2004

# Commissural, association and projection fibers

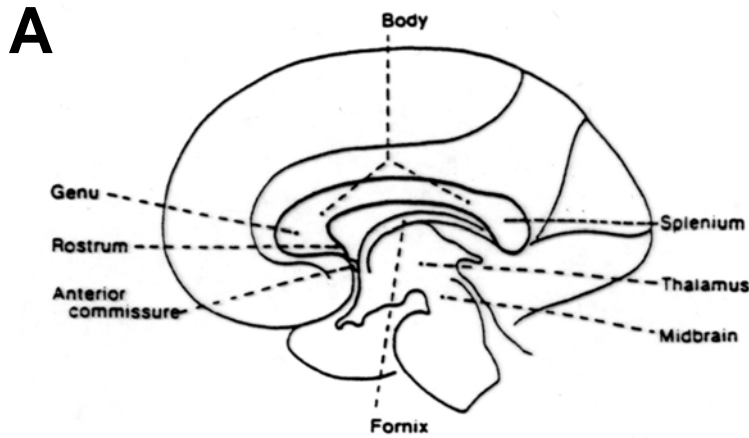


Dorsal view of the prosencephalon and brainstem showing the development of commissural, association and projection fibers (DeMyer, 1988).

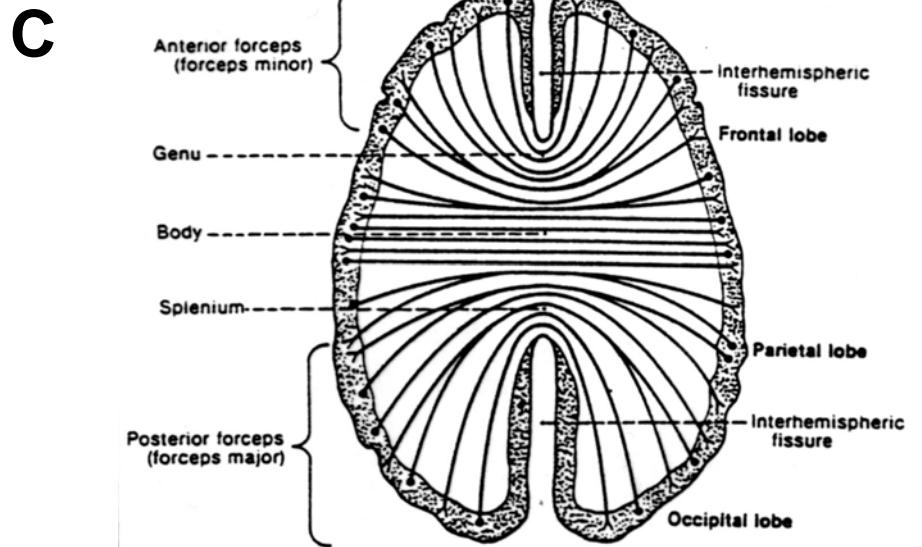


Dorsal view of the prosencephalon showing the development of the short, arcuate, association fibers. Transverse and vertical association fibers of intermediate length criss-cross the deep white matter (DeMyer, 1988)

# The corpus callosum

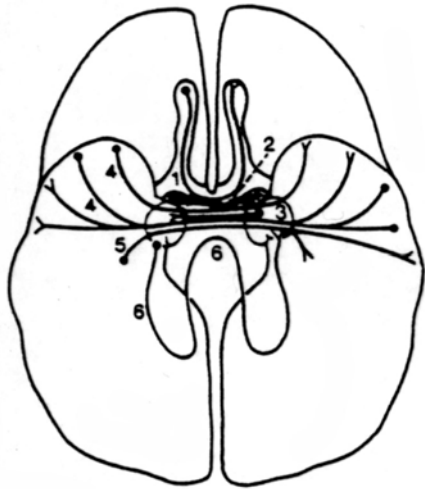


A: Sagittal section of the corpus callosum showing its division into four compartments: rostrum, genu, corpus, splenium (DeMyer, 1988). B: Distribution of degenerating fibers after transection of the entire cc. Note the absence of commissural fibers in area 17, the S1 and M1 hand region (this latter one is not visible because it is largely buried in the central sulcus (Myers, 1965). C: Horizontal section showing the pattern of crossing of callosal fibers (DeMyer, 1988).



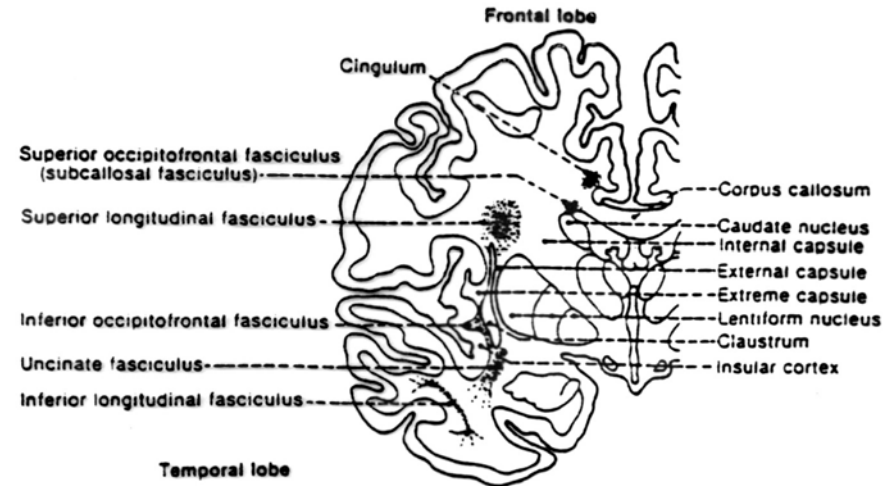
# Anterior commissure and long association fibers

**A**

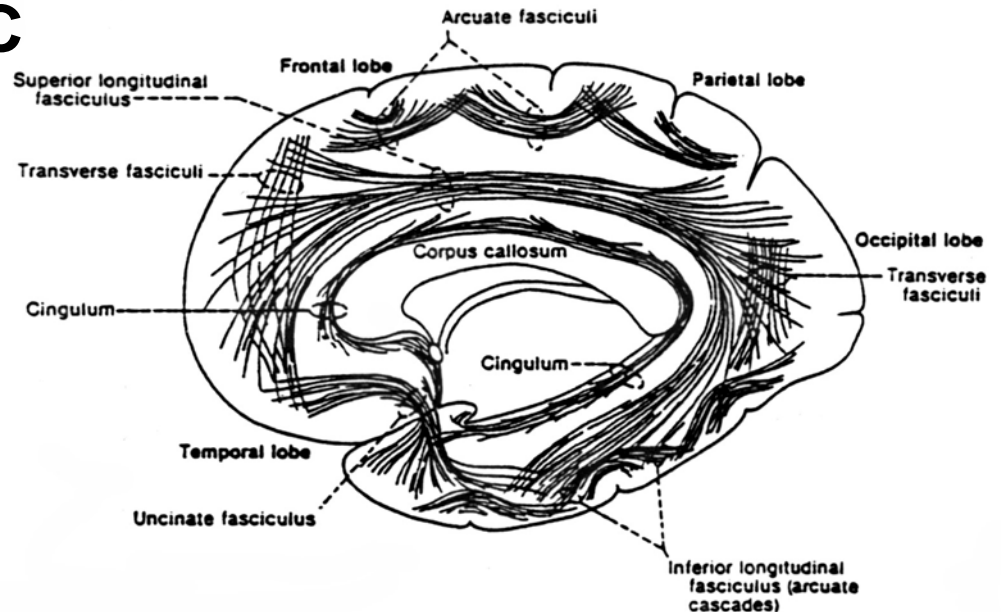


**A:** Ventral view showing of the fibers of the anterior commissure. 1: interbulbar (to bulbus olfactorius); 2: intertubercular (to olfactory tubercle); 3: interamygdaloid; 5: interparahippocampal; 6: stria terminalis (interamygdaloid). **B:** Coronal section showing several of the long association fibers; **C:** Sagittal section. Note the location of the superior longitudinal fascicle connecting fronto-occipital areas, the inferior longitudinal fascicle, the uncinate fascicle (fronto-temporal fibers), the cingulum (cingulate-parahippocampal fibers). The short association (arcuate fibres) are also shown (DeMyer, 1988).

**B**



**C**



# Thalamocortical connections

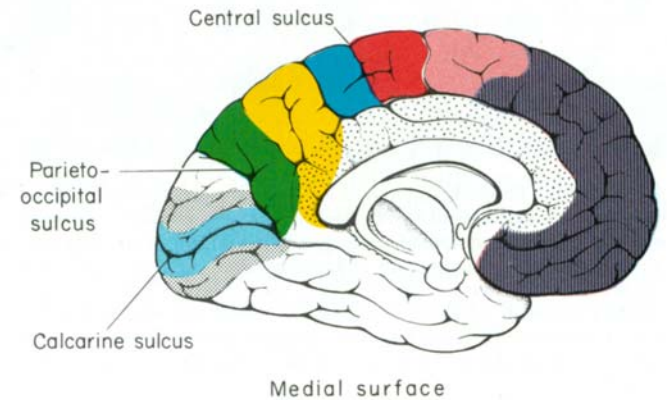
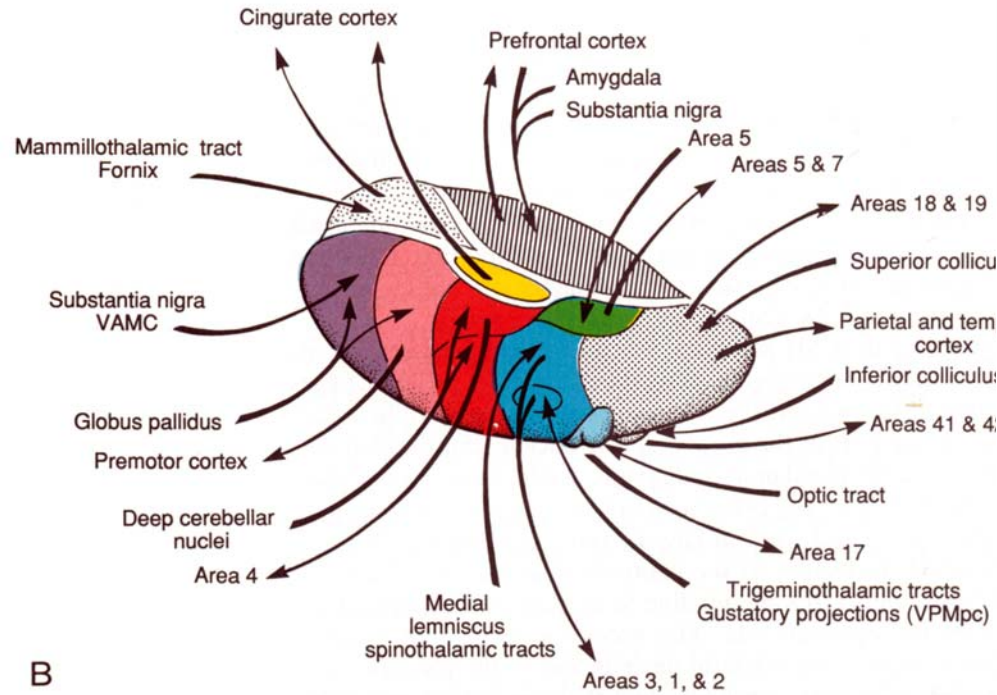
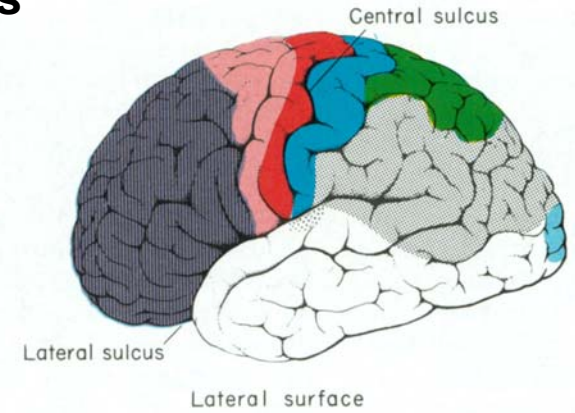
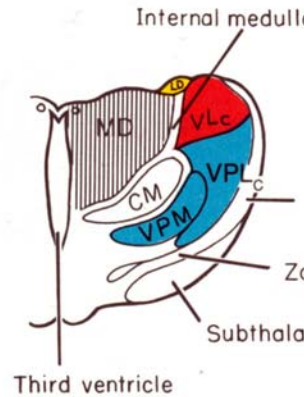
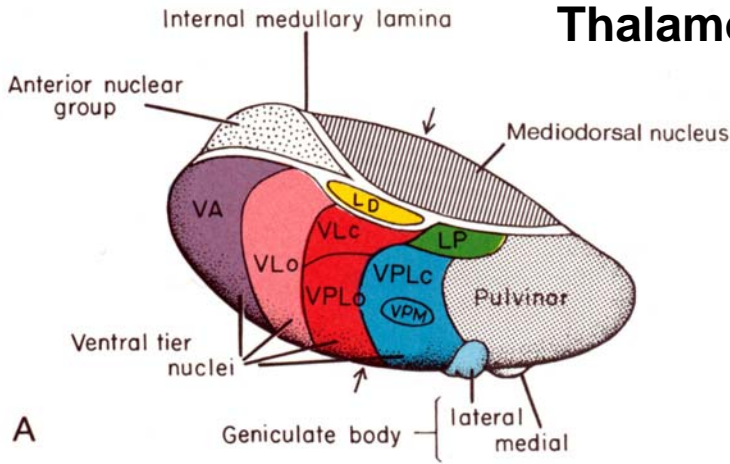
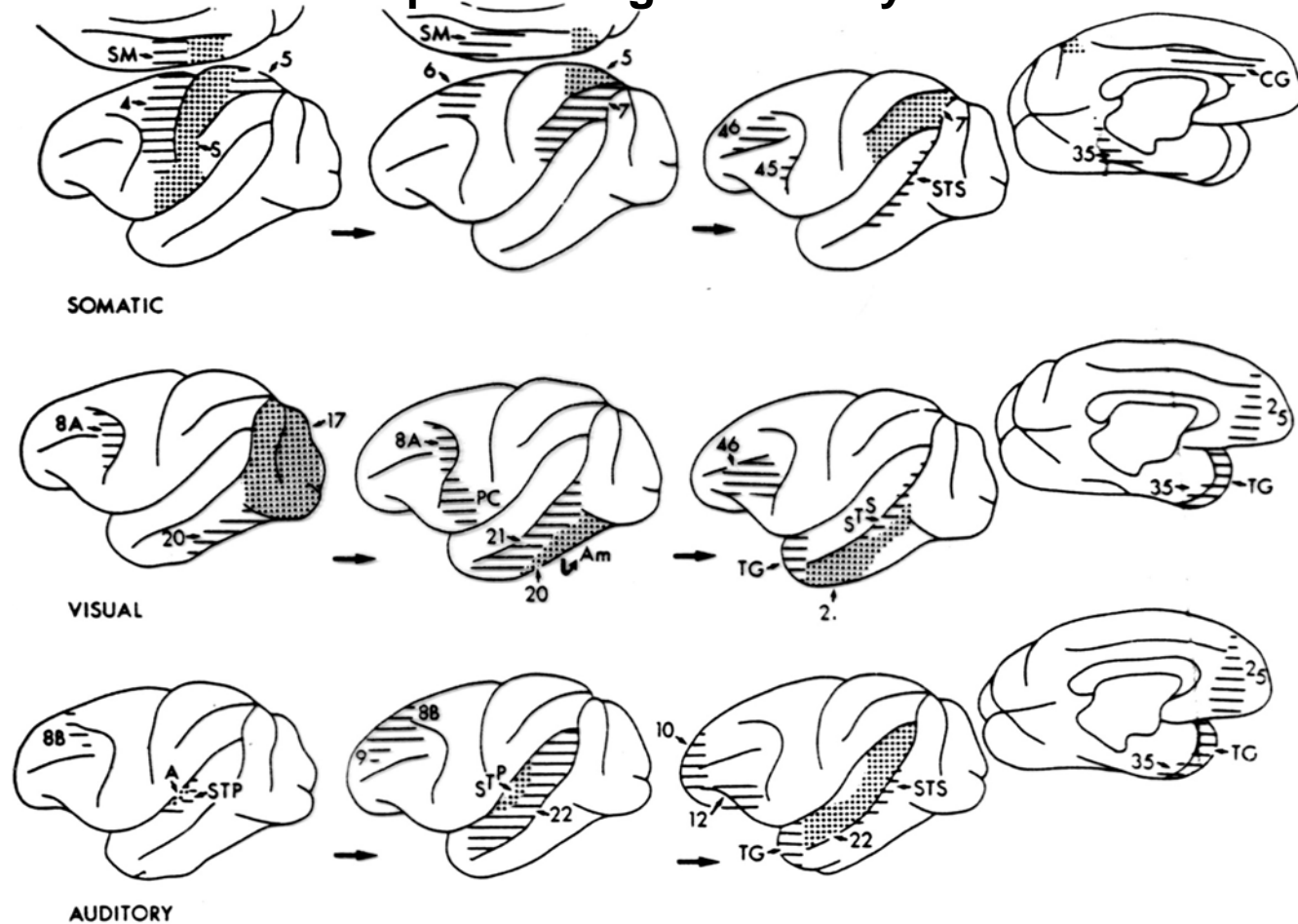


Diagram of the major thalamic nuclei, their inputs and their cortical projection areas. Color coding in the cortex is the same as for the thalamus (Carpenter, 1991)

**TABLE 5.3. Cortical Afferents**

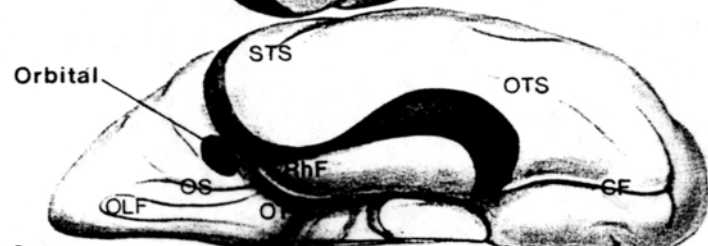
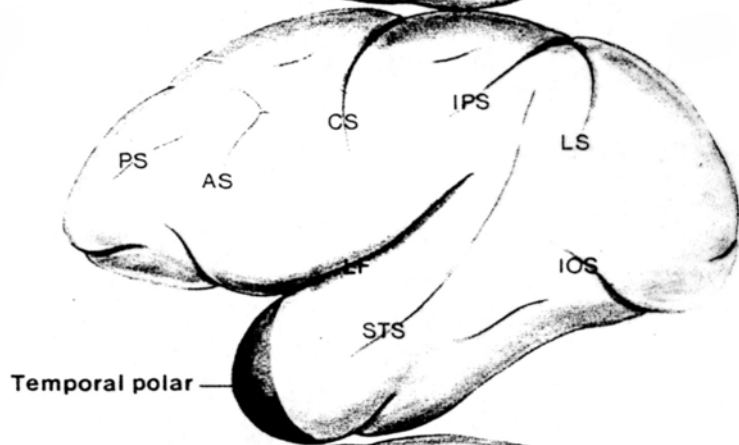
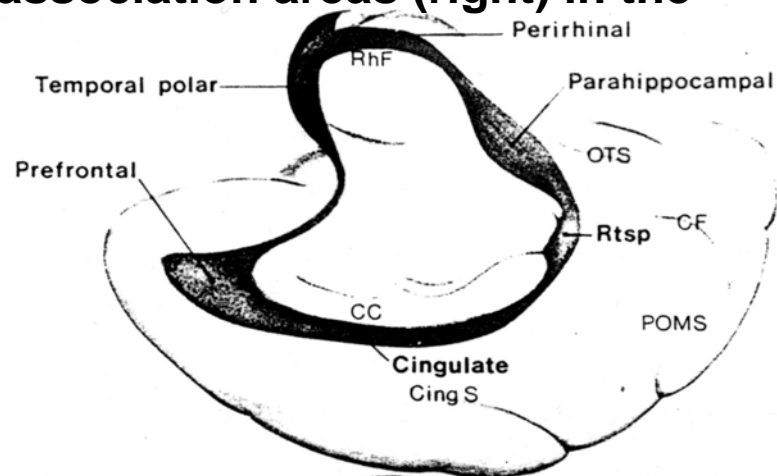
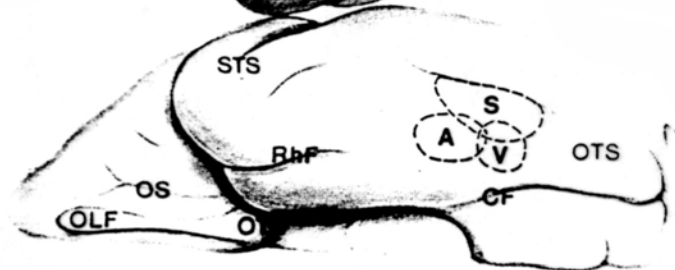
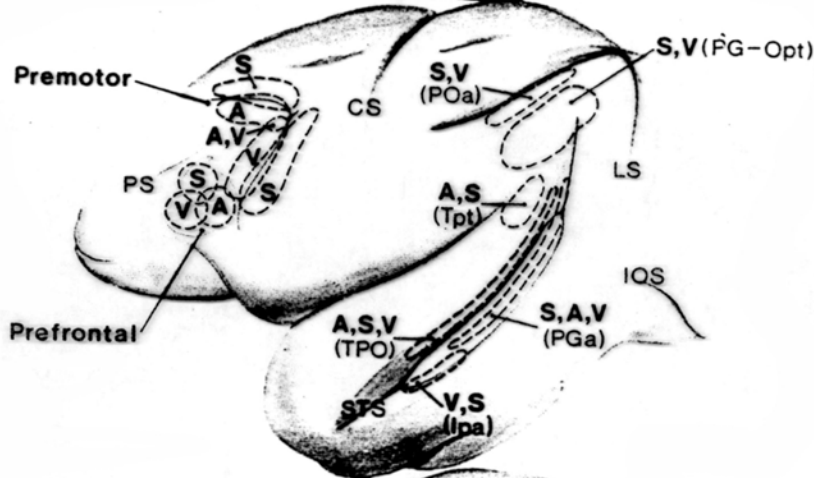
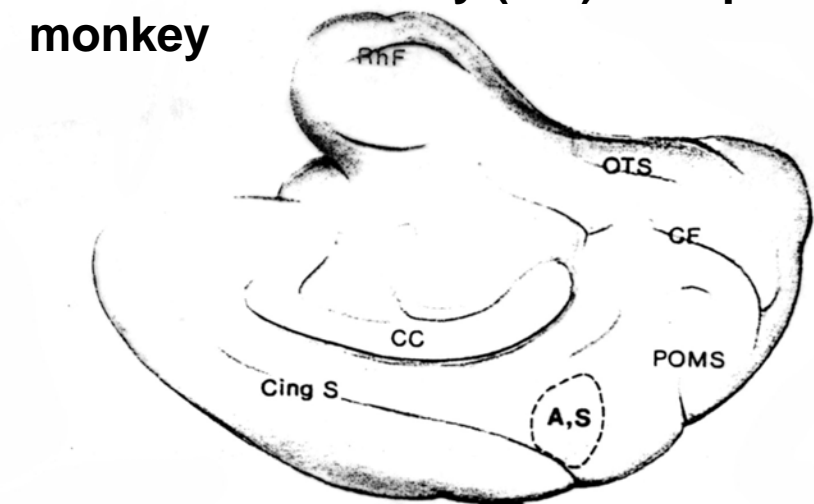
Source	Axons	Distribution	Transmitter	Termination layer
VL, VPL, Pulv, LG, MG, LP	Specific thalamo-cortical afferents	Columnnar	Glu	III, IV
Thalamus paralaminar	Nonspecific thalamo-cortical afferents	Regional	Glu	I
Thalamus intralaminar	Nonspecific thalamo-cortical afferents	Regional		V, VI
Cortex, other hemisphere	Callosal afferents	Columnnar	Glu	III, IV
Cortex, same hemisphere	Corticocortical afferents	Columnnar	Glu	II, III, IV
Nucleus of the raphe	Serotonergic	Diffuse	5HT	I + all layers
Substantia nigra	Dopaminergic afferents	Prefrontal, limbic archicortex	Dopamine	V, VI (prefrontally)
Locus coeruleus	Noradrenergic afferents	Diffuse	Noradrenaline	All layers
Basal forebrain nuclei	Cholinergic afferents	Regional	Acetylcholine	In particular lower layers

## Hierarchical processing of sensory information



Summary diagram showing progression of connections from primary sensory cortices to unimodal association cortices and finally to polymodal association areas. In each diagram, dotted pattern shows projection *origins* and horizontal lines delimit *termination* regions. In the somatosensory systems, for example, S1 gives rise to projections to motor cortex (area 4) and to parietal association area (area 5). Area 5, in turn, gives rise to projections to premotor cortex (area 6) and to posterior parietal cortex (area 7). This latter region projects to polysensory zones in the superior temporal cortex (STS), cingulate gyrus (CG) and perirhinal cortex (area 35). (Jones and Powell, modified by Amaral, 1987)

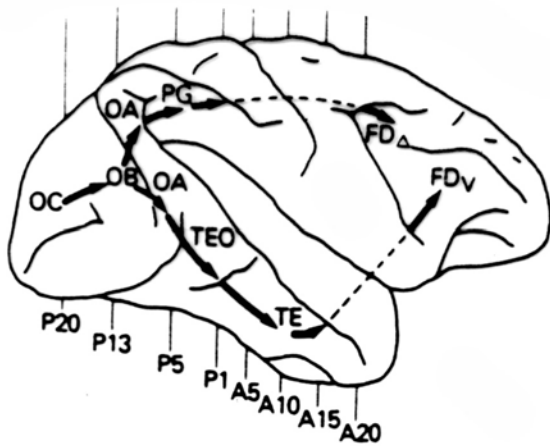
# Multimodal sensory (left) and 'paralimbic' association areas (right) in the monkey



A:auditory, S: somatosensory, V: visual; CS: central sulcus; Cing S: cingulate sulcus; RhF: rhinal fissure; AS: arcuate sulcus; IPS: intraparietal sulcus; PS: principal sulcus

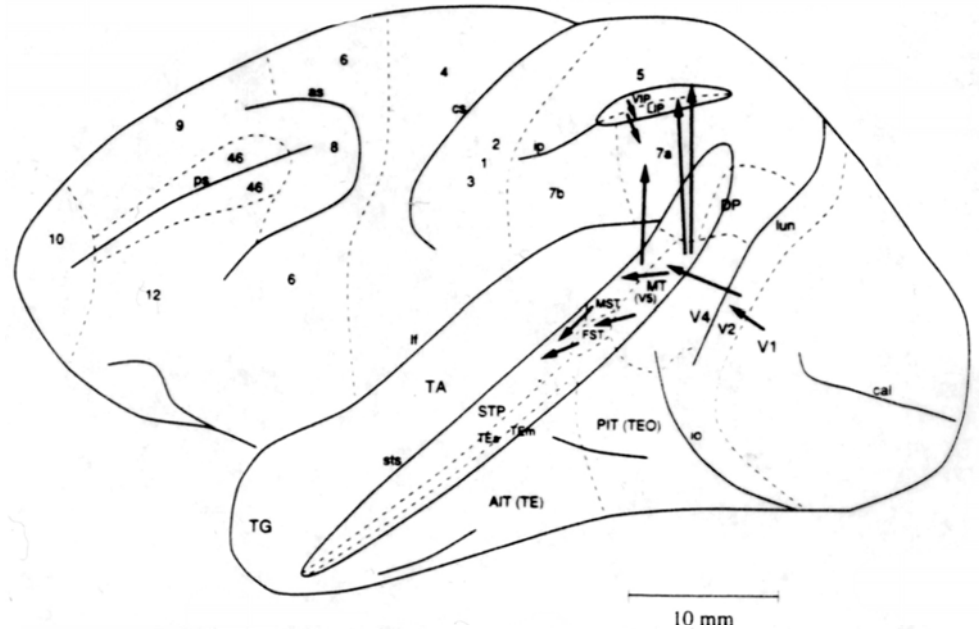
# Visual associational connections

**A**

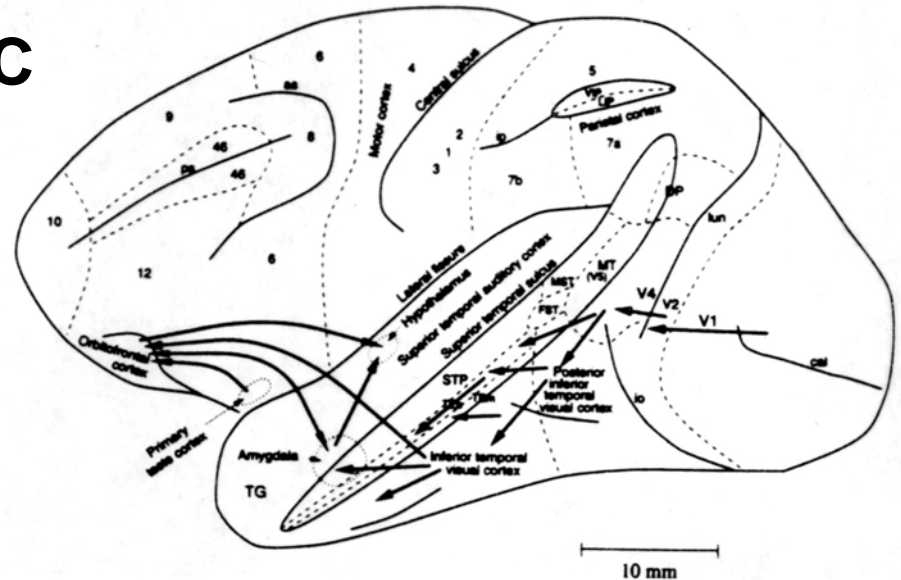


**A:** Two visual cortical pathways in the monkey. Both pathways begin in the primary visual cortex (OC) and diverge in the peristriate cortex (OA and OB) to end in inferior temporal (TEO and TE) and parietal areas (PG). The ventral area is essential for object, the dorsal for spatial vision (Mishkin et al., 1983). **B:** Lateral view of the macaque monkey showing the connection of the dorsal stream from V1 to V2, MST, with some connection reaching the frontal eye field. **C:** Connection of the ventral stream from V1, V2 and V4, the inferior temporal visual cortex, etc with some connections reaching the amygdala and orbitofrontal cortex (B and C from Rolls and Treves, 1998)

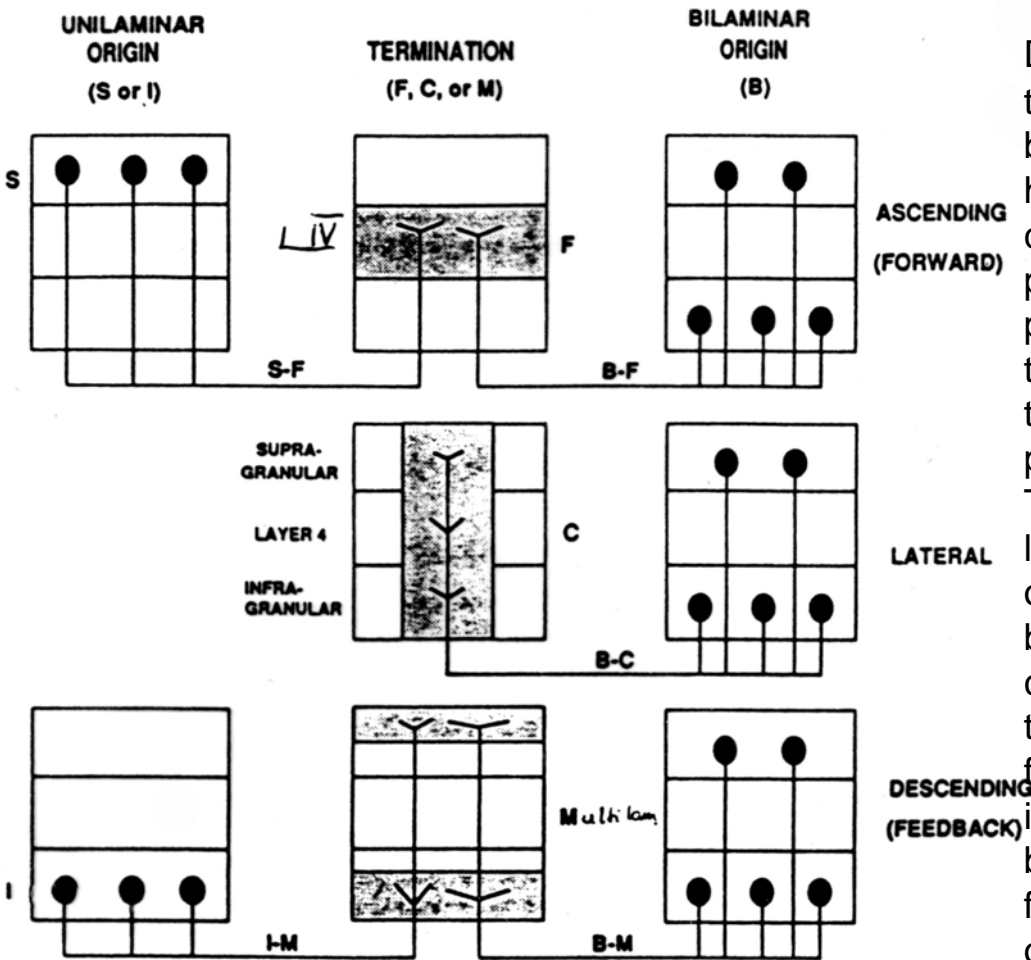
**B**



**C**

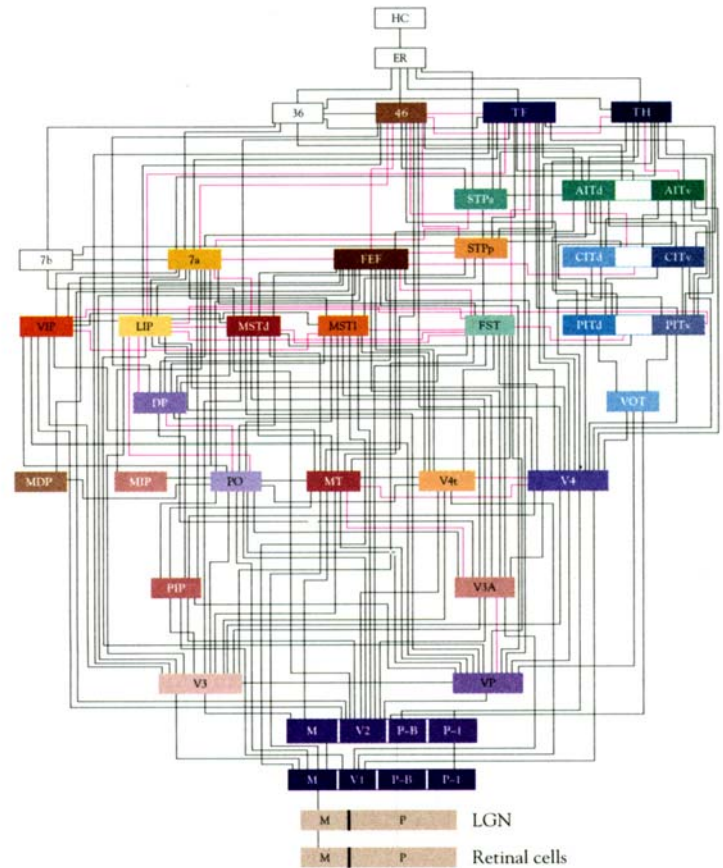
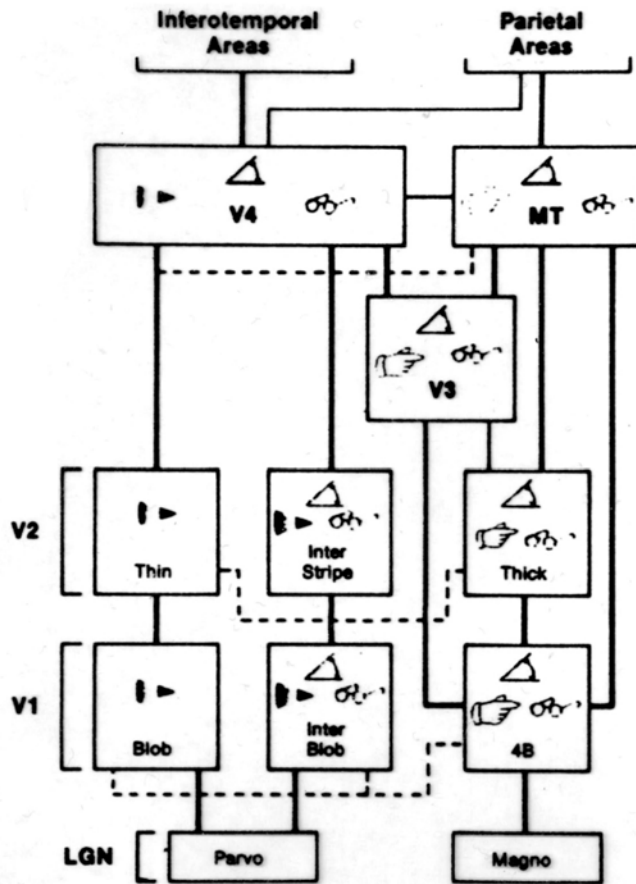


# Analysis of the pattern of neocortical connectivity



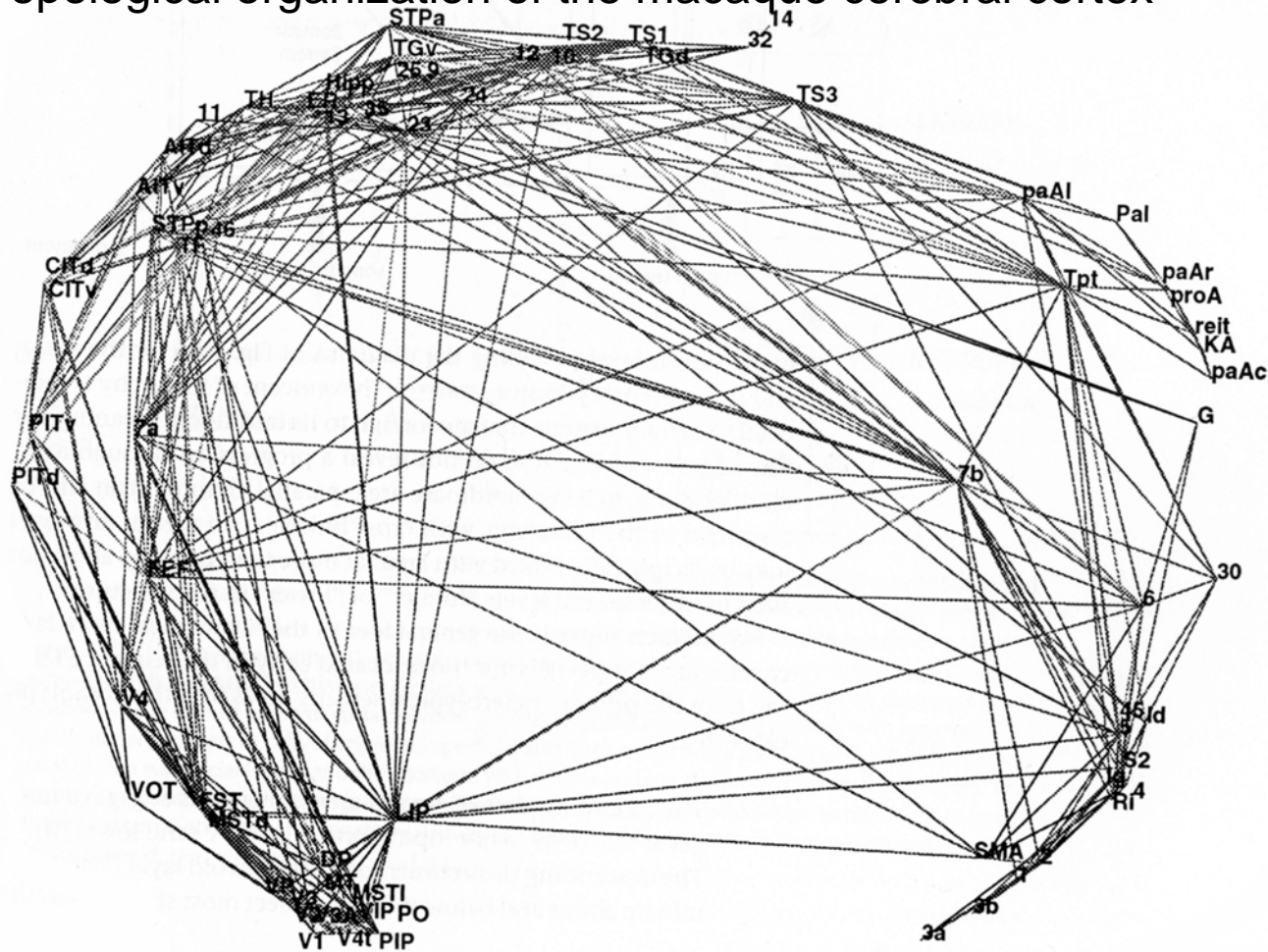
Diagrams of the laminar patterns of origin and termination of cortico-cortical connections used by Felleman and Van Essen (1991) to assign hierarchical positions to cortical areas. The central column shows the characteristic patterns of terminations: the **F** pattern –with preferential termination in L 4; the **C** pattern – the columnar pattern with equal density of terminations in all cortical layers; and the **M** pattern- a multilamellar pattern that avoids L 4. There are several characteristic patterns of locations of cells of origin. The **S** pattern, with origins in superficial layers and the **B** pattern: bilaminar with approximately equal numbers of cells of origin in superficial and deep layers with termination in L 4 are characteristic for feed-forward connections. The **I** pattern, with origins in the infragranular layers and the **B** pattern with bilaminar terminations are characteristic for feedback connections. Finally, the bilaminar origin and columnar termination is typical for lateral (equifunctional) connections.

# Distributed and hierarchical organization in neocortical systems



**A:** Schematic diagram of the main anatomical connections and neuronal selectivities in the immediate visual areas of the macaque monkey. LGN=lateral geniculate nucleus with the parvocellular (narrow-band) and magnocellular (broad-band) parts; 4B lamina 4B of V1. Blob and thin stripes rich in cytochromoxidase (CO) regions; Thick: thick stripes rich in CO; rainbow: tuned or opponent wavelength selectivity by at least 40% of neurons; angle: orientation selectivity by at least 20% of neurons; spectacles: binocular disparity selectivity by at least 20% of neurons; pointing hand: direction of motion selectivity by at least 20% of neurons **B:** Parallel and hierarchical organization in visual cortical areas: there are 305 pathways linking areas termed visual (A: DeYoe and van Essen, 1988; B: Felemann and van Essen, 1991)

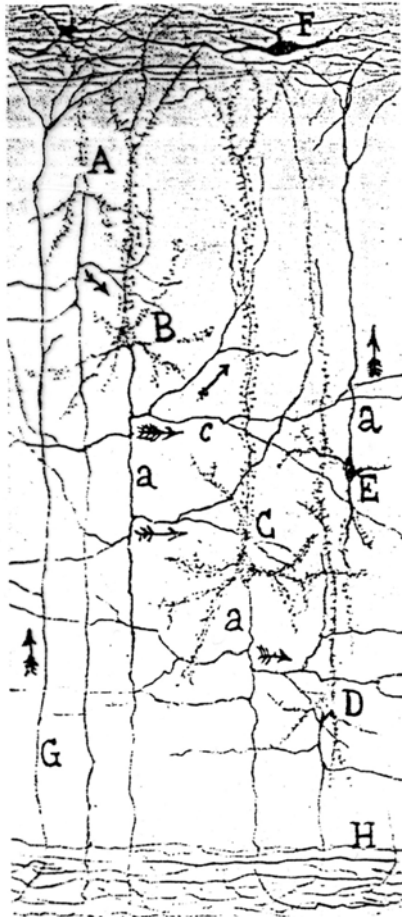
# Topological organization of the macaque cerebral cortex



The topological organization of the macaque cortical areas in terms of their ipsilateral connections, as known prior to 1993. A total of 758 connections between 72 cortical areas are shown; of these 136 are one-way. The connections shown are only 15% of the total possible connections. The structure is a best-fit representation of the topology of the system in two dimensions. The position of each area is specified as to minimize distance between interconnected areas, and maximize distances to areas which is not interconnected. Areas with similar patterns of inputs and outputs tend to be placed close together, those with dissimilar patterns far apart. The cortex is represented in a state of connective tension, not in its true anatomical space (Young, 1993)

## CORTICAL CIRCUITS: Cajal

A

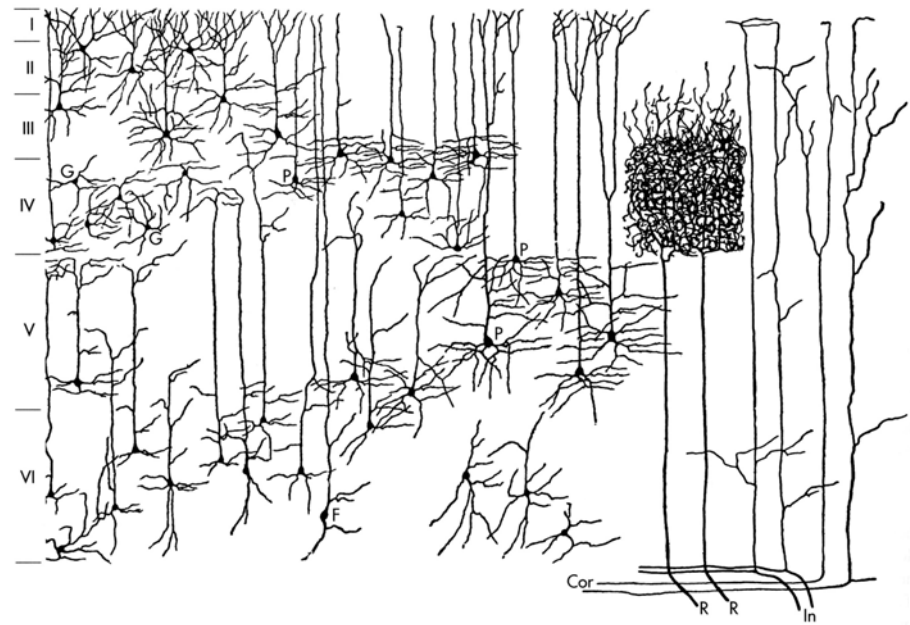


A: Cortical circuits. B: Type of spines of cerebral pyramids of rabbit, a child of two months, spines of a one-month-old cat; portion of a dendrite of a spinal motor neuron of a cat (Cajal, 1933)

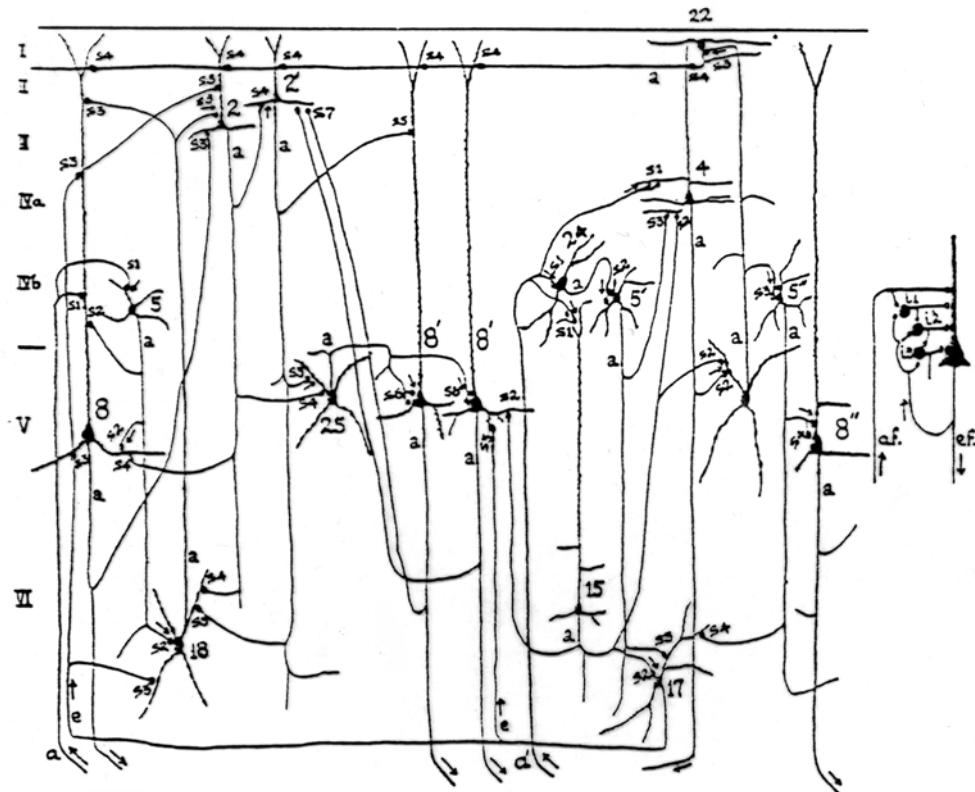
B



# CORTICAL CIRCUITS: Lorente de No



Cells, arborization of corticopetal axons and intracortical circuits (Lorente de No, 1938). Note the recurrent (reverberating) circuits.



# CORTICAL RESIDENT CELLS: E.G. Jones

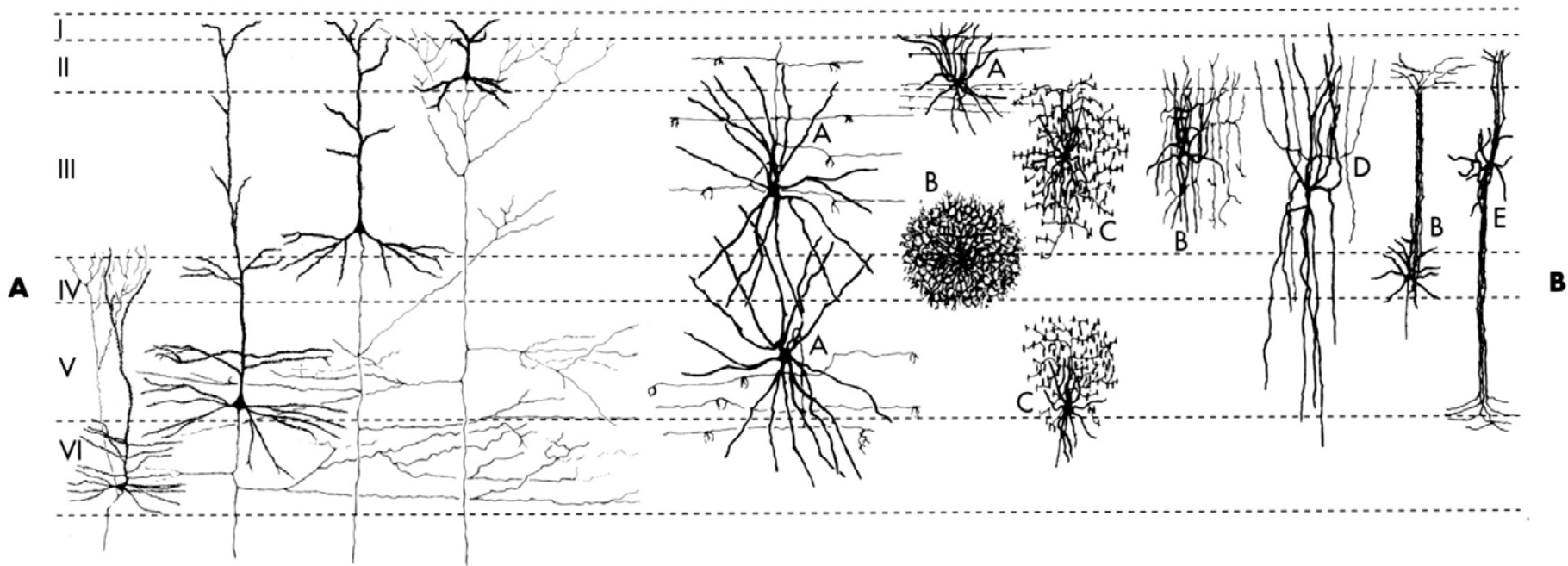
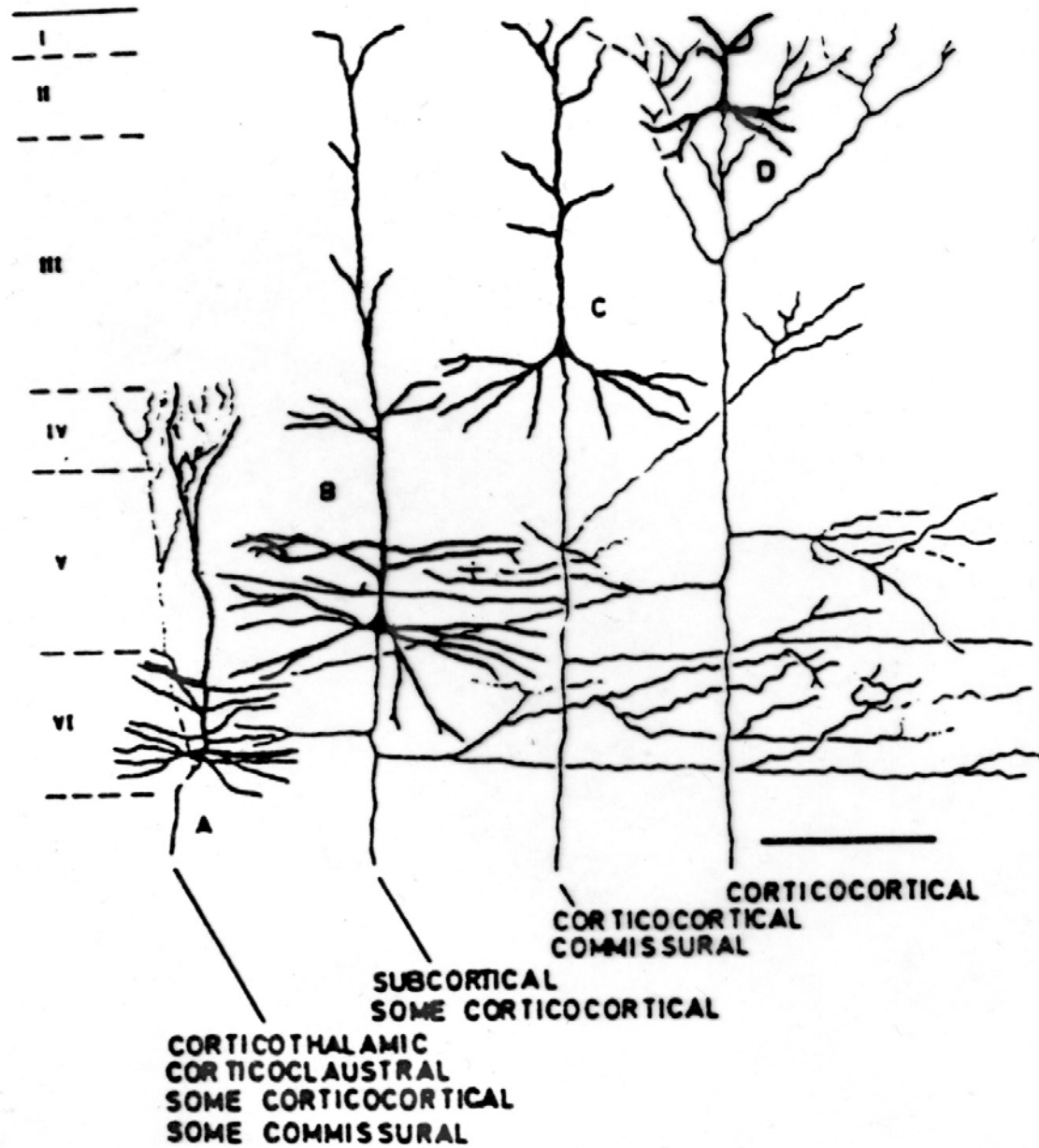


FIGURE 22-4

Neocortical neurons. **A**, Pyramidal neurons in different layers have characteristically different soma sizes and patterns of distribution of axon collaterals. **B**, Nonpyramidal neurons come in a variety of sizes and shapes; many have names attributable to their shapes. Basket cells (**A**) are usually large and make basket-shaped endings that partially surround the cell bodies of pyramidal cells. Other kinds of smaller multipolar cells (**B**) may have elaborate dendritic and axonal arborizations. Chandelier cells (**C**) have vertically oriented synaptic “candles” that end on the initial segments of pyramidal cell axons. Bipolar cells (**D**) have dendrites that both ascend and descend, and double bouquet cells (**E**) have axons that both ascend and descend. (**A** from Jones EG: Identification and classification of intrinsic circuit elements in the neocortex. In Edelman GM, Gall WE, Cowan WM, editors: *Dynamic aspects of neocortical function*, New York, 1984, John Wiley and Sons. **B** from Hendry SHC, Jones EG: *J Neurosci* 1:390, 1991.)

Pyramidal cells contain glutamate, most of the nonpyramidal cells, except the small spiny, putatively excitatory cell of layer IV are likely to be GABAergic. Long, bitufted cell colocalizes GABA and neuropeptides or acetylcholine and peptides.



Schematic drawing of the major targets of pyramidal cells in different layers of the of the somatosensory cortex in monkeys (E.G. Jones, 1985)

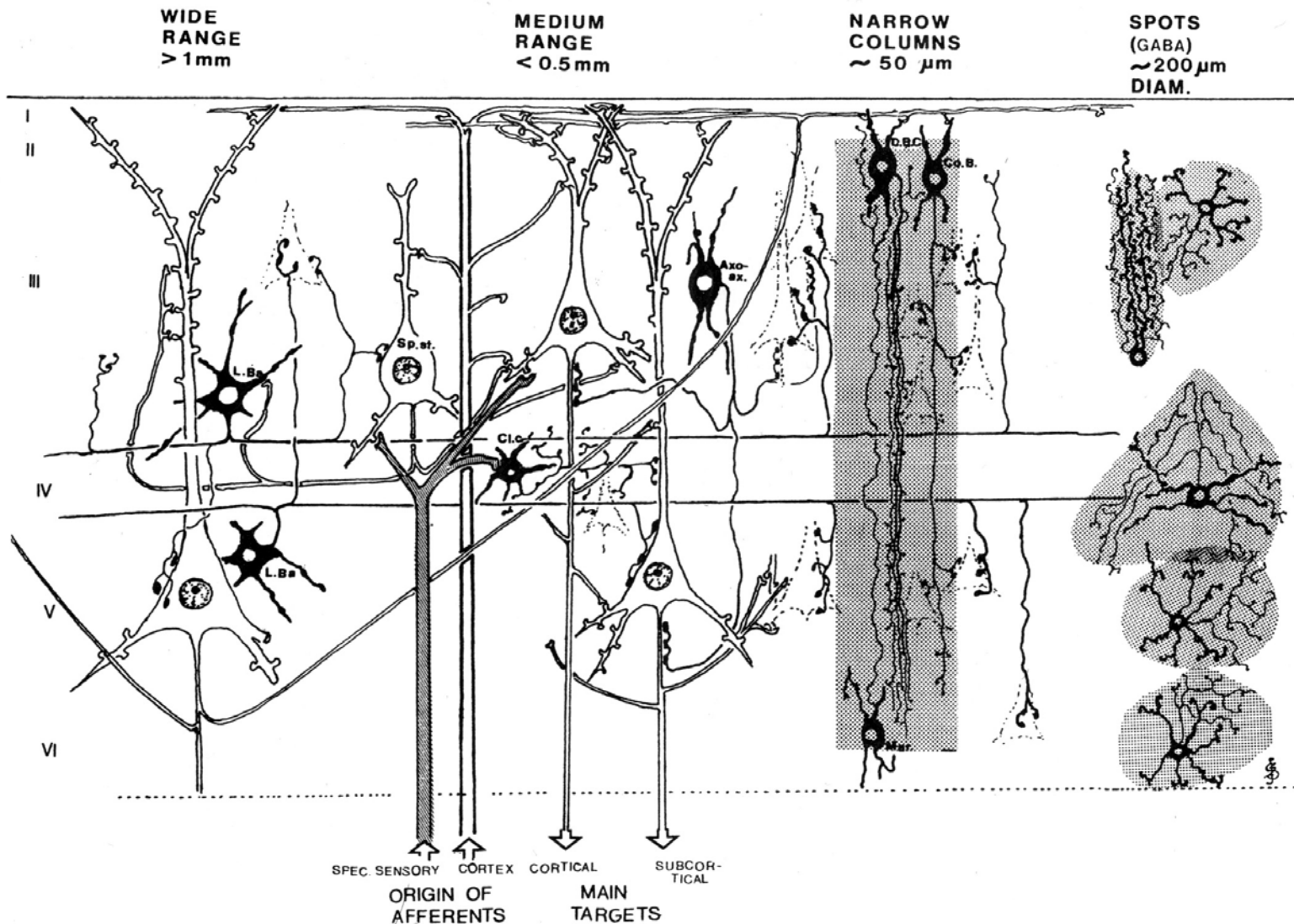


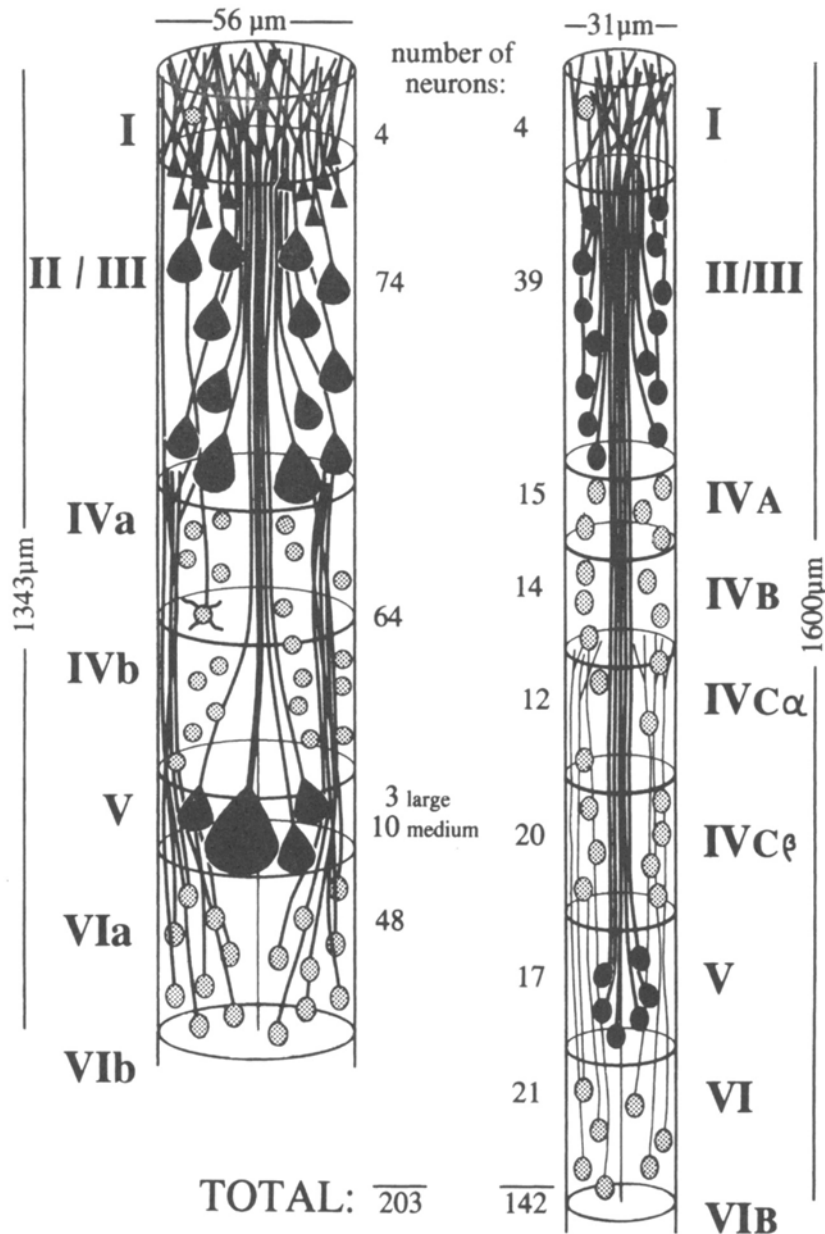
Diagram illustrating the main internal connections of the cerebral cortex. Excitatory neurons and their connections are drawn in outlines, inhibitory neurons in full black. Large-distance excitatory connections (1-5 mm) are given by large pyramidal cells of layer V. Large basket cell (L.Ba) are causing tangential inhibition at distances of 1 mm. The excitatory spiny stellate cells (Sp.st) act mainly at medium range distances. The two main input lines (specific sensory afferents indicated by hatching and cortico-cortical afferents) act at medium range. Inhibitory neurons: axo-axonic; columnar basket (CoB), double bouquet cells of Cajal (C.B.), Martonotti (Mar). Various inhibitory neurons with spot-like regions are indicated at right (Szentagothai, 1993)

# AREA 17

## CAT

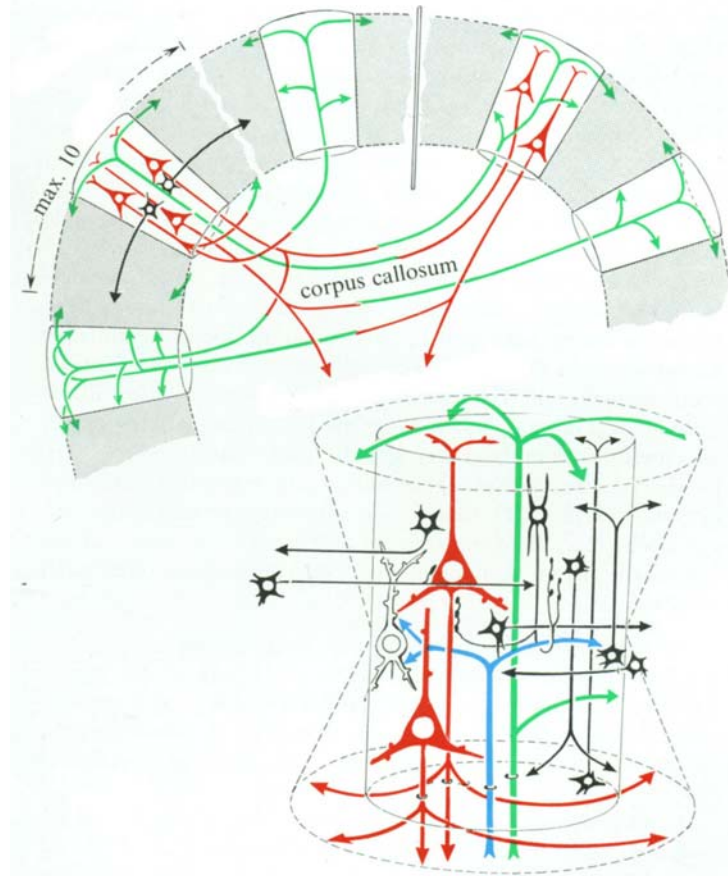
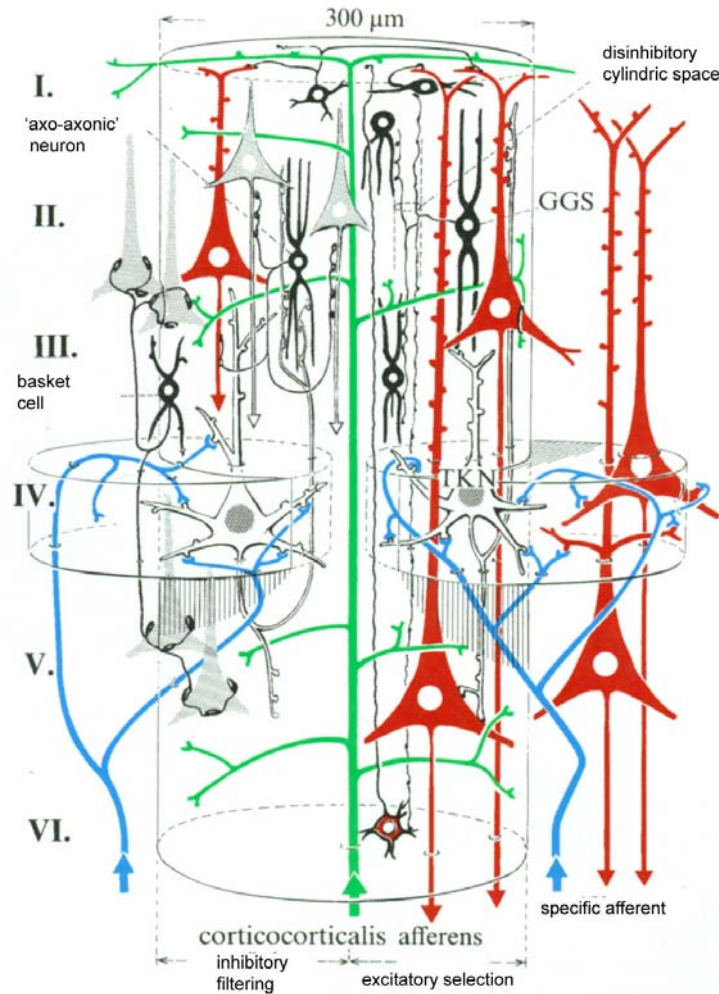
## MONKEY

### Cortical Moduls I. Dendritic bundles



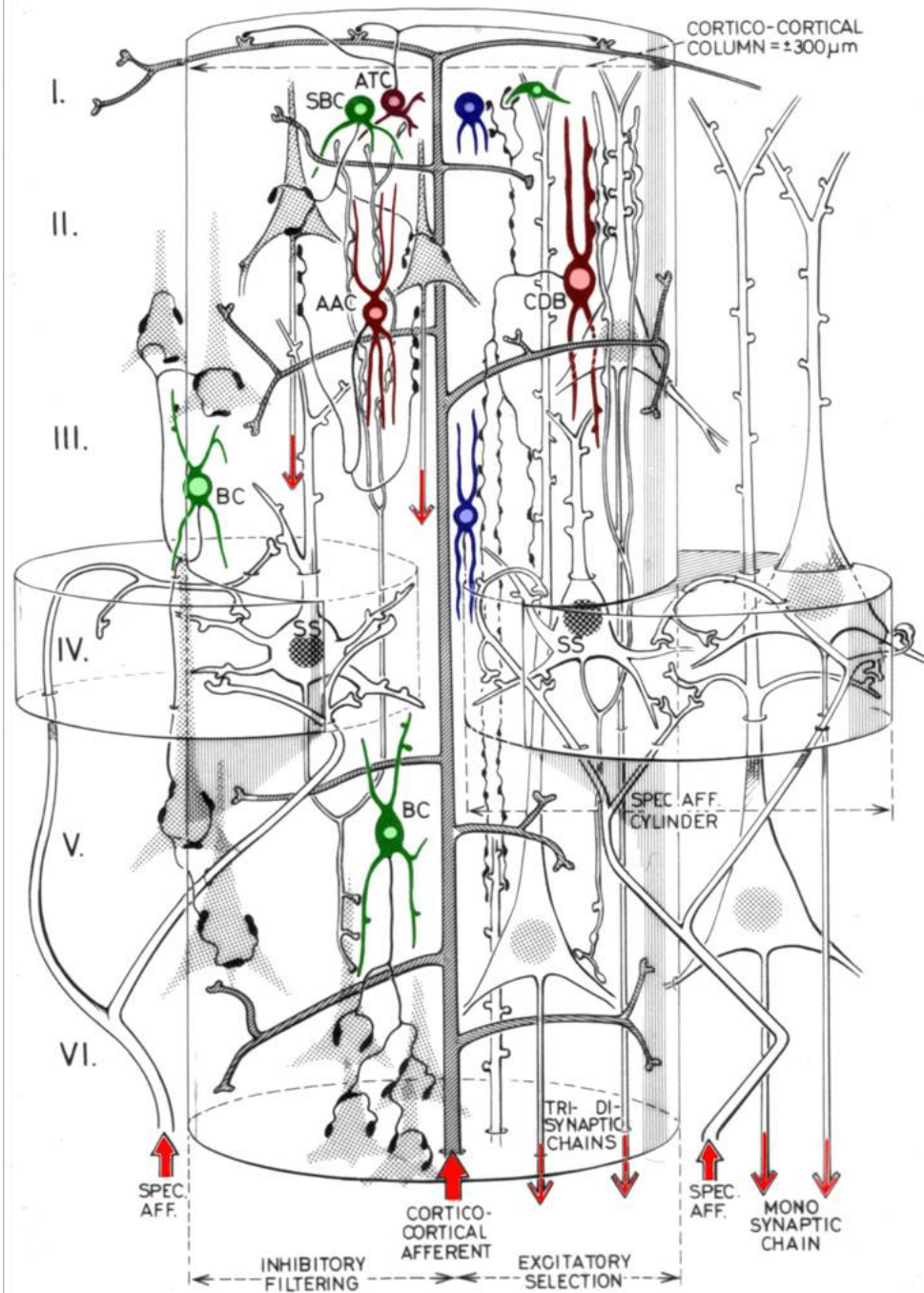
The pyramidal cell modules in cat and monkey visual cortex, drawn to show the relative thickness of the cerebral layers, the numbers of neurons in each layer, and the dendritic bundles of L V pyramidal neurons. The inhibitory interneurons (16-20% of the total) are not shown. Cells of L IV shown without dendrites are spiny stellate cells, the excitatory interneurons (lightly shaded). The dendrites of L VI pyramidal cells (also lightly shaded) project vertically tp only to L IV. (Peters and Yilmez, 1993).

# Cortical Moduls II. The callosal and associational columns: Szentagothai



Interconnections of associational and callosal columns. The output of each column originate from pyramidal cells, their terminals axonal arborizations are labeled green. Ipsilateral connections maximally upto 10 columns. The lower right scheme shows some of the dynamic features: in L I and VI the excitation expands the diameter of the column, in L IV, the inhibition shrinks the cylinder (Szentagothai)

Arrangement of neurons and local circuits in one cortical columnar module. Pyramidal cells :red; specific afferents blue; cortico-cortical afferents: green; inhibitory neurons: solid black; TKN: spiny stellate excitatory neuron; GGS: inhibitory neuron (double-bouquet cell of Cajal) connected to other inhibitory neurons. The effect of the Martinotti cell in L VI spread upto LI (see fig. on following page)



CORTICO-CORTICAL COLUMN =  $\pm 300\mu\text{m}$

I.  
II.  
III.  
IV.  
V.  
VI.

SBC ATC

AAC CDB

BC SS

SS

BC

TRI- DI- SYNAPTICAL CHAINS

SPEC. AFF.

SPEC. AFF.

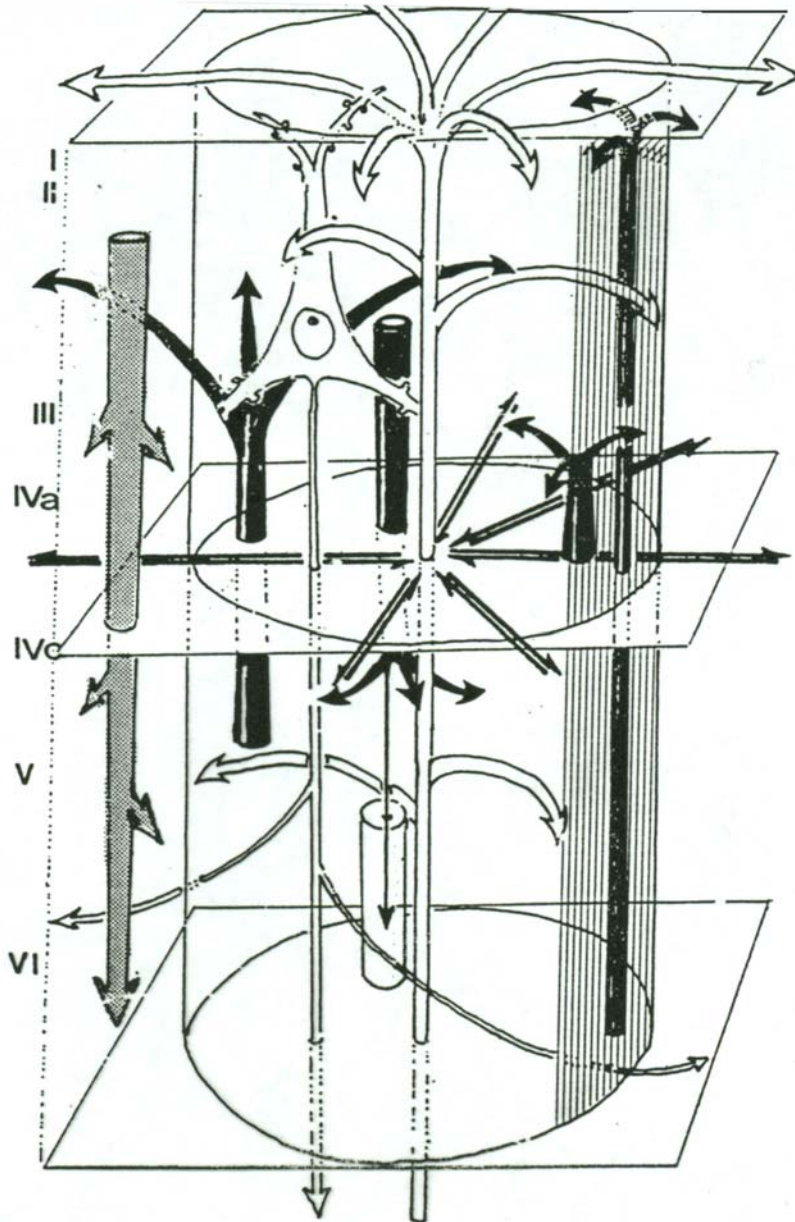
MONO SYNAPTIC CHAIN

CORTICO-CORTICAL AFFERENT

INHIBITORY FILTERING

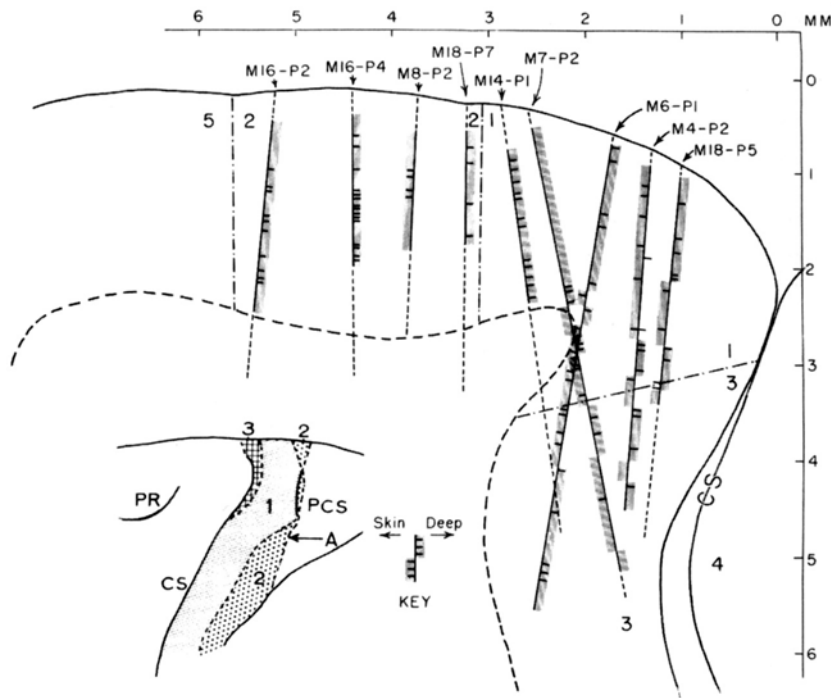
EXCITATORY SELECTION

## Intracolumnar Inhibitory modules

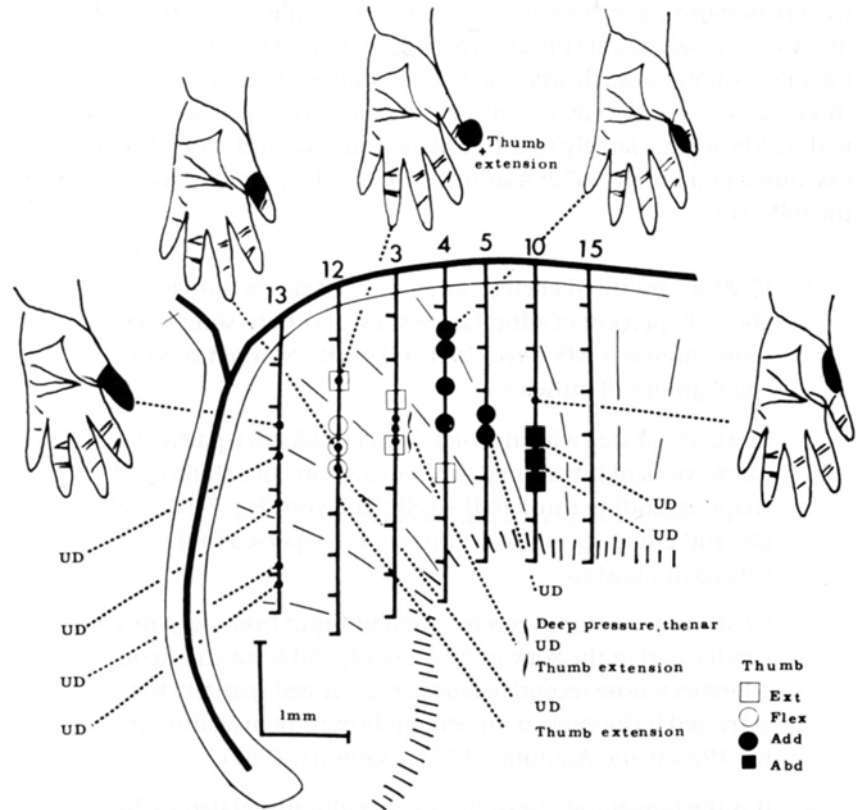


Interlaminar connexions for excitation and inhibition are shown by arrows connecting different layers of the visual cortex. A cortico-cortical (excitatory) afferent is drawn in the middle of the cylinder. Specific sensory afferents are omitted. A L III pyramidal cell is drawn in upper left. Inhibitory connections are most widely spread in L IVc and from L IVc to IVa (large basket cell). There is a major inhibitory input from L V cell into L III and from L VI to L I and II (extreme right: Martinotti cell). There is a massive inhibitory input from L III to the bottom of L IV and into the upper layers of L V. Descending stippled arrow at extreme left corresponds to vertically descending largely disinhibitory connexions by double bouquet cells (Szentagothai).

# Columnar organization of the sensory and motor cortices

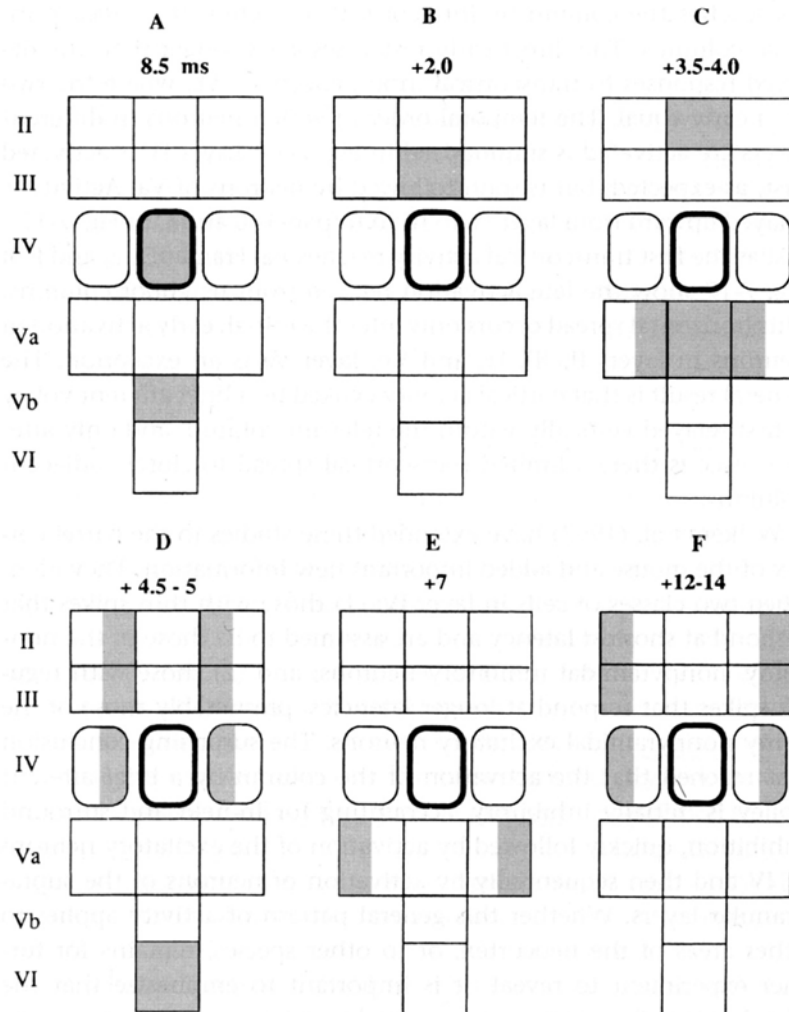


Lower inset shows the cytoarchitectural areas through which the electrode penetrations were made. Penetrations made perpendicular to the cortical surface and passing down parallel to its radial axis encountered neurons all of the same modality type. As the penetrations were made more anteriorly in areas 1 and 3, where the vertical axis of the cortex rolls, blocks of cells with different modality alternates (Powell and Mountcastle, 1959)



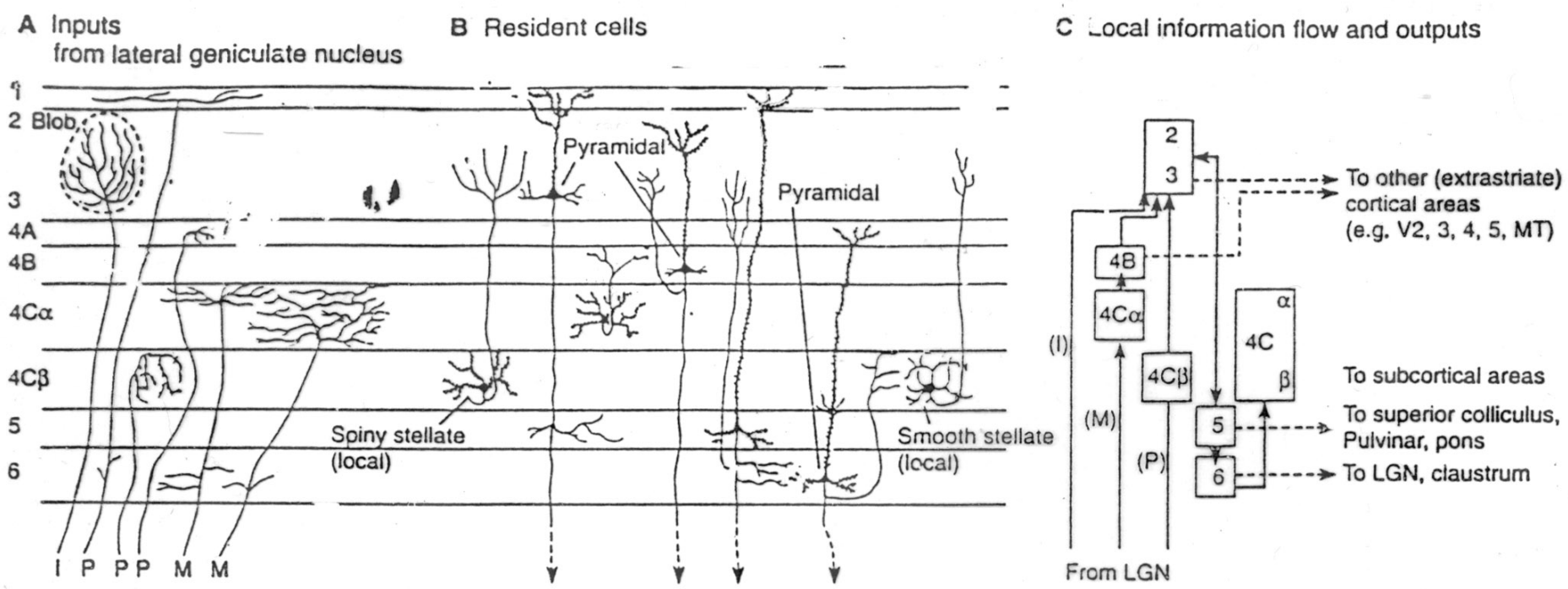
Intracortical microelectrode stimulation in the precentral motor cortex of a monkey that revealed some aspects of the input-output relation for the contralateral thumb and the columnar organization of this cortical area. Microelectrode penetrations are shown by solid lines and numbers. Short horizontal lines indicate sites at which weak currents did not evoke motor responses. Locations where movements were produced and receptive fields of the cells studied are marked by dots or squares and are connected by dashed lines to figurines showing the receptive fields (Asanuma, 1975)

# Columnar organization in the barrel cortex



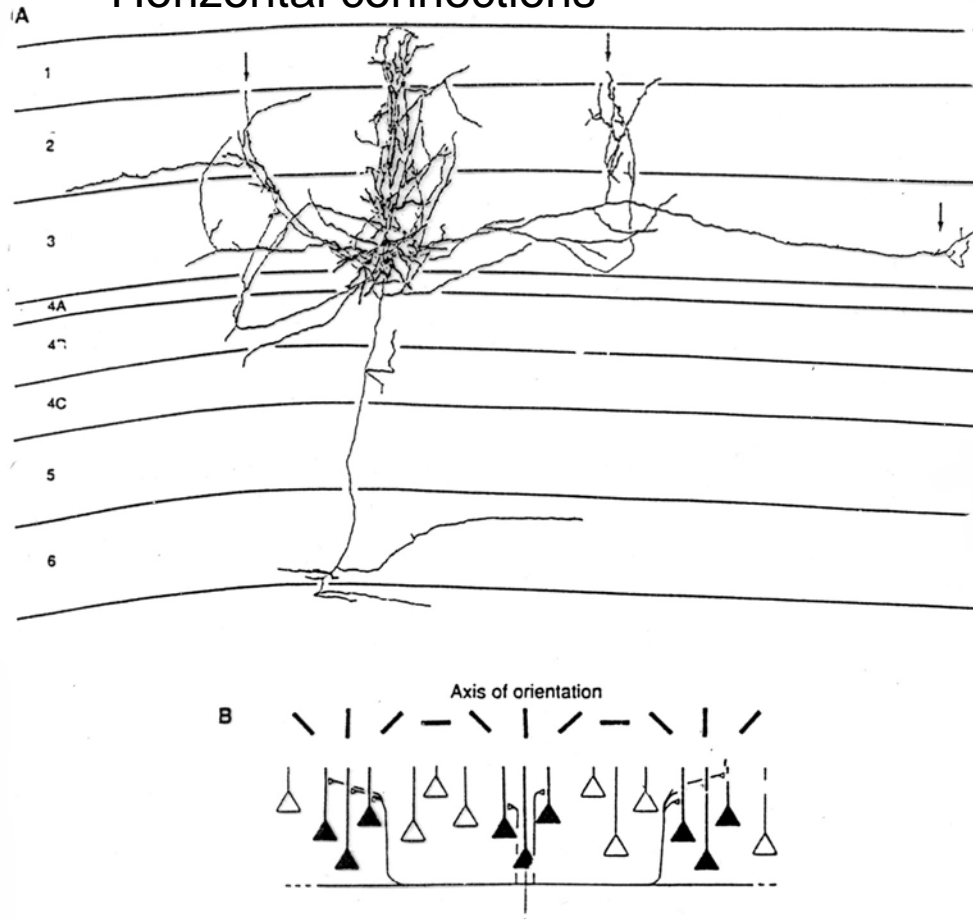
Intracolumnar and pericolumnar flow of activity in a barrel in the anesthetized adult rat, evoked by brief deflection of the related contralateral whisker. Cellulart discharges were recorded with extracellular microelectrodes. Cells in L IV are activated at a mean latency of 8.5 msec. Sequential activation of laminae and sublaminar units at the mean latencies after panel A. Cells within column in layer II and Vb are activated 2.4 msec after those of L IV, near simulataneously with L Va cells in near-neighbor columns (A-C). Activity then spreads to near-neighbor layers and columns (D—F) (Armstrong-Jones et al., 1992).

# Resident cells and local flow of information in the primary visual cortex

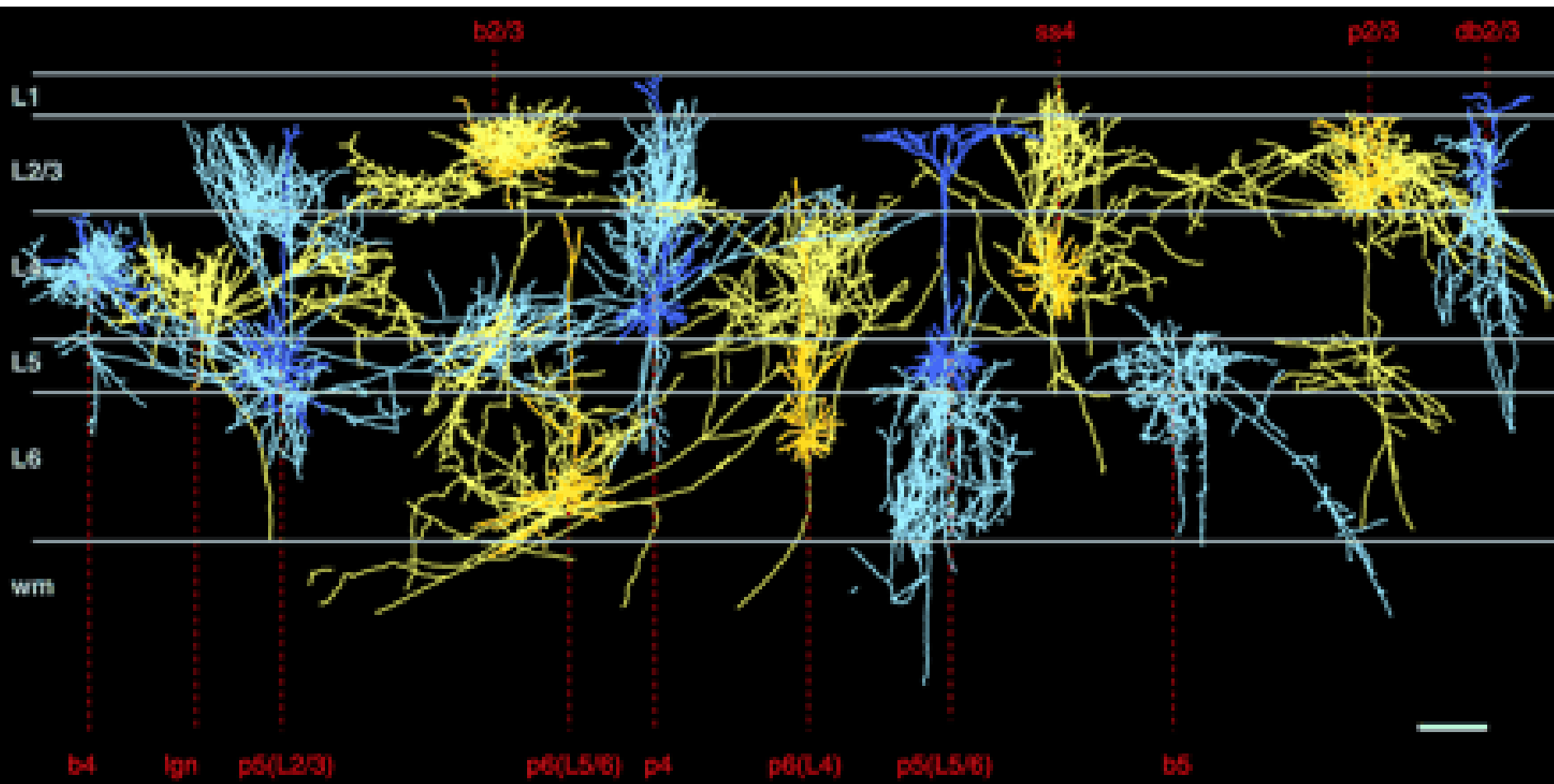


**A:** inputs from the LGB. **B:** resident cells. **C:** Afferents from M and P cells of the LGN end on spiny stellate cells in layer 4C, and these cells project axons to layer 4B and the upper layers 2 and 3. Cells from the interlaminar zones (I) in the LGN project directly to layers 2-3. From there, pyramidal cells project axon collaterals to L5 pyramidal cells, whose axon collaterals project both to L6 cells as well as back to cells in L2-3. Axon collaterals of L6 pyramidal cells then make a loop back to L4C onto smooth stellate cells. Each layer, except for 4C, has different outputs. The cells in L5 project to the superior colliculus, the pons, and the pulvinar. Cells in L6 project back to LGN and the claustrum (Lund, 1988) .

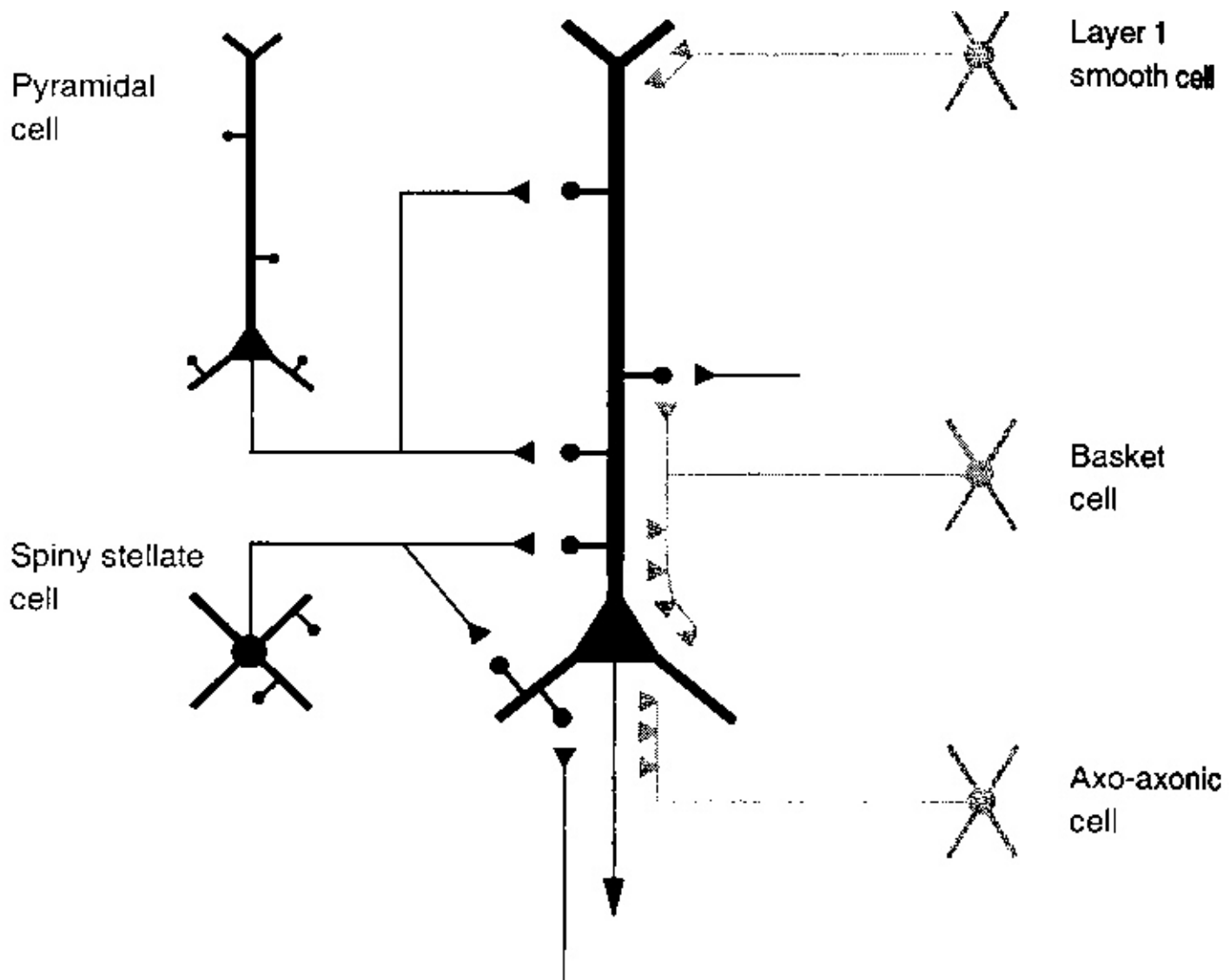
## Horizontal connections



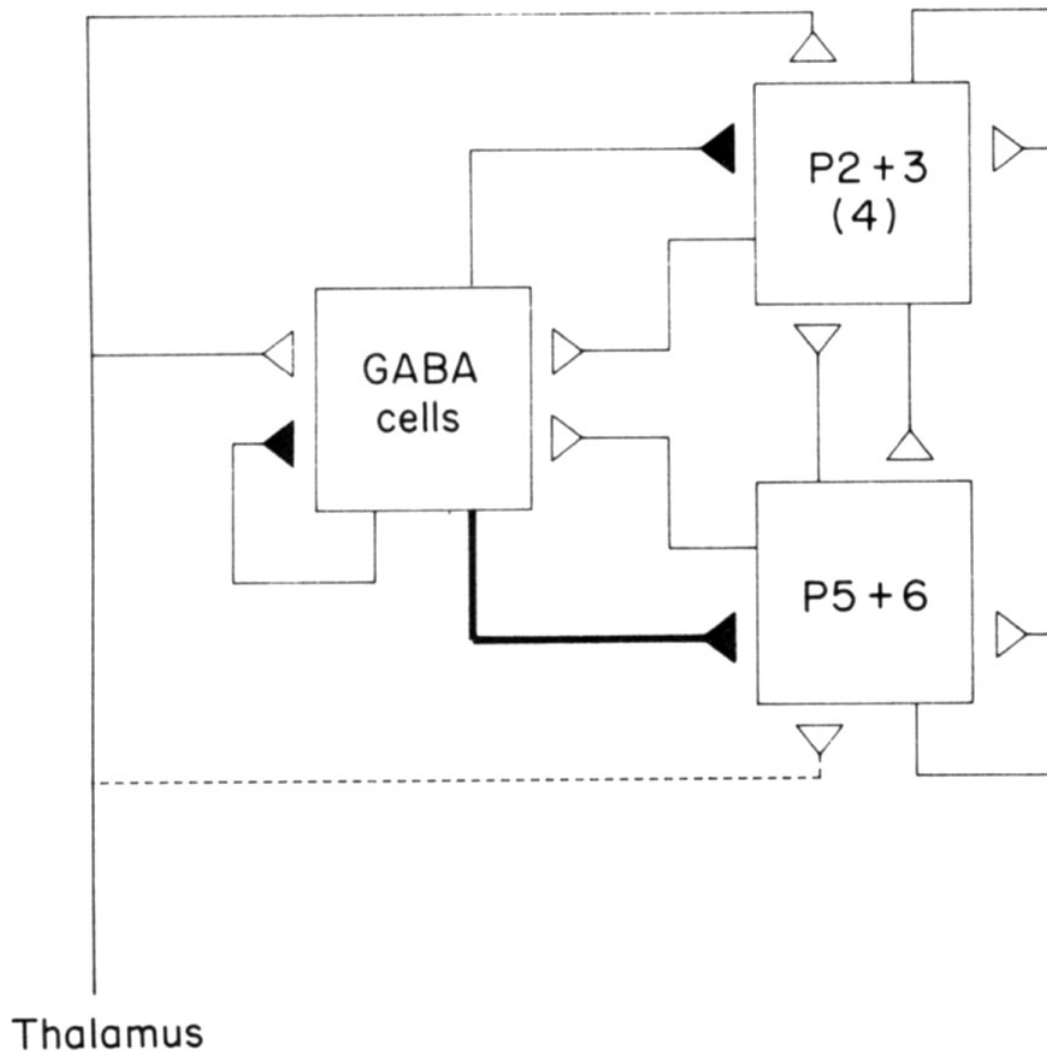
A: camera lucida reconstruction of a pyramidal cell injected with horseradish peroxidase in L 2-3 in a monkey. Several axon collaterals (arrow) branch off the axon and ramify near the dendritic tree and in three other clusters. This collateral system is thought to interconnect cells in different cortical columns with similar functional properties (McGuire et al., 1990). B: The functional specificity of the long-range clustered horizontal connections. The axon of one pyramidal neuron, in the center of the diagram, synapses on other pyramidal cells in the immediate vicinity as well as on pyramidal cells some distance away. The axon makes connection only with cells with the same functional specificity (Tso's, Gilbert, Wiesel, 1986)



**Reconstructed cells in the visual cortex.** For better viewing, two-color schemes (blue and yellow) were used. Axons are shown in bright blue or bright yellow, and dendrites are shown in dark blue or dark yellow. Boutons are skipped for visibility. Cell types are indicated at the top. b2/3, b4, b5, Basket cells in layer 2/3, 4, and 5; db2/3, double bouquet cell in layer 2/3; p2/3, p4, p5, p6, pyramidal cells in layer 2/3, 4, 5, and 6; ss4, spiny stellate cells in layer 4. Spiny stellate cells and pyramidal cells in layer 5 and 6 were further distinguished by the preferred layer of the axonal innervation [ss4(L4) (data not shown), ss4(L2/3), p5(L2/3), p5(L5/6), p6(L4) and p6(L5/6)]. X/Y thalamic afferents of type X and Y. Horizontal lines indicate the approximate cortical layers L1, L2/3 (layer 2 and 3 were merged), L4, L5, and L6. Also indicated is the white matter (wm). Scale bar, 300  $\mu\text{m}$  (Binzegger et al., 2004).

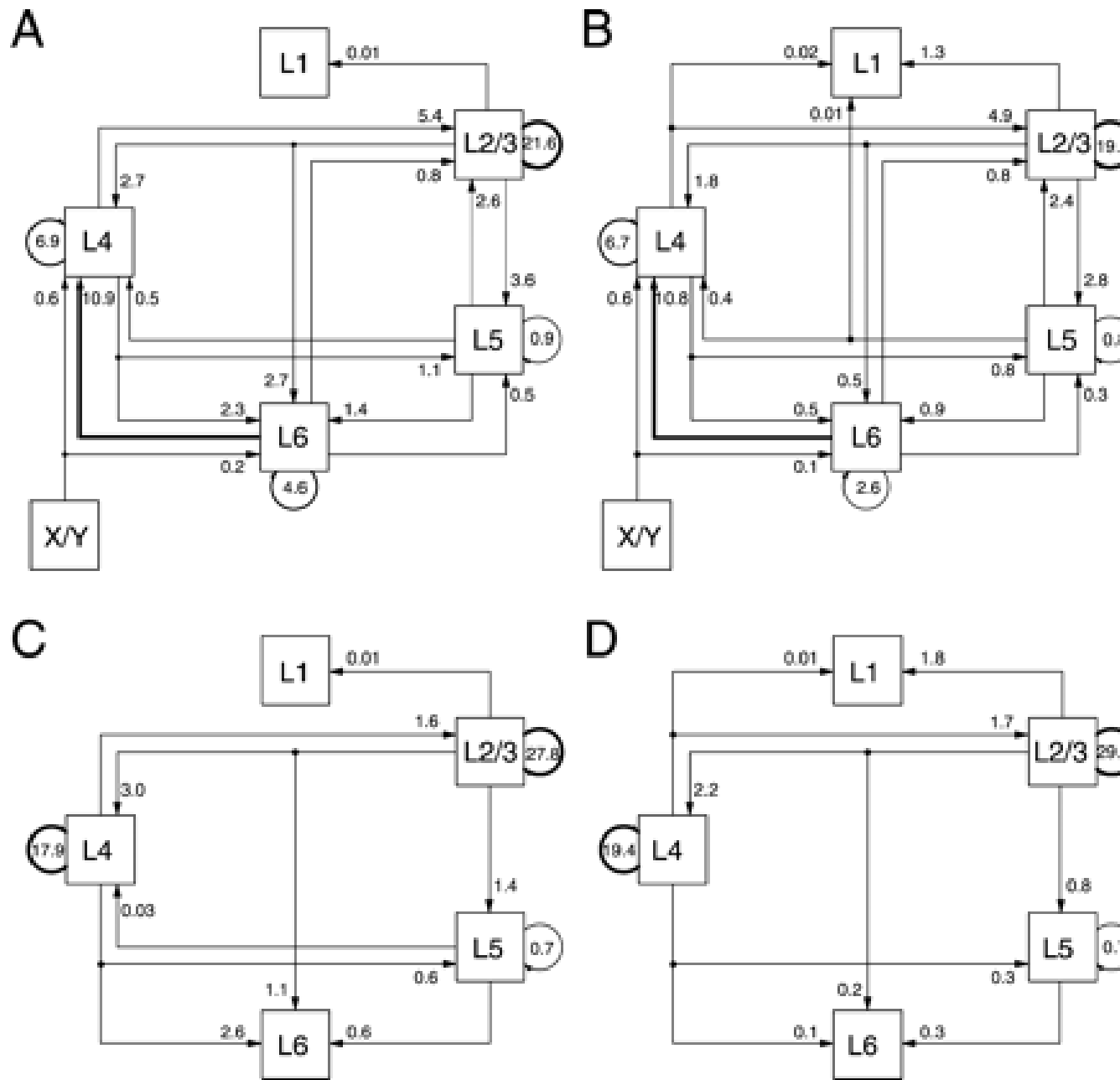


## The canonical microcircuit.



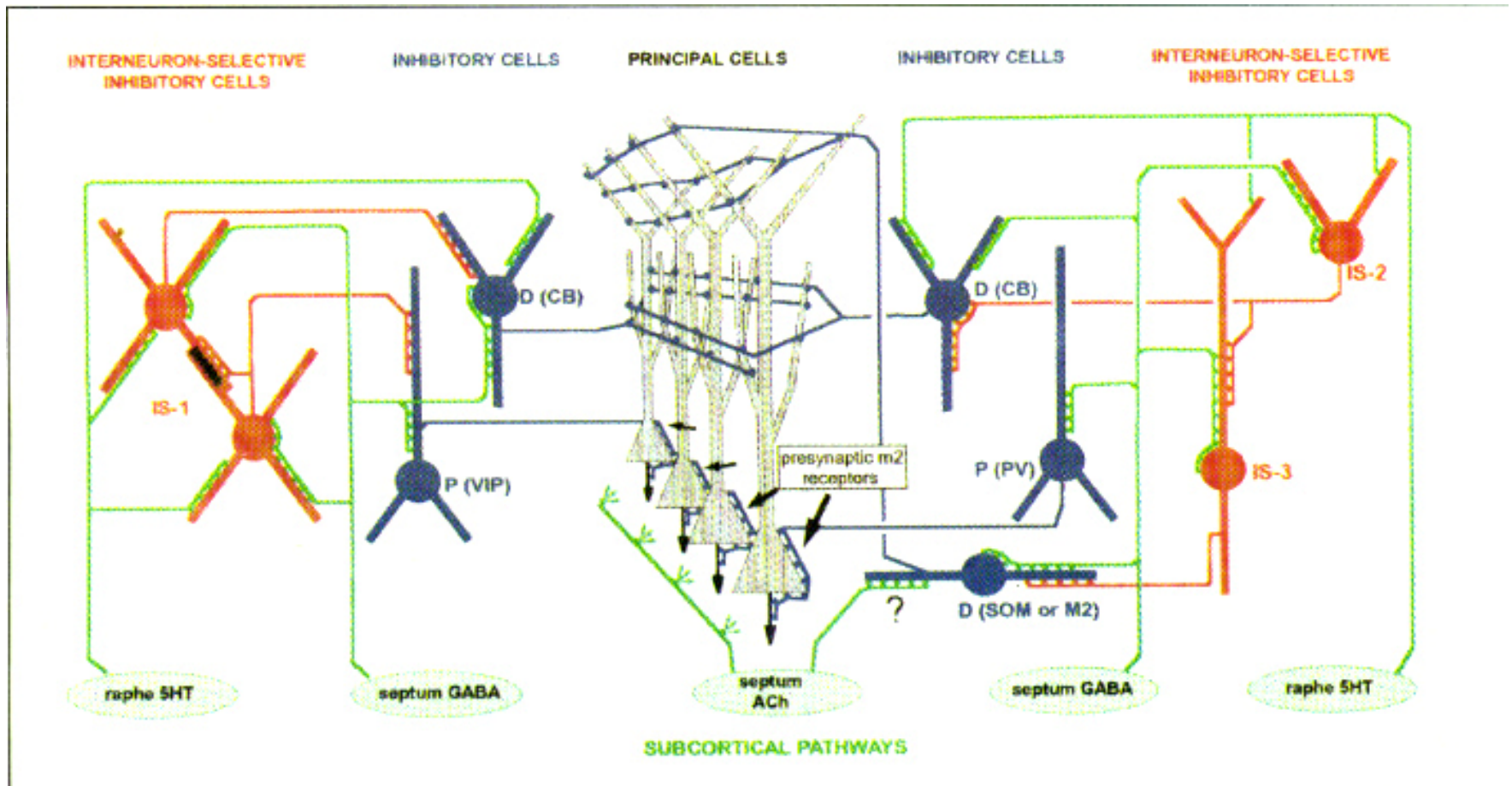
It is applicable to all cortical areas so far examined. Three population of neurons interact with one another. One population is inhibitory (GABAergic cells, solid synapses) and two are excitatory (open synapses) representing superficial (P2+3) and deep (P5+6) pyramidal neurons. The properties of L4 stellate (4), which contribute 10% of neurons in granular cortex, less elsewhere, are similar to those of the superficial pyramids. The thickness of the connecting lines indicates the functional strength of the input. Note that the dominant connections is between excitatory neurons, so that a relatively weak thalamic input can be greatly amplified by the recurrent excitation of the spiny neurons (Douglas and Martin, 1990).

# Numbers of synapses between excitatory and inhibitory neurons in the visual ctx

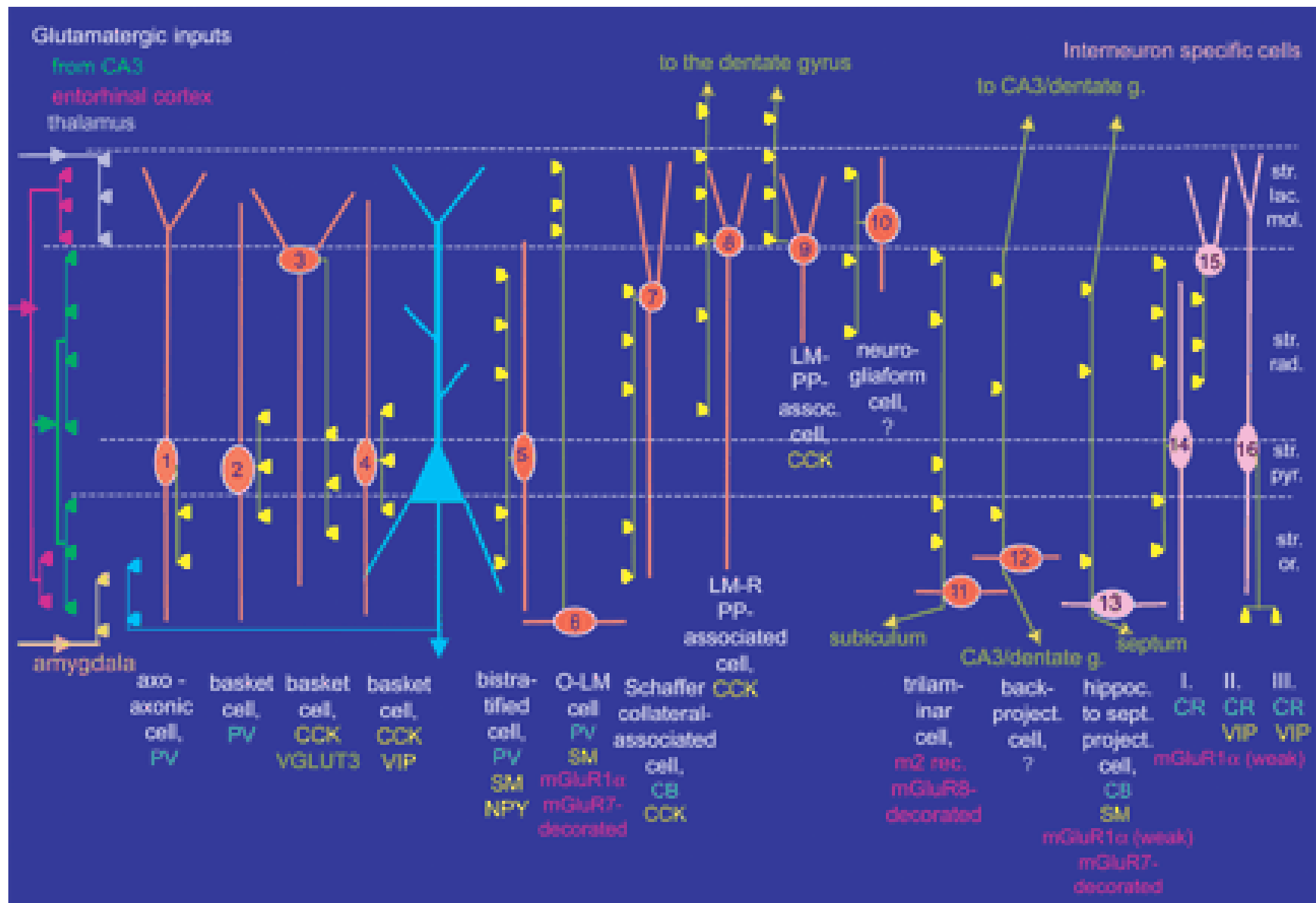


A between excitatory neurons (A), from excitatory onto inhibitory neurons (B), from inhibitory onto excitatory neurons (C), and between inhibitory neurons (D). **A, Total number of synapses between excitatory neurons is  $13.6 \times 10^{10}$ .** The proportion of asymmetric unassigned synapses that the excitatory neurons in each layer receive is 0.1% (layer 1), 6% (layer 2/3), 10% (layer 4), 2% (layer 5), and 12% (layer 6). These synapses are presumably formed by the afferents originating outside area 17. **B, Total number of synapses from excitatory neurons onto inhibitory neurons is  $2.1 \times 10^{10}$ .** The proportion of asymmetric unassigned synapses that the inhibitory neurons in each layer receive is 17% (layer 1), 5% (layer 2/3), 9% (layer 4), 0.5% (layer 5), and 11% (layer 6). **C, Total number of synapses from inhibitory neurons onto excitatory neurons is  $2.4 \times 10^{10}$ .** The proportion of symmetric unassigned synapses that the excitatory neurons in each layer receive is 0.1% (layer 1), 6% (layer 2/3), 12% (layer 4), 6% (layer 5), and 19% (layer 6). **D, Total number of synapses between inhibitory neurons is  $0.4 \times 10^{10}$ .** The proportion of symmetric unassigned synapses that the inhibitory neurons in each layer receive is 11% (layer 1), 5% (layer 2/3), 10% (layer 4), 4% (layer 5), and 15% (layer 6).

# Hippocampal circuitry anno 1998



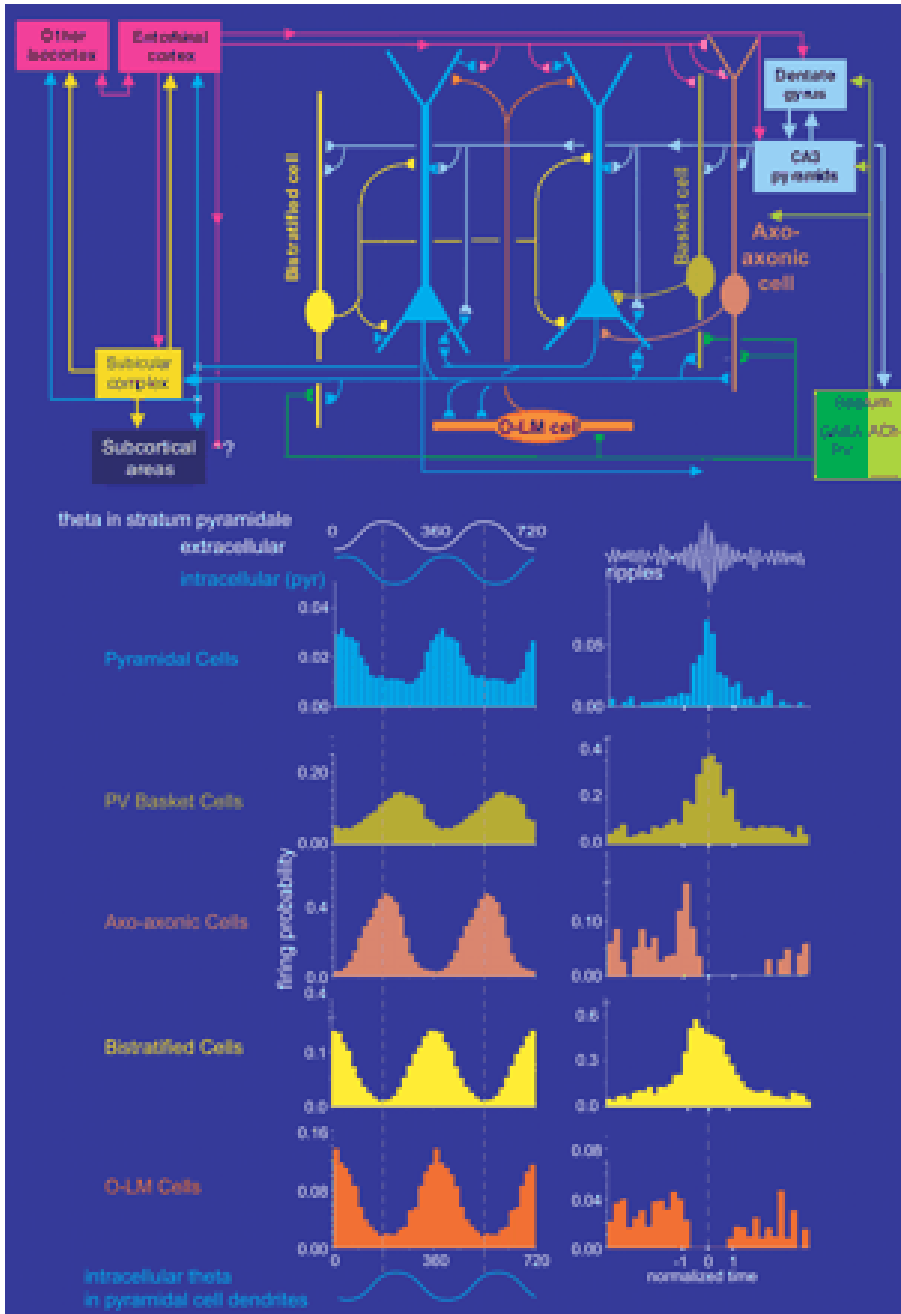
# HIPPOCAMPAL CIRCUITRY (2005)



Innervation of pyramidal cells by 12 types of GABAergic interneuron and interneurons by 4 types of interneuron specific cell in the CA1 area of the hippocampus

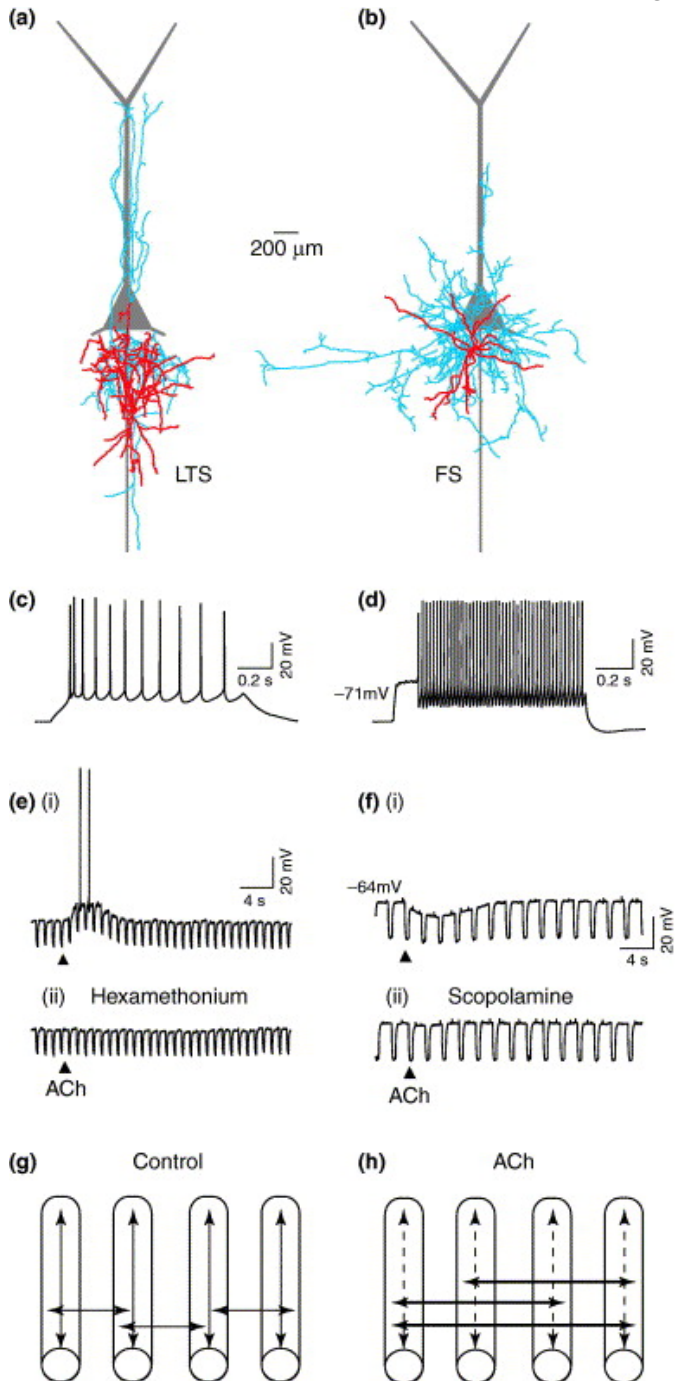
(Somogyi and Klausberger, 2005)

# Firing patterns of pyramidal cells and four types of interneurons in the hippocampus



The schematic drawing summarizes the main synaptic connections in the CA1 area of pyramidal cells (blue), parvalbumin expressing basket, axo-axonic, bistratified and O-LM cells. The cells have differential temporal firing patterns during theta and ripple oscillations (mean of several cells). For clarity two theta cycles are shown in the firing probability histograms. The Y axis of the spike probability plots was constructed by including all events and cycles in the analysed period irrespective of whether the individual recorded cell fired or not. The phase relationship of the extracellularly recorded field potential (schematic white wave) used in the spike alignments and the phase shifted oscillation in the membrane potential oscillation of pyramidal cells reported from intracellular studies (blue waves) is shown schematically. For the ripples, time was normalized to the beginning, highest amplitude and end of ripple episode. The spike probability plots show that during different network oscillations representing two distinct brain states, interneurons of the same connectivity class show *different* firing activities and therefore modulate their specific postsynaptic target-domain in a brain-state-dependent manner. Interneurons belonging to different connectivity classes fire preferentially at distinct time points during a given oscillation. Because the different interneurons innervate distinct domains of the pyramidal cells, the respective compartments will receive GABAergic input at different time points. This suggests a role for interneurons in the temporal structuring of the activity of pyramidal cells and their inputs via their respective target domain in a co-operative manner, rather than simply providing generalized inhibition (SOMOGYI AND Klausberger, 2005).

# Intra and intercolumnar connections: role of ACh



Differential modulation of LTS and FS interneurons by ACh in layer 5 of rat neocortex. **(a)** A biocytin-filled and reconstructed LTS interneuron in neocortical layer 5. The cell body and dendrites are in red, the axon is in blue, and a schematic pyramidal neuron is in gray. Note that the axonal plexus is vertically oriented, extending toward the more superficial cortical layers. LTS interneurons tend to make synapses more prominently on pyramidal neuron dendrites than do FS interneurons. **(b)** A biocytin-filled and reconstructed FS cell in neocortical layer 5. Color code as in (a). Note the extensive axonal arborization in the perisomatic region. **(c,d)** Characteristic firing behavior of a LTS interneuron (c) and an FS interneuron (d) in response to a suprathreshold depolarizing current injection. **(e)** Puff application of ACh depolarizes LTS cells, causing action potential firing (i), through nicotinic ACh receptor activation that is blocked by hexamethonium (ii). **(f)** By contrast, ACh application hyperpolarizes FS interneurons (i), an effect blocked by the muscarinic receptor antagonist scopolamine (ii). Arrowheads in (e,f) indicate the time of ACh application. **(g,h)** The hypothetical change in the flow of excitation induced by ACh. Single cortical columns are drawn as cylinders. Under control conditions (g), intracolumnar excitation (vertical arrows) and intercolumnar excitation (horizontal arrows) are counteracted by inhibitory output of LTS and FS interneurons, respectively. When ACh is released (h), inhibition of FS interneurons (as in f) and excitation of LTS cells (as in e) results in an increase of intercolumnar excitation (dark horizontal arrows) and in a decrease of intracolumnar excitation (dashed vertical arrows) (Bacci et al, 2005).